# Role of RAI2 protein in the progression of prostate and breast cancer

DISSERTATION

Dissertation
With the aim of obtaining a doctoral degree (Dr. rer. nat.)
at the Department of Biology
Faculty of Mathematics, Informatics and Life Sciences
University of Hamburg

Submitted by
KATHARINA BESLER

Born in Kostanay, Kazakhstan

Hamburg, May 2020

The present study was carried out between April 2016 and April 2020 at the University Medical Center Hamburg-Eppendorf in the Institute of Tumour Biology under the direction of Prof. Dr. Klaus Pantel and the supervision of Dr. Stefan Werner and Prof. Dr. Harriet Wikman-Kocher.


| | |
|---|---|
| 1. Reviewer: | Prof. Dr. Christian Lohr |
| 2. Reviewer: | Prof. Dr. Wikman-Kocher |

Date of oral defense: September 11th 2020

# Abstract

The *RAI2* gene was first identified as a novel metastasis suppressor gene in breast cancer patients with hormone-dependent disease. Moreover, low RAI2 expression was significantly associated with early occurring bone micro-metastasis and poor patients' outcome. Molecular characterization of the RAI2 protein in the ER-positive luminal breast cancer cell lines suggested that the RAI2 protein could act as a transcriptional co-regulator involved in differentiation of hormone-dependent breast cancer cells, and might play an active part in the transcriptional network of hormonal response. In this study the role of RAI2 in prostate and breast cancer, both steroid hormone driven cancers, was evaluated focusing mainly on its impact on hormone response and progression to a hormone therapy resistant disease.

First, the prognostic relevance of RAI2 expression in prostate cancer was determined from published GEO datasets. To clarify whether there is a functional relationship between RAI2 and hormone receptor expression, knockdown or inhibition of either oestrogen (ER) or androgen receptors (AR) and RAI2 depletion were performed in hormone-dependent breast or prostate cancer cell lines. Furthermore, quantitative PCR analyses were performed to investigate the expression of AR-regulated genes in RAI2-depleted LNCaP prostate cancer cells. In addition, a possible molecular interaction between RAI2, CtBP and the AR proteins was analysed using immunofluorescence staining. To study the effect of the RAI2 protein on breast and prostate cancer cell line progression, both RAI2 knockout and RAI2 overexpression systems were generated. The effects of modified RAI2 expression on proliferation, cell response to pharmacological inhibition, anchorage-independent growth and cell migration were also investigated. Also, growth and dissemination of LNCaP prostate cancer cells with RAI2-knockout was analysed in a xenograft model. Finally, to evaluate the clinical relevance of RAI2 expression in blood samples of advanced prostate patients, a method was established to measure RAI2 mRNA expression of circulating tumour cells. The feasibility of this method was tested within a small pilot study comprising 36 patients with metastatic prostate cancer.

Results of this study showed, on the one hand, a decrease in ER and AR expression in all tested breast and prostate cancer cell lines as a result of RAI2 knockdown. On the other hand, the depletion of the respective HR increased the RAI2 protein expression in all tested cell lines of both tumour entities. This implies an interdependent regulation of the expression of these two proteins. Furthermore, pharmacological inhibition of HR led to significant changes in RAI2 expression, which in most cases correlated with the expression of the growth hormone receptor. Since RAI2 depletion causes elevated PSA gene expression in LNCaP cells and the RAI2 protein is colocalised

with CtBP factors in the nucleus, it is likely that the protein acts as transcriptional coregulator also in prostate cancer cells.

With regard to proliferation and cell viability, the RAI2 knockout did lead to divergent results in the cell lines tested. Only in the LNCaP cells could a significant increase in proliferation be detected, which was also found increased in RAI2-KO cells even under inhibition of the AR. Moreover, the RAI2 knockout was associated with an increased migration of LNCaP cells and an increased resistance to the anoikis. However, neither increased tumour growth nor increased dissemination of LNCaP RAI2-KO cells could be detected in the xenograft mouse model. Finally, a method was successfully established that allows determination of gene expression of *RAI2*, as well as other genes relevant for the progression of prostate cancer in CTCs. In the analysed blood samples from patients with metastatic prostate cancer, RAI2 expression strongly correlated with the CTC status and the expression of AR, it's constitutively active variant and the AR-regulated genes *PSA* and *PSMA*. Furthermore *RAI2* expression was associated with increasing serum PSA levels, anemia and a tendency to worse overall survival.

Taken together, the results of this study show a strong correlation and functional association between the RAI2 protein and the steroid hormone receptors ER and AR in cell line models and patient material. Furthermore, a coregulatory function of the RAI2 protein is likely, mainly due to its interaction with the CtBP proteins, which act as coregulators of ER- and AR-mediated transcription. Despite the observed similarities between the tested breast and prostate cancer cell lines, proliferation and resistance to hormone therapy seems not only to depend on RAI2 but also on the cell-specific genetic aberrations of the individual cell line. Furthermore, a newly established liquid biopsy approach allows detection of the presence of CTC in the blood of patients with metastatic prostate cancer based on the gene expression of *RAI2*, *AR*, *AR-V7*, *PSA (KLK3)* and *PSMA (FOLH1)*. However, the exact molecular function of the RAI2 protein requires clarification as well as whether detection of *RAI2* gene expression could be exploited to enhance the treatment of metastatic prostate cancer.

# Zusammenfassung

Das RAI2-Gen wurde erstmals als ein mögliches Metastasierungssuppressor-Gen bei Brustkrebspatientinnen mit hormonabhängiger Erkrankung identifiziert. Darüber hinaus korrelierte eine geringe RAI2-Expression mit früh auftretenden Micro-Knochenmetastasen und damit einhergehendem verschlechtertem Krankheitsverlauf bei den betroffenen Patientinnen. Die molekulare Charakterisierung des RAI2-Proteins in den ER-positiven, luminalen Brustkrebszelllinien ließ zudem vermuten, dass das RAI2-Protein als transkriptioneller Co-Regulator bei der Differenzierung von hormonabhängigen Brustkrebszellen wirken und möglicherweise eine aktive Rolle im transkriptionellen Netzwerk der Hormonreaktion spielen könnte. In dieser Studie sollte die Bedeutung von RAI2 für die Progression des Brust- und Prostatakarzinoms weitergehend analysiert werden. Aufgrund des hormonabhängigen Wachstums beider Krebsarten wurde ein besonderer Fokus der Analysen auf den Einfluss des RAI2 Proteins auf die Hormonantwort, sowie die Entwicklung einer gegenüber Hormontherapie resistenten und Erkrankung gelegt.

Um die prognostische Relevanz von RAI2 beim Fortschreiten des Prostatakarzinoms erstmalig zu untersuchen, wurde zunächst auf bereits publizierte GEO Datensätze zurückgegriffen. Um zu klären, ob es einen funktionellen Zusammenhang zwischen der RAI2-Expression und der Expression der Hormonrezeptoren gibt, wurden diese Proteine wechselseitig in Hormon-abhängigen Krebszelllinien depletiert. Des Weiteren wurden quantitative PCR Analysen durchgeführt, um die Expression von AR-regulierten Genen in RAI2-depletierten LNCaP Prostatakrebs Zelllinien zu untersuchen. Unter Anwendung einer Immunfluoreszenzfärbung, sollte zudem eine mögliche Interaktion zwischen dem RAI2, dem AR und den CtBP Proteinen untersucht werden. Um die Auswirkung des RAI2 Proteins auf die Progression von Brust- und Prostatakrebs-Zelllinien zu untersuchen wurden Zelllinien mit einer RAI2-Inaktivierung und mit konstitutiver RAI2-Überexpressions generiert. Die Auswirkungen dieser Modifikationen auf die Proliferation, das Ansprechen der Zellen auf pharmakologische Inhibition sowie das verankerungsunabhängige Wachstum und die Zell Migration wurden anschließend in den genetisch modifizierten Zellen untersucht. Darüber hinaus wurde das Wachstum und die Dissemination der modifizierten LNCaP Prostatkrebszellen in einem Xenograft Model, analysiert. Um die klinische Relevanz der RAI2-Expression bei fortgeschrittenen Prostatapatienten zu evaluieren, wurde außerdem eine Methode zur Messung der RAI2-Expression in zirkulierenden Tumorzellen etabliert und innerhalb einer kleinen Studie an 36 Patienten mit metastatischem Prostatakarzinom getestet.

Untersuchungen dieser Arbeit zeigten, zum einen eine Verringerung der ER- und AR-Expression bei allen getesteten Brust- und Prostatakrebs Zelllinien infolge eines RAI2-Knockdowns. Andererseits erhöhte die Depletion des jeweiligen HR die RAI2 Protein Expression in den Zelllinien

beider Tumorentitäten, was eine voneinander abhängige Regulation der Expression beider Proteine impliziert. Des Weiteren führte die pharmakologische Inhibition der HR zu einer signifikanten Veränderung der RAI2-Expression, die in den meisten Fällen mit der Expression des wachstumstreibenden Hormonrezeptors korrelierte. Zusammen mit der erhöhten Expression des PSA Gens in vollständig RAI2-depletierten LNCaP Zellen und einer Interaktion der RAI2 und CtBP Proteine, wurde somit weitere Evidenz geschaffen, die eine Beteiligung an der transkriptionellen Regulation der Hormonantwort durch das RAI2 Protein begründen. In Hinblick auf die Proliferation und die Viabilität der Zellen führte der RAI2-knockout zu keinem einheitlichen Ergebnis. So konnte lediglich in den LNCaP Zellen eine signifikante Erhöhung der Proliferation detektiert werden, die auch unter der Inhibition des AR verstärkt in den RAI2-depletierten Zellen zu detektieren war. Eine RAI2-Inaktivierung führte zudem zu einer erhöhten Motilität der LNCaP Zellen sowie zu einer erhöhten Resistenz gegenüber der Anoikis. Dennoch konnte in den verwendeten Xenograft Mausmodel weder vermehrtes Tumorwachstum, noch eine vermehrte Dissemination der LNCaP RAI2-KO Zellen nachgewiesen werden. Schließlich wurde erfolgreich eine Methode etabliert, die es ermöglicht die Expression des RAI2 Gens, sowie weiterer für die Progression des Prostatakarzinoms relevanter Gene, in zirkulierenden Tumorzellen zu analysieren. In einer Pilotstudie mit 36 Blutproben von Patienten mit metastatischen Prostatakarzinom, korrelierte die RAI2-Expression mit dem CTC Status und der Expression des *AR*, seiner konstitutiv aktiven Variante sowie der AR-regulierten Gene *PSA* und *PSMA*. Darüber hinaus war die RAI2-Expression mit steigenden PSA-Werten im Serum, Anämie und einer Tendenz zu schlechterem Gesamtüberleben assoziiert.

Zusammengefasst zeigen die Ergebnisse dieser Studie eine starke Korrelation sowie eine funktionelle Assoziation des RAI2-Proteins mit den Steroidhormonrezeptoren ER und AR in den getesteten Zelllinienmodellen und Patientenmaterial. Darüber hinaus bleibt eine Funktion des RAI2-Proteins als transkriptioneller Koregulator möglich. Evidenz hierfür ist, hauptsächlich die Interaktion mit den CtBP-Proteinen, die als Koregulatoren der ER- und AR-vermittelten Transkription fungieren. Trotz der festgestellten Ähnlichkeiten zwischen den getesteten Brust- und Prostatakrebszelllinien scheint die Proliferation und die Resistenz gegenüber Hormontherapien nicht nur von RAI2, sondern auch von den zellspezifischen genetischen Aberrationen jeder Zelllinie abzuhängen. Die hier etablierte Liquid Biopsy-Methode erlaubt es die Präsenz von CTC im Blut von Patienten mit metastatischen Prostatakarzinom basierend auf der Gen-Expression von *RAI2*, *AR, AR-V7*, *PSA (KLK3)* und *PSMA (FOLH1)* zu detektieren. Es bleibt weiterhin zu klären, nach welchen molekularen Prinzipien das RAI2-Protein in der Hormonantwort wirkt und welche Relevanz die *RAI2* Expression als Biomarker für eine Verbesserung der Behandlung von Patienten mit metastasiertem Prostatakarzinoms einnimmt.

# Contents

Abstract ..... I

Zusammenfassung ..... III

List of abbreviations ..... IX

List of tables ..... XII

Register of illustrations ..... XIII

1 Introduction ..... 1

1.1 Fundamentals of cancer progression ..... 1

1.2 Prostate Cancer: Epidemiology, anatomy, risk factors and disease management ..... 3

1.3 Breast cancer: Epidemiology, anatomy, risk factors and disease management ..... 5

1.4 Hormone signalling/ Steroid receptor signalling pathway ..... 8

1.5 Hormone therapy in prostate and breast cancer ..... 10

1.6 Mechanisms of resistance to hormone therapy ..... 13

1.7 The concept of Liquid Biopsy for clinical management of cancer patients ..... 15

1.8 Retinoic acid-induced protein 2 ..... 17

1.9 Objectives of this study ..... 19

2 Material and Methods ..... 21

2.1 Material ..... 21

2.1.1 Laboratory equipment ..... 21

2.1.2 Software ..... 23

2.1.3 Consumables ..... 24

2.1.4 Chemicals and reagents ..... 25

2.1.5 Buffer and media ..... 27

2.1.6 Commercial Kits ..... 28

2.1.7 Hormones, Inhibitors and Cytostatics used in cell culture experiments ..... 29

2.1.8 Vectors and Expression plasmids ..... 29

2.1.9 Oligonucleotides ..... 30

2.1.10 Antibodies ..... 31

2.1.11 Human cell lines ..... 32

2.1.12 Mouse material ..... 33

2.1.13 Patient material ..... 33

2.2 Cell culture methods ..... 33

2.2.1 Resuscitation of frozen cells ..... 34

2.2.2 Cultivation of cells ..... 34

2.2.3 Cryopreservation of cell lines ..... 34

2.2.4 Cell number determination ..... 35
2.2.5 Cell line authentication ..... 35
2.2.6 Retroviral gene transfer for overexpression of *RAI2* gene in cell lines ..... 35
2.2.7 Lentiviral gene transfer for downregulation of gene expression in cell lines 36
2.2.8 CRISPR/Cas-9 genome editing to knockout RAI2 expression in LNCaP cell line ..... 36
2.3 Functional assays to analyse the hallmarks of cancer ..... 37
2.3.1 MTT assay ..... 37
2.3.2 Colony formation assay ..... 37
2.3.3 Transwell migration assay ..... 38
2.3.4 Soft agar assay ..... 38
2.4 Molecular biologic Methods ..... 39
2.4.1 Genomic DNA isolation from human cell lines ..... 39
2.4.2 Sequencing ..... 39
2.4.3 Quantity and quality measurement of nucleic acids ..... 40
2.4.4 RNA isolation from human cancer cell lines ..... 40
2.4.5 Complementary DNA (cDNA) synthesis by reverse transcription of RNA .. 40
2.4.6 Polymerase-chain-reaction (PCR) with AmpliTaq Gold® polymerase ..... 40
2.4.7 Agarose gel electrophoresis ..... 41
2.4.8 Quantitative real time-PCR (qRT-PCR) ..... 42
2.5 Protein biochemical methods ..... 43
2.5.1 Cellular extract preparation ..... 43
2.5.2 BCA assay ..... 43
2.5.3 SDS-polyacrylamide gel-electrophoresis ..... 44
2.5.4. Western blot analysis ..... 44
2.5.5 PamStation ..... 45
2.5.6 Immunofluorescence staining of cultured cells ..... 46
2.6 Xenograft experiment ..... 46
2.6.1 Enrichment of CTC from murine EDTA-blood by the Parsotix™ system ... 47
2.6.2 Isolation and processing of murine bone marrow cells ..... 47
2.6.3 Immunofluorescence staining for the detection of CTCs and DTC ..... 47
2.6.4 *Alu*-PCR for DTC detection in murine organs ..... 48
2.7 Enrichment and detection of CTC from peripheral blood of prostate cancer patients ..... 48
2.7.1 Ficoll density gradient for isolation of PBMCs from healthy donors ..... 48
2.7.2 Bisulfide conversion ..... 49
2.7.3 CTC enrichment from PCa-patients by “AdnaTest ProstateCancer”-kit ..... 49
2.7.4 Preamplification ..... 49
2.7.5 Expression analysis qRT-QPCR and data analysis ..... 50
2.8 In Silico analyses ..... 50

3 Results ..... 51
3.1 In Silico Analysis of RAI2 expression in Prostate Cancer ..... 51
3.2 Analysis of the relationship between RAI2 and Hormone receptors ..... 51
3.2.1 Analysis of the relationship between RAI2 and the Oestrogen Receptor ..... 52
3.2.2 Analysis of relationship between RAI2 and Androgen Receptor ..... 53
3.3. Effects of hormone receptor inhibition on RAI2 expression ..... 54
3.3.1 Inhibition of ERα activity in human breast cancer cells lines ..... 54
3.3.2 Inhibition of AR activity in human prostate cancer cells ..... 55
3.4 Analysis of possible interaction partners of RAI2 protein in prostate cancer cells ..... 56
3.5 Establishment of a *RAI2*-gene knockout in human LNCaP cell line by CRISPR-Cas9 editing ..... 57
3.6 Androgen response in RAI2-depleted LNCaP cells ..... 59
3.7 Viability of RAI2 modified prostate cancer cells ..... 60
3.7.1 Cell viability of MCF-7 breast cancer cells with RAI2-KO ..... 61
3.7.2 Cell viability of LNCaP and VCaP prostate cancer cells after RAI2-KO ..... 62
3.7.3 Cell viability of PC-3 prostate cancer cells with RAI2 overexpression ..... 63
3.8 Colony formation ability of RAI2 modified cells ..... 64
3.8.1 Clonogenic ability of LNCaP cells with RAI2-knockout ..... 64
3.8.2 Clonogenic ability of PC-3 prostate cancer cells overexpressing RAI2 ..... 65
3.8.3 Analysing LNCaP cell recovery after reintroduction of RAI2 protein into RAI2-KO cells ..... 66
3.9 Anchorage independent growth of RAI2 modified cells ..... 67
3.10 Cell motility of RAI2 modified cells ..... 68
3.11 Serine/threonine kinase activity after RAI2-knockout ..... 69
3.12 Analysis of tumour progression in a xenograft model ..... 71
3.12.1 Survival Analysis of LNCAP RAI2-KO inoculated ..... 72
3.12.2 Detection of cell dissemination by IF staining and *Alu*-PCR ..... 72
3.13 Establishment of a liquid biopsy test to detect RAI2 expression status in patients ..... 74
3.13.1 First establishment steps for RAI2 promoter methylation status analysis on ctDNA level ..... 75
3.13.2 Gene expression analysis of CTCs from metastatic prostate cancer patients 76

4 Discussion ..... 81
4.1 Prognostic relevance of RAI2 based on published datasets ..... 82
4.2 Relevance of RAI2 expression on the hormone response ..... 82
4.3 Effect of RAI2 depletion on BrCa and PCa progression ..... 86
4.4 Potential of RAI2 as a novel biomarker of liquid biopsy ..... 93

5 Conclusion and outlook ..... 96

6 Appendix ..... 101
A Heat maps of phosphorylated peptides /PAMstation ..... 101

7 Bibliography.....103

Danksagung.....116

Eidesstattliche Erklärung.....118

English certificate .....119

# List of abbreviations

| | |
|---|---|
| °C | Degree Celsius |
| µm | Micrometre |
| µM | Micromolar |
| AKT | Protein kinase B |
| APS | Ammonium persulfate |
| AR: | Androgen receptor |
| AR-V7 | Androgen receptor variant 7 |
| BIC | Bicalutamide |
| BrCa | Breast cancer |
| BSA | Bovine serum albumin |
| BSSQ | Bisulfite sequencing |
| Cas9 | CRISPR associated protein 9 |
| CD45 | Protein tyrosine phosphatases, receptor-type, C |
| cDNA | Complementary DNA |
| ChIP | Chromatin immunoprecipitation |
| Co-IP | Co-immunoprecipitation |
| Cq | Cycle quantification |
| CRC | Colorectal cancer |
| CRISPR | clustered regularly interspaced short palindrome repeats |
| CST | Cell Signalling Technologies |
| DAPI | 4', 6-diamidine-2-phenylindole |
| DHT | Dihydrotestosterone |
| DMEM | Dulbecco's Modified Eagle's Medium |
| DMSO | Dimethyl sulfoxide |
| DNA | Desoxyribonucleic acid |
| dNTP | Deoxyribonucleoside triphosphates |
| DTT | Dithiothreitol |
| DU145 | Duke University 145 |
| ECL | Enhanced chemiluminescence |
| EGFR | Epidermal growth factor receptor |
| EMT | Epithelial-to-mesenchymal transition |
| ENZ | Enzalutamide |
| EpCAM | Epithelial cell adhesion molecule |
| ER: | Oestrogen receptor |
| FACS | Fluorescence-activated cell sorting |
| FCS | fetal calf serum |

| | |
|---|---|
| FCS | Fetal calf serum |
| FDA | Food and Drug Administration |
| g | Gram |
| GAPDH | Glyceraldehyde-3-phosphate dehydrogenase |
| gDNA | Genomic desoxyribonucleic acid |
| GEO | Gene Expression Omnibus |
| GFP | Green fluorescent protein |
| h | Hour/s |
| $H_20$ | Water |
| $H_20_2$ | Hydrogen peroxide |
| HD | Hormone-deprived |
| HER2 | Receptor tyrosine-protein kinase erbB-2 |
| HR | Hormone receptor |
| HRP | Horseradish peroxidase |
| HSC70 | Heat shock cognate 71 kDa protein |
| ICI | Fulvestrant |
| IF | Immunofluorescence |
| IgG | Immunoglobulin G |
| Indel | Insertion and deletion |
| ITB | Institute of Tumour Biology |
| kb | Kilo base pairs |
| KD | Knockdown |
| kDa | Kilodaltons |
| KO | Knockout |
| LNCaP | Lymph Node Carcinoma of the Prostate |
| M | Molar |
| MCF-7 | Michigan Cancer Foundation-7 |
| MET | Mesenchymal-to-epithelial transition |
| min | minutes |
| mL | Millilitre |
| mM | Millimolar |
| MME | Neprilysin, membrane metallo-endopeptidase |
| mRNA | Messenger ribonucleic acid |
| mTOR | mechanistic Target of Rapamycin |
| MTT | Methylthiazol diphenyl tetrazolium bromide |
| MTT | 3-(4,5-Dimethylthiazol-2-yl)-2,5-diphenyltetrazoliumbromide |
| NaCl | Sodium chloride |
| NaOH | Sodium hydroxide |
| nm | Nanometre |
| nM | Nanomolar |

| | |
|---|---|
| NT | Non-target |
| OE | Overexpression |
| PBMC | peripheral blood mononuclear cell |
| PBS | Phosphate buffered saline |
| PCa | Prostate cancer |
| PCR | Polymerase chain reaction |
| PFA | Paraformaldehyde |
| Pfp/Rag$^{-/-}$ | Perforin and recombination activating gene 2 double knockout |
| PI3K | Phosphatidylinositol-4,5-bisphosphate 3-kinase |
| PI3KCA | Phosphatidylinositol 4,5-bisphosphate 3-kinase catalytic subunit alpha isoform |
| PSA | Prostate-specific antigen |
| PSMA | Prostate-specific membrane antigen |
| qRT-PCR | Quantitative Real-time PCR |
| RAI2: | Retinoic acid-induced protein 2 |
| rcf | Relative centrifugal force |
| RPLP0 | Ribosomal protein lateral stalk subunit P0 |
| rpm | Revolutions per minute |
| RPMI | Rosewell Park Memorial Institute |
| RTK | receptor tyrosine kinase |
| SDS | Dimethyl sulfoxide |
| SDS | Sodium dodecyl sulfate |
| SDS-PAGE | Sodium dodecyl sulfate polyacrylamide gel electrophoresis |
| sec | Second |
| SERD | Selective oestrogen receptor degrader |
| SERM | Selective oestrogen receptor modulator |
| SGK-1 | Serine/threonine-protein kinase |
| shRNA | Short hairpin ribonucleic acid |
| STK | serine/threonine kinase |
| TAM | Tamoxifen |
| TEMED | *N*,*N*,*N*′,*N*′-Tetramethylethane-1,2-diamine |
| UKE | University Medical Center Hamburg-Eppendorf |
| UV | Ultraviolet |
| V | Volt |
| VCaP | Vertebral-Cancer of the Prostate |

# List of tables

Tab. 2-1 List of Laboratory equipment used in this study ..... 21
Tab. 2-2 List of microscopes used ..... 23
Tab. 2-3 List of softwares used for data acquisition, analysis and image editing ..... 23
Tab. 2-4 List of consumables used ..... 24
Tab. 2-5 List of chemicals and reagents used ..... 25
Tab. 2-6 Composition of buffer and media ..... 27
Tab. 2-7 Commercial Kits used ..... 28
Tab. 2-8 Hormoones, inhibitors and cytostatics used in this study ..... 29
Tab. 2-9 List of vector and expression plasmids used ..... 29
Tab. 2-10 Oligonucleotides used for quantitative Real-Time -PCR ..... 30
Tab. 2-11 Oligonucleotides used for DNA amplification by PCR ..... 31
Tab. 2-12 Primary antibodies used for Western blot and Immunofluorescence staining ..... 31
Tab. 2-13 Fluorophore-conjugated primary antibodies ..... 32
Tab. 2-14 Fluorophore- and HRP-conjugated secondary antibodies ..... 32
Tab. 2-15 Human cell lines ..... 32
Tab. 2-16 PCR components for a 25 µL reaction mixture ..... 41
Tab. 2-17 Cycling program for qPCR ..... 43
Tab. 2-18 Components for preparation of stacking and separation gel ..... 44

# Register of illustrations

Fig. 1-1 Overview of the metastatic cascade. ....2
Fig. 1-2 Top cancer per country in men of all ages, estimated number of new cases in 2018.....3
Fig. 1-3 Zonal compartments of the prostate....4
Fig. 1-4 Top cancer per country, estimated age-standardized incidence rates (World) in 2018 in females of all ages.. ....6
Fig. 1-5 Schematic representation of the breast....7
Fig. 1-6 Activation of androgen receptor signalling. ....9
Fig. 1-7 Overview of resistance mechanisms to hormone therapy in PCa. ....14
Fig. 1-8 Preliminary analysis of RAI2 expression in BrCa and PCa cell lines....18
Fig. 3-1 *RAI2* mRNA expression in publicly available GEO-datasets. ....51
Fig. 3-2 Western blot analysis after shRNA-mediated knockdown (KD) of *RAI2* and *ERα* mRNA in BrCa-cells. ....52
Fig. 3-3 Western blot analysis after shRNA-mediated knockdown (KD) of RAI2 and AR mRNA in PCa-cell lines. ....53
Fig. 3-4 RAI2 and ERα protein expression after inhibition of oestrogen receptor activity. ....55
Fig. 3-5 RAI2 and AR protein expression after inhibition of androgen receptor activity. ....56
Fig. 3-6 Distribution of fluorescent labelled RAI2, AR and CtBP1 protein in PCa cell lines. ....57
Fig. 3-7 Validation of a LNCaP cell line with RAI2 knockout. ....58
Fig. 3-8 Gene expression analysis of *PSA*; *MME* and *SGK*-1 gene in LNCaP cells. ....59
Fig. 3-9 Western blot analysis of RAI2- modified cell lines used in this study. ....60
Fig. 3-10 Cell viability of RAI2 depleted MCF-7 cells after inhibition of the ER or the Akt/mTOR proliferation pathway....61
Fig. 3-11. Cell viability of RAI2 depleted PCa-cells after inhibition of the AR or the Akt/mTOR proliferation pathway and the cell cycle. ....62
Fig. 3-12 Cell viability of RAI2 overexpressing PC-3 cells after inhibition of the Akt/mTOR pathway and the cell cycle. ....63
Fig. 3-13 Colony formation of LNCaP cells after inhibition of proliferation controlling processes. ....65
Fig. 3-14 Colony formation of PC-3 cells overexpressing RAI2. ....66
Fig. 3-15 Colony formation of LNCaP cells with a RAI2 knockout after reintroduction of RAI2 protein expression. ....67
Fig. 3-16 Anchorage independent growth of RAI2 modified LNCaP and PC-3 prostate cancer cells. ....68
Fig. 3-17 Cell migration of RAI2 modified LNCaP and PC-3 prostate cancer cells. ....69
Fig. 3-18 Comparison of serine/threonine kinase activity in parental and RAI2-knockout KPL-1 cells, treated with 1 μM fulvestrant. ....70

Fig. 3-19 Comparison of serine/threonine kinase activity in parental and RAI2-knockout LNCaP cells, treated with 3 μM bicalutamide. ....71
Fig. 3-20 Kaplan Meyer survival analysis of pfp/rag2$^{-/-}$ mice injected with LNCaP RAI2-KO cells. ....72
Fig. 3-21 Detection of CTCs and DTCs in pfp/rag2$^{-/-}$ mice injected with parental or RAI2-KO LNCaP cells. ....73
Fig. 3-22 Metastatic spread of parental and RAI2-KO LNCaP cells to distant organs detected by *Alu*-PCR....74
Fig. 3-23 Methylation profile of RAI2 promotor detected by bisulfide sequencing (BSSQ) in PBMCs of five healthy donors.. ....75
Fig. 3-24 Classification of analysed genes and CTC samples from healthy donors (HD) and metastatic prostate cancer patients (PC)....76
Fig. 3-25 Classification of samples and genes by principle component analysis (PCA). ....77
Fig. 3-26 Pearson correlation.. ....78
Fig. 3-27 Correlation of *RAI2* mRNA expression in CTCs with clinical parameters of metastatic prostate cancer patients. ....79
Fig. 3-28 Kaplan Meyer estimation showing overall survival in months of metastatic prostate cancer patients based on RAI2 expression in CTCs and available follow up data. ....80
Fig. 6-1 Heat map visualising log2 transformed signal intensities of phosphorylated peptides after incubation with whole cell extracts from parental and RAI2-KO (K47 clone) KPL-1 breast cancer cells. ....101
Fig. 6-2 Heat map visualising log2 transformed signal intensities of phosphorylated peptides after incubation with whole cell extracts from parental and RAI2-KO LNCaP prostate cancer cells....102

# 1 Introduction

Cancer incidence rates have steadily increased during the last decade and has become the second leading cause of death worldwide after cardiovascular disease[1]. According to WHO estimations that include all cancers, ages and both sexes, the number of cancer incident cases of 18.1 million in 2018 will further increase to 29.5 million (+63.4 %) cases in 2040[2]. The increase in cancer burden is mainly explained by a growing and aging global population as well as other risk factors, such as tobacco smoking, urbanisation and the pollution that comes with it, obesity, dietary patterns and hereditary determinants[1,3]. Especially, increased wealth and greater access to high quality healthcare contributes to increased life span and thus to accumulation of mutations thereby cancer initiation[1]. Prostate and breast cancer are the leading causes for cancer incidences in men or women worldwide and the fifth leading and leading causes of cancer deaths respectively, showing the need for better disease management for both entities[2]. In spite of significant progress in understanding and treating primary cancers, the metastatic disease remains largely incurable and the least understood aspect of cancer biology, accounting for about 90% of cancer-associated deaths[4]. Therefore, the identification and functional characterisation of metastasis-associated genes is of paramount importance to improve early diagnosis and the generation of more efficient, targeted therapies for this late stage disease.

## 1.1 Fundamentals of cancer progression

A review article published by HANAHAN and WEINBERG in 2000, has comprehensively summarised the distinct and accumulative changes normal cells have to undergo to become malignant cells and to progress into lethal metastatic disease. Based on data from decades of cancer research, they have defined six hallmarks of cancer consisting of sustaining proliferative signalling, evading growth suppressors, resisting cell death, enabling replicative immortality, inducing angiogenesis and activating invasion and metastasis[5]. Additionally, genomic instability, leading to genetic mutations as well as the deregulation of cellular energetics and epigenetics emerged as pivotal features in the initiation and progression of cancer. Finally, the ability of tumours to promote inflammation and to communicate with the cellular microenvironment has been accepted to further nurture the tumorigenesis[6]. However, the capacity to metastasise is considered as the central hallmark of cancer, since metastasis is the leading cause of cancer-related deaths[7]. The establishment of metastases is preceded by a series of steps including local invasion of the primary tumour by the cancer cells prior to their intravasation into the tumour vasculature. Inside the blood system single circulating tumour cells (CTCs) or tumour cell clusters have to survive several natural obstacles,

including anoikis, shear forces, the immune system and oxidative stress[8]. Arrested in capillaries of distant sites, the tumour cells extravasate and move into the tissue of the target organs. Within the new environment disseminated tumour cells (DTCs) can survive in a dormant state for years before eventually growing into an overt metastasis, that requires most of the introduced hallmarks of cancer[8,9].

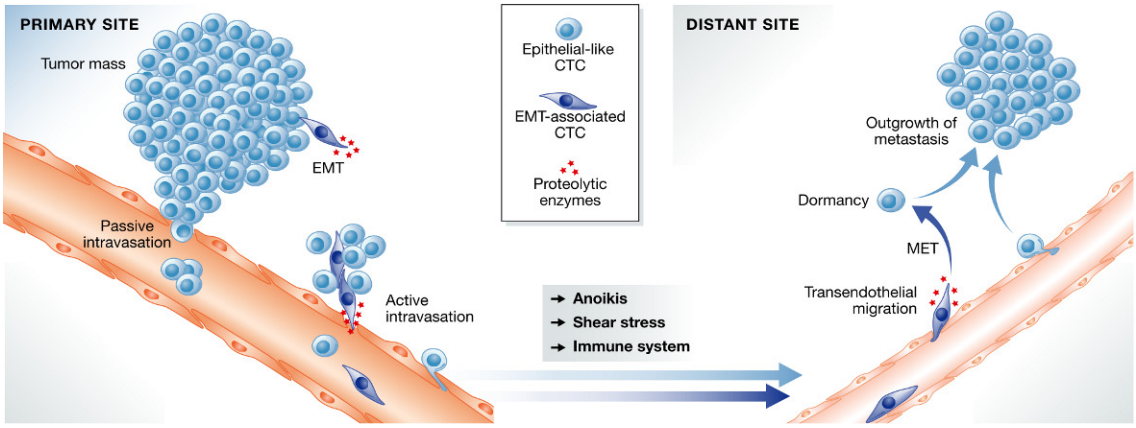


**Fig. 1-1** Overview of the metastatic cascade. The main steps of metastasis include invasion, passive or active intravasation of the tumour cells into the circulatory system, their extravasation into distant organs where they can remain in dormant state or outgrow into metastases. Figure taken from JOOSSE et al.[8]. EMT, epithelial-mesenchymal transition; MET, mesenchymal-epithelial transition, CTC, circulating tumour cell.

Guided by genetic abnormalities and a number of growth factors the epithelial-mesenchymal transition (EMT) is considered to be crucial for metastasis formation. During this transdifferentiation process, epithelial cells lose their cell to cell contact and detach from their neighbouring extracellular matrix, gaining a mesenchymal phenotype and the ability to invade, resist stress and disseminate[7]. After extravasation however, cancer cells have to undergo a reverse mesenchymal to epithelial transition (MET) to proliferate and form a bulk of secondary tumour mass[10]. Furthermore, it has been understood that the transition is a dynamic process with multiple stages between the epithelial and mesenchymal phenotype[11]. On the molecular level, epithelial cells as well as the intermediate phenotypes to a different extent are characterized by the expression of epithelial markers, such as E-cadherin, cytokeratin and EpCAM[12,13]. Our institute as well as other researchers make use of the expression of these molecules to enrich and detect CTCs from peripheral blood in the course of liquid biopsy, which is described in more detail in a following chapter.

## 1.2 Prostate Cancer: Epidemiology, anatomy, risk factors and disease management

Based on estimations of the GLOBOCAN database, prostate cancer was the most commonly diagnosed cancer among men in 2018 in 106 countries, dominating in Central and South America, Western and Northern Europe, and sub-Saharan Africa. In contrast, prostate cancer was estimated as the leading cause of cancer deaths, excluding non-melanoma skin cancer, in only 46 countries located mainly in sub-Saharan Africa and Latin America, showing geographic variations[14]. Of note across ethnicity, African-descent men are showing the highest prostate cancer risk, while the lowest is observed for Asians. This might be in part explained by existing ethnicity-specific differences in allele and genotype frequencies of candidate prostate cancer susceptibility genes[15,16]. In line with that, the highest estimated prostate cancer mortality rates in 2018 were found in countries, which are characterized by predominantly African-descent population, i.e. the Caribbean and Southern and Middle Africa, while the lowest rates were found in most parts of Asia but also North Africa[14].

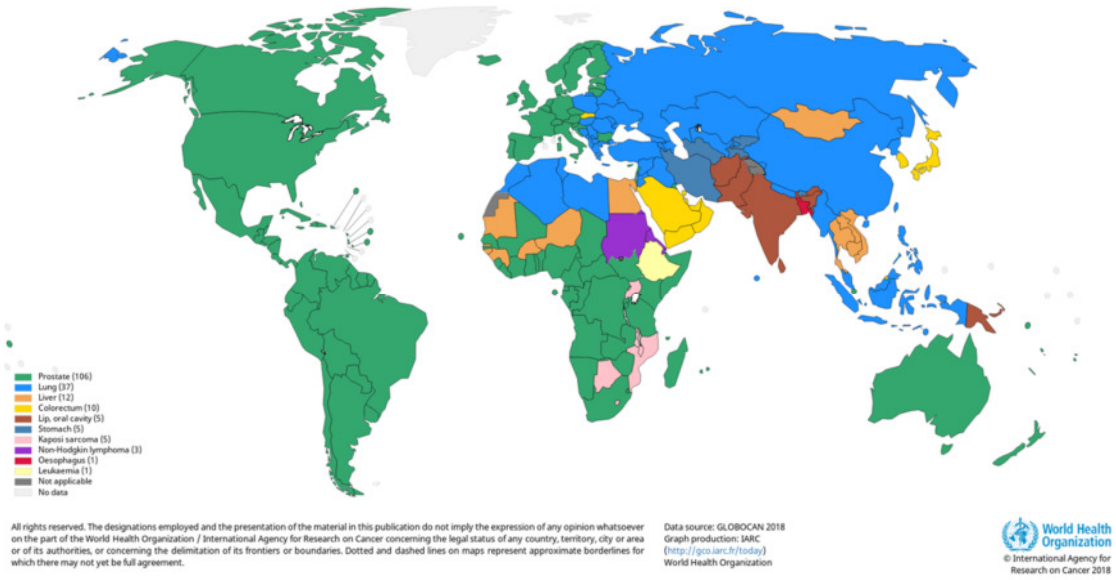


**Fig. 1-2** Top cancer per country in men of all ages, estimated number of new cases in 2018. Nonmelanoma skin cancer was excluded from calculation. Illustration was taken from GLOBOCAN 2018[17]. Top five cancer sites: prostate (green, 106 countries), lung (blue, 37 countries), liver (orange, 12 countries), colorectum (dark-yellow, 10 countries), lip oral cavity (brown, 5 countries).

In Germany, 57,370 men were diagnosed with prostate cancer, and approximately 14,417 deaths were attributed to this disease in 2016, according to the Robert Koch Institute. With a share of about 22.7%, prostate cancer remained the most frequent cancer in men and with 11.9% it was

the second leading cause of cancer-related deaths after lung cancer (23.5%). The median age of onset of the disease was 72 years[18].

The prostate is a walnut-shaped accessory gland of the male reproductive system. It is localized above the pelvic floor directly in front of the rectum surrounding the urethra below the bladder. In 1981, MCNEAL characterised the exocrine gland into four anatomic zones, each of which has a different share in the origin of prostate carcinoma. With high importance to further disease management, he outlined that 75% of cancer arises from the peripheral zone, while 20% and 5% of carcinomas develop within the transitional or central zone[19]. Although he considered the fourth anterior zone as not important for pathology, nowadays this zone is estimated to harbour 17% of all prostate cancer[19,20]. On the cellular level, prostate cancer is hypothesized to arise predominantly from luminal epithelial cells, which are the functional cells of the gland, that secrete the human prostate specific antigen (PSA), express the androgen receptor (AR) and are thus androgen responsive[21]. In search for genes increasing the susceptibility for prostate cancer, several studies identified aberrations in *BRCA2*, *BRCA1*, *CHEK*, *ATM*, *TP53* and *HOXB13* which were associated with inherited disease[22,23]. Moreover, PCa is characterized by large-scale genomic rearrangements and substantial copy number alterations including multiple chromosomes which frequently result in loss of tumour suppressor genes like *PTEN*, *NKX3.1*, *TP53* and *CDKN1B* and to oncogenic fusions, like *TMPRSS2-ERG*, which is detectable in 50 % of prostate tumours[24].

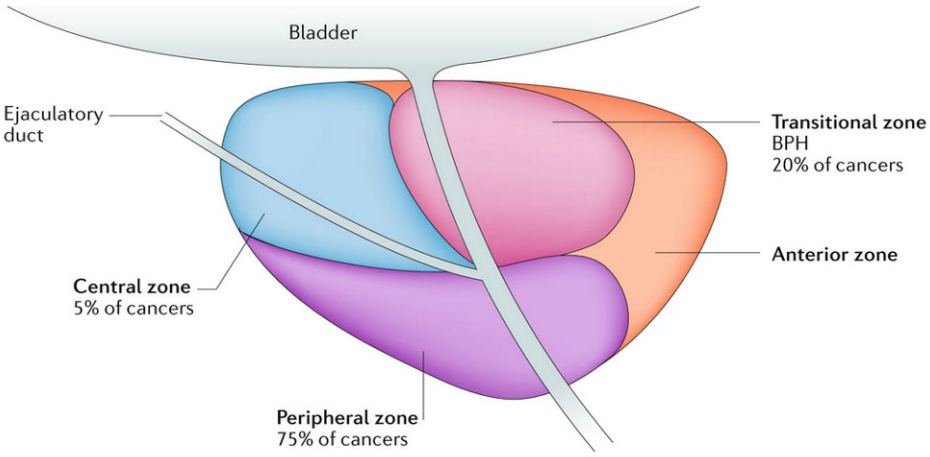


**Fig. 1-3** Zonal compartments of the prostate. Schematic illustration of four anatomic distinct zones of the prostate gland and their impact on prostate cancer development, as elucidated by the work of MCNEAL. Illustration was taken from SATHIANATHEN et al.[25].

Nontargeted transrectal ultrasound (TRUS)-guided biopsy is standard practice for the diagnosis of prostate cancer in men who show abnormalities of the gland during digital rectal examination and/or serum prostate-specific antigen (PSA) levels higher than 4 ng/mL. During this procedure prostate tissue is systemically removed with 12 punch cylinder under ultrasound guidance before

it is histologically examined and graded according to the Gleason scoring system and its latest modifications by EPSTEIN et al.[25,26]. As for many other cancers staging is largely based on the TNM-system, rating the size and extent of tumour (T), involvement of lymph nodes (N) and the presence of metastasis (M)[27]. The combination of clinical stage, Gleason score and the serum PSA level are used for risk stratification as well as for prediction of pathological stage or biochemical recurrence after surgery, playing a pivotal role for treatment decisions/ disease management[25]. Current treatment for clinically localized prostate carcinoma involves either radical prostatectomy or radiotherapy with curative intentions, although in men with low risk disease active surveillance is accepted, which includes regular monitoring for disease progression[28,29].

Since almost all prostate cancers begin in an androgen-dependent state and the AR influences the tumour growth mainly throughout the disease, standard care of the advanced, metastatic PCa is based on targeted drugs against the androgen receptor (AR) signalling pathway[29,30,31]. After initial tumour regression and the decline of the androgen receptor regulated protein PSA measured in the patient's serum, tumour cells acquire resistance to hormone therapy and progress to castration resistant prostate cancer (CRPC)[28]. Therapy options for this lethal phenotype are aimed to prolong overall survival and include treatment with either the androgen synthesis inhibitor abiraterone, the second-generation anti-androgen enzalutamide, the taxane based chemotherapeutic drug docetaxel or radiotherapy in case of osseous metastasis[32].

## 1.3 Breast cancer: Epidemiology, anatomy, risk factors and disease management

Breast cancer is the most prevalent cancer among women worldwide. In 2018, approximately every 18 seconds a woman was newly diagnosed with breast cancer, accounting 2.1 million new cases in total. With estimated 626,679 deaths breast cancer was furthermore the leading cause of cancer-related deaths in women[33]. Worldwide, the incidence correlated with the country's income and is highest in North America, Australia, New Zealand and northern and western Europe. The access and the utilisation of mammography for diagnosis of breast cancer is seen as one justification for this observation. Furthermore, in high-income countries, breast cancer is usually diagnosed at an early stage, while in low and middle-income countries the cancer is commonly detected at a late stage, which is associated with poor prognosis and thus with higher mortality in countries such as those in sub-Saharan Africa and developing Asian countries[34–36].

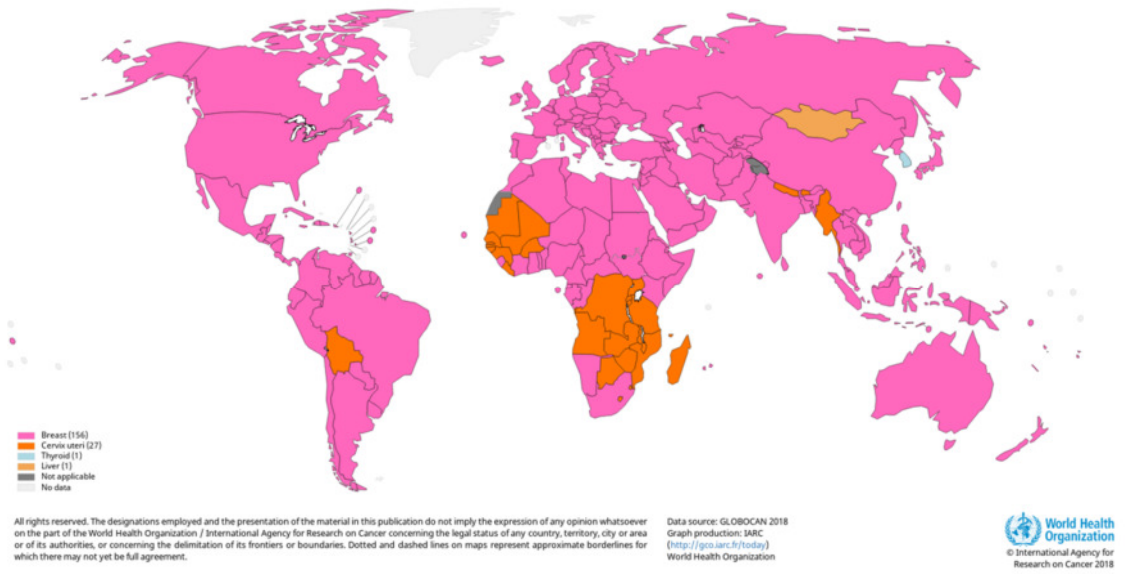


**Fig. 1-4** Top cancer per country, estimated age-standardized incidence rates (World) in 2018 in females of all ages. Taken from GLOBOCAN 2018[32]. Pink, breast cancer: 156 countries; orange, cervix uteri: 27 countries; light blue, thyroid: one country; yellow, liver: one country; grey not applicable; white, no data.

In Germany, breast cancer was newly diagnosed in 68,950 women in 2016 and led to 18,570 deaths in the same year. With either 29.5% or 17.6%, breast cancer represents the most frequent tumour side of all new cancer diseases and the leading cause of cancer-related deaths in Germany. Based on current incidence rates, about one in eight women will develop breast cancer during their lifetime. However, with the introduction of the mammography screening in 2005 fewer women suffer from advanced tumours than before[18].

In general, breast tissue consists of lobules, which are glands necessary for milk production, ducts that connect the lobules to the nipple, connective tissue as well as fatty- and lymphatic tissue[35]. All breast cancer arises from the terminal duct lobular units[37]. There are 21 histologically distinct breast cancers, while the most common histological subtypes include the invasive ductal and lobular carcinomas and their pre-invasive counterparts ductal and lobular carcinoma in situ, respectively[35,37]. On the molecular level breast cancer is a heterogeneous disease, which allows in combination with histological features the classification into five different clinical intrinsic subtypes. The majority of tumours (~70%) are oestrogen receptor (ER) and progesterone receptor (PR) positive, but negative for the human epidermal growth receptor 2 (HER2) and are grouped into the luminal A-like subtype. Similarly, hormone receptor expression is observed in the luminal B-like subtype, even though to a lower extent than the luminal A-like type. Additionally, this subtype is further divided according to the HER2 status into a negative or positive group. The fourth subtype is non-luminal and mainly characterised by an enrichment of HER2 and a negative hormone receptor status. Tumours that neither express ER, PR nor HER2 are classified as triple negative

breast cancers (TNBC)[37]. Further features of the surrogate intrinsic subtypes that are significant for disease management are depicted in figure 1.3.

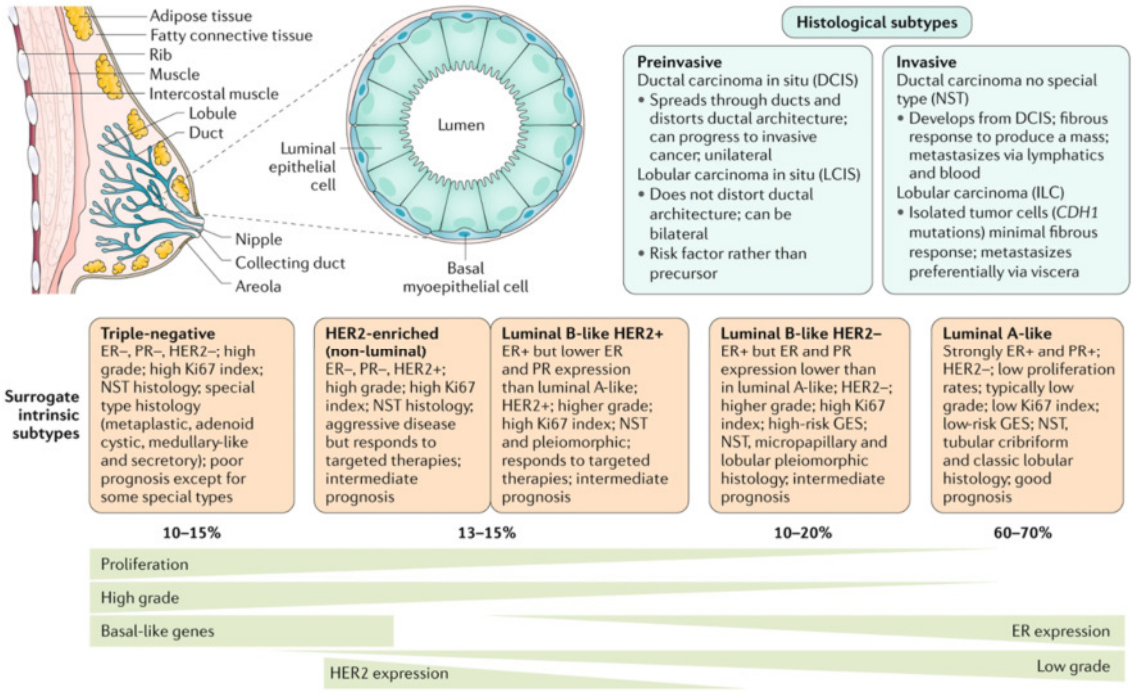


**Fig. 1-5** Schematic representation of the breast, showing the structure of the terminal duct lobular units, the functional units of the collecting duct. Histological most frequent breast cancer subtypes are described on the top right. Besides histological features, the expression of key proteins such as the oestrogen receptor (ER), progesterone receptor (PR), human epidermal growth receptor 2 (HER2) and the proliferation marker are assessed for classification of five surrogate intrinsic subtypes, that are decisive for disease management. The percentage of the respective subtype in breast cancer, as well as other characteristics like proliferation, grade, the expression of ER, HER2 or basal like genes are aligned with the subtype boxes. Picture was taken and modified from HARBECK et al.[37].

Several risk factors for breast cancer have been identified, among others increasing age, race, breast characteristics, menarche history and reproductive patterns as well as hormone use, diet, physical activity or the consumption of tobacco and alcohol[35]. About 5-10% of breast cancers are inherited and approximately 25% of hereditary cases are caused by mutations in one of the highly penetrant genes *BRCA1*, *BRCA2*, *PTEN*, *TP53*, *CDH1* and *STK11*, which are responsible for up to 90% risk to develop breast cancer over the course of a lifetime[38,39]. Additionally, a twofold increase in risk is observed due to mutations in the genes *CHEK2*, *BRIP1*, *ATM* and *PALB2*, which furthermore account for 2%-3% of cases[39]. Testing for mutations is currently recommended for women with personal and/or familial breast cancer history. Besides familial predispositions, participation in the national mammography screening programme is recommended for every woman between 50 to 69 of age to enable early detection of symptom free disease[40]. The x-ray examination is the only method with proven reduction of breast cancer mortality[41,42]. In the event

of abnormal findings by means of mammography or other imaging techniques, histological clarification is carried out by punch biopsy, vacuum biopsy and, in exceptional cases by open excision biopsy[40]. Breast cancer is curable in 70-80% of patients with non-metastatic, early-stage disease, while advanced breast cancer with metastases in distinct organs is not curable under the current available treatment options[37]. In general, the management of breast cancer is multidisciplinary and includes loco-regional therapy, such as surgery or radiation as well as systemic therapy. The choice of systemic therapy depends on the molecular features of the respective intrinsic subtype and includes either treatment with targeted approaches against the HER2 receptor, chemotherapy, bone stabilizing agents, poly (ADP-ribose) polymerase inhibitors for BRCA mutations carriers and hormone therapy for the hormone receptor positive disease[37]. Since the oestrogen receptor ER is the main driver of the majority of breast cancers, the most common hormone therapy for breast cancer works by blocking the interaction of hormones with their specific receptor or by decreasing the body's production of hormones[37].

## 1.4 Hormone signalling/ Steroid receptor signalling pathway

Even though breast and prostate cancer develop from organs of different anatomy and physiological functions, both organs need the sex steroid hormones oestrogen or androgen not only for their development, but also for the rise and progression of their hormone-dependent cancers[43]. The steroids act as ligands to their respective receptors, the oestrogen receptors-α (ERα) and ERβ or the androgen receptor (AR). Both steroid receptors are nuclear transcription factors and members of the nuclear receptor superfamily that drive specific gene expression programmes orchestrating a plethora of physiological functions, including cell cycle progression and proliferation[44]. The structure of the steroid receptors is divided into four functionally separate domains: an amino-terminal domain, harbouring the N-terminal ligand-independent activation functional domain (AF-1), a DNA binding domain (DBD) and a flexible hinge region, connecting the DBD domain with the carboxy-terminal ligand-binding domain (LBD), including the second transcriptional activation domain AF-2[45,46]. Since the biochemical mechanisms by which the steroid receptors carry out their function are similar and this thesis is mainly based on prostate cancer progression, the underlying mechanisms are illustrated in this section using the androgen receptor. The majority of the androgen testosterone is released by the testes into the peripheral blood stream, where it circulates mostly bound to sex hormone-binding globulin (SHBG) and albumin[47–49]. It is suggested that only free testosterone is able to enter the prostate cells by passive diffusion, where it is converted to dihydrotestosterone (DHT) by the enzyme 5α-reductase (SRD5A2)[49,50]. Although testosterone and DHT both act as agonist on the AR, DHT is the main androgen found in the nucleus of prostatic cells, where it stimulates the AR target genes ten-times

more potent than testosterone[51]. In the unbound state the androgen receptor is located in the cytoplasm in a complex with heat shock proteins (HSP) and other chaperon proteins[52]. Ligand binding induces a conformational change in the AR that not only leads to dissociation from HSP-proteins and receptor phosphorylation but also to an expose of AF-2 which mediates the receptor homodimerization and stabilization of the ligand within the binding pocket[53,54]. After translocation into the nucleus via the bipartite nuclear localization signal (NLS) within the hinge region, the AR binds to specific androgen response elements (AREs) in the promoter region of target genes. Upon DNA binding, the steroid receptor recruits coregulators, general and specific TFs as well as the RNA polymerase II for a regulated transcription of genes, leading to cell growth, survival and the synthesis of PSA[54,55].

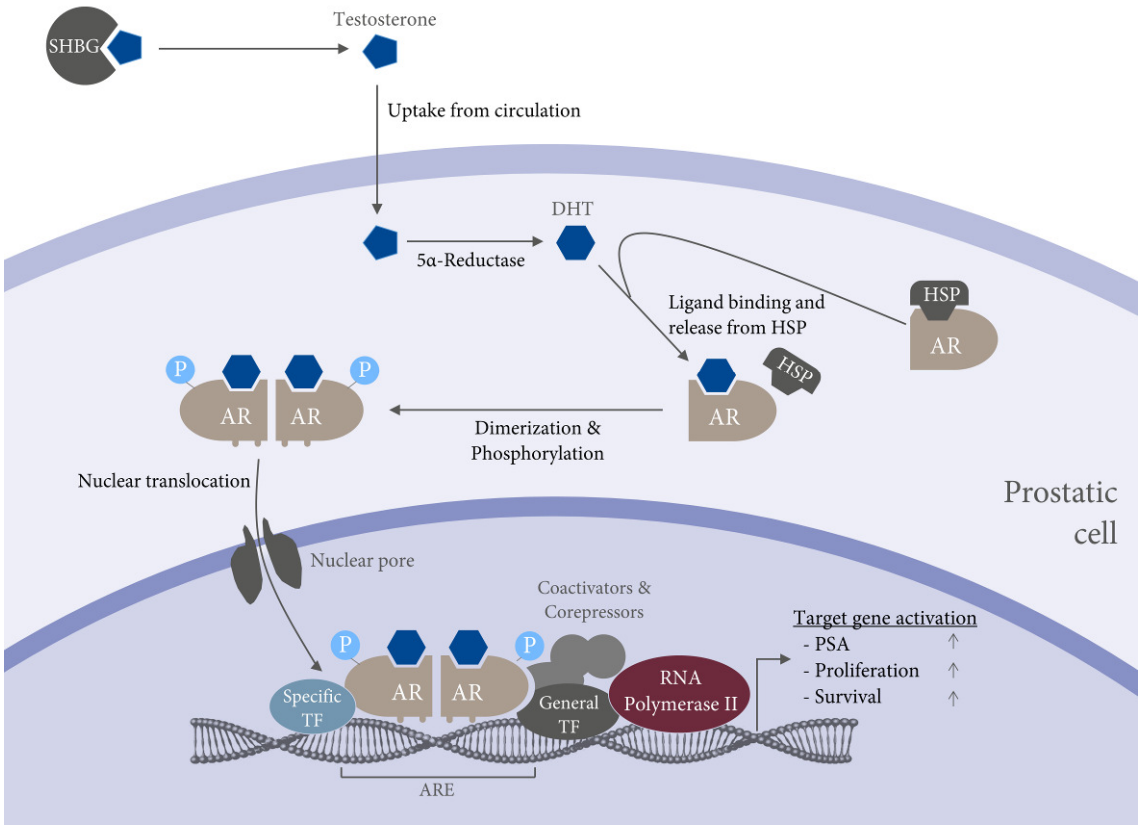


**Fig. 1-6** Activation of androgen receptor signalling. Unbound to SHBG, testosterone is able to enter prostatic cells where it is converted to dihydrotestosterone (DHT) by the 5α-reductase. Binding of DHT to the AR leads to dissociation from (HSP) and phosphorylation of the receptor. After dimerization the receptor binds to androgen response elements (ARE) in the promoter region of target genes and recruits TF, coregulators and the RNA polymerase for their transcription. The target gene activation leads to growth, survival and PSA secretion. Figure is taken and modified in collaboration with Christoph Raschdorf from FELDMAN & FELDMAN[56]. SHBG, sex hormone binding protein; P, phosphate; TF, transcription factor; PSA, prostate-specific antigen.

Depending on whether the recruited coregulators have an enhancing or reducing effect on the transactivation of steroid receptors, these are defined as coactivators or corepressors. By displaying a diverse array of functions, coregulators are able to influence the AR-mediated transcription either through chromatin remodelling, histone residue modifications, recruitment of TF, regulation of the proteosomal protein degradation or stabilization of the AR, just to name a few[55]. Thereby direct protein-protein interactions take place via LXXLL motifs of the coregulators and the AF-2 region of the nuclear receptors LBD[57,58]. Furthermore, the AR-LBD shows an additional unique binding ability to FXXLF motifs[59]. The steroid nuclear receptors AR and ER guide cyto-differentiation and homeostasis in benign epithelial cells, the change of their behaviour however is a major event in tumorigenesis, as receptors become primary drivers of malignant neoplastic cells[60,61]. Thus, a lot of strategies have been developed to block the action of the AR and ER in prostate and breast cancer cells to improve patient's outcome[43]. Hormone therapies that become standard of care as well as resistance mechanisms involved into the maintenance of hormone receptor signalling are reviewed below.

## 1.5 Hormone therapy in prostate and breast cancer

Based on the success of first oophorectomies and the observation of local disappearance of mammary tumour growth, George Beatson was the first person to suggest surgical removal of ovaries to "control and overcome" breast cancer[62]. Similarly, Huggins and Hodges have shown that reducing serum androgen levels by orchiectomy or exogenous administration of oestrogen led to regression of prostate tumours and palliation of symptoms, which was awarded the Nobel prize in 1966[63,64]. With the discovery of ER and the AR as the key drivers of both cancer entities and the elucidation of steroid biosynthesis a large amount of therapeutic strategies were established to inhibit hormone synthesis or to block the receptor function[43].

In particular, the synthesis of testosterone is regulated by the hypothalamic-pituitary-gonadal axis. First the gonadotropin-releasing hormone (GnRH) is pulsatile released by the hypothalamus to stimulate the secretion of the luteinizing hormone (LH) from the anterior pituitary, which on the other hand activates the synthesis of testosterone from cholesterol in the testis. The pulsatile release of GnRH is mandatory for continued LH secretion, whereas persistent GnRH stimulation would lead to desensitization, which is the goal of the administration of long-acting GnRH agonist for androgen deprivation therapy (ADT). Serum testosterone concentrations are similarly effectively suppressed with GnRH analogues as after orchiectomy, but are associated with less morbidity and deaths, which is why they are used as the standard first-line treatment in men with advanced-stage prostate cancer[65,66]. A common addition to castration at disease progression is the use of antiandrogens in combination with androgen depletion approaches[66]. First-generation

antiandrogens compete with testosterone and DHT for binding with the AR-LBD pocket, thereby leading to conformational changes of the receptor and reversible inhibition of transcription[28,66]. This drug class includes steroidal agents like cyproterone acetate and non-steroidal substances, which were originally developed due to off-target effects and a partial agonist activity of the steroidal ones. After first FDA approval of the non-steroidal antiandrogen flutamide, the approval for nilutamide and bicalutamide followed[28]. Although the analysis of different trials performed in the 1980s have shown only a modest improved overall and cancer-specific survival of patients with advanced prostate cancer after combination of medical or surgical castration with either nilutamide or flutamide, a significant survival benefit was shown for the combination of a GnRH agonist with bicalutamide compared with GnRH agonist alone. Furthermore, treatment with nilutamide or flutamide was associated with adverse effects and quality of life, while bicalutamide did not reduce the tolerability in patients[66–68]. The improved safety profile and an ease of daily use made bicalutamide to the most commonly prescribed antiandrogen[28]. However, most men with advanced disease develop resistance to first line AR inhibition and progress to a lethal castration resistant PCa[69]. The cytostatic drug docetaxel was the only treatment for CRPC approved by European and American health authorities that showed a survival benefit, until better understanding of the resistance mechanisms against hormone therapy led to development of new AR-directed therapies[70,71]. The therapeutic landscape has been enriched with the second-generation antiandrogen enzalutamide, which not only binds the androgen receptor with an eight-time higher affinity than bicalutamide, but also reduced its translocation into the nucleus and inhibits the recruitment of coactivators[72]. Additionally, abiraterone acetate has been synthesized to inhibit CYP17A, a key enzyme of androgenic-biosynthesis, to deplete the synthesis of androgens through the adrenal route that have not been addressed by GnRH nor orchiectomy, resulting in remaining testosterone and DHT levels (25% and 10% of pre-treatment level) even after 3 months of castration[73]. Abiraterone acetate and enzalutamide have been shown to improve survival and have been approved by the FDA for the treatment of CRPC in 2011 and 2012[74,75]. Based on the ARCHES trail, enzalutamide was furthermore approved on December 16$^{th}$ 2019 for patients with metastatic castration sensitive prostate cancer (mCSPC) According to the agency's recommendations CRPC and mCSPC patients should receive enzalutamide in combination with a GnRH analogue concurrently or should have had bilateral orchiectomy[75]. Despite life-prolonging effects of both agents, patients develop new resistances tied to reactivation of androgen synthesis and receptor signalling[76].

In premenopausal women, the major oestrogen 17β-estradiol (E2) is mainly produced in the ovaries from cholesterol by series enzymatic reactions which eventually lead to aromatization of androstenedione to estrone and conversion to E2. The production is controlled similarly to testos-

terone synthesis by hypothalamic-gonadal axis, since synthesis shares a common pathway[43,77]. Released E2 functions as a circulating hormone that acts on distal target tissues. In menopausal women, however, the production of E2 and other types of oestrogen takes place in extra-gonadal sites, including the fatty tissue, osteoclasts and chondrocytes of the bone, vessels and brain through aromatization of circulating testosterone. In these sites' oestrogen acts locally as a paracrine or even intracrine factor[78]. Besides the capability of E2 to activate both oestrogen receptor types ERα and ERβ, E2 action in breast cancer is mainly mediated by ERα, which is predominantly expressed in breast tumours and therefore regarded as the most suitable target for hormonal therapy, which was shown to be effective in the adjuvant setting after surgery to minimize the risk of relapse, and also in patients with metastatic disease to delay the disease progression[79,80]. The hormonal therapy of ER positive breast cancer is dictated by three main therapeutic modalities, in particular the selective ER modulators (SERMs), the selective ER down-regulators (SERDs) and aromatase inhibitors (AIs). Furthermore, combination of either AI with mTOR inhibitor or CDK4/CDK6 inhibitors as well as combined treatment with SERDs and CDK4/CDK6 are complementing the hormone therapy landscape[77,81]. One prominent SERMs agent is the antiestrogen tamoxifen which antagonizes ER by competing with E2 for binding to LBD of ER and recruiting corepressors to promoter region of oestrogen-target genes and blocking their transcription in BrCa cells, while maintaining the activation in the bone[82,83]. However, oestrogen agonist effects of SERMs and cross-resistance between endocrine therapies with comparable mechanism of action have led to development of SERDs. As one representative of the SERDs, fulvestrant was developed to act as a pure ER antagonist. With a binding affinity of 89% of E2, fulvestrant is more potent in the competitive inhibition of E2 binding than tamoxifen, whose binding affinity is 2.5% that of E2. Additionally, fulvestrant-ER binding compromises receptor dimerization and nuclear translocation of the receptor. Moreover, any fulvestrant-ER complex that enters the nucleus is transcriptional inactive due to disabled AF1 and AF2 domains. Besides that, the complex is less stable than E2-or tamoxifen bound ER, leading to an accelerated degradation of the ER protein[84]. The main strategy of AIs is the deprivation of oestrogens by inhibiting the oestrogen biosynthesis, moreover to decrease the conversion of androgens to oestrogens by aromatase proteins. Meanwhile, third-generation AIs are widely used for postmenopausal women. The choice of the right hormone therapy is a factor of age, menopausal status, comorbidities and the toxicity profile of the drug[77]. Sequential use of the introduced agents, with different modes of action, enables extension of treatment within the generally well tolerated hormone therapeutic agents despite acquired resistances to previous hormone therapy. However, to further prolong the time before cytotoxic chemotherapy becomes unavoidable, understanding of the mechanisms of resistances are necessary to generate effective new agents[84]. Thus, based on the improved understanding, the above mentioned mTOR inhibitors and CDK4/6 inhibitors made it into clinical use as complementary inhibitors of ER action.

## 1.6 Mechanisms of resistance to hormone therapy

Even though, most hormone-dependent breast and prostate cancer tumour, initially respond to hormone therapy with tumour regression, most patients develop resistance and their tumours progress to a lethal disease. Nevertheless, in the majority of hormone-resistant cases, the relevant steroid receptor remains active and decisive for tumour proliferation and survival. So far, several mechanisms have been elucidated that contribute to preservation of receptor activity in breast and prostate cancer, showing similarities between both entities[44]. One mechanism to circumvent hormone ablation therapy is by increasing sensitivity to very low levels of steroid ligand. This is achieved on the one hand by receptor gene amplifications resulting in an increased AR or ER expression itself, which can be observed in 30%-52% of prostate- and around 2% of breast tumours that recurred under respective hormone therapy[85–87]. On the other hand, hypersensitivity to low androgens can be achieved by increased receptor stabilization and enhanced nuclear localization, as it was observed for AR in recurrent tumour cells or ER after mutations in the LBD leading to an enhanced ER-transcriptional activity[88,89]. Alternatively, tumour cells might have increased expression or activation of coregulators, resulting in the induction of transactivation of hormone receptors. In PCa and BrCa, amplifications of AR and ER coregulator genes *NCOA2* and *NCOA3* are associated with a higher risk of resistance to receptor antagonist. Likewise, overexpression of the hormone receptor pioneer transcription factor FOXA1 promotes resistance to ER/AR signalling impeding therapies[44]. Finally, the effect of hormone ablation therapies can be circumvented by intratumoural steroid biosynthesis[43]. Thus, weak adrenal androgens DHEA and androstenedione can be converted to testosterone and DHT in prostate, resulting in higher intraprostatic androgen levels than in serum of castrated men[90]. Comparable, levels of E2 are up to tenfold higher in breast cancer of postmenopausal women than in their serum, due to conversion of androgens to oestrogens by CYP19A1 aromatase in breast adipose tissue[91,92]. Other adaptation to low ligand environment prostate cancer cells are based on AR-mutations in the LBD that broaden specificity of the receptors, creating so-called promiscuous androgen receptor. As a result, other steroid hormones such as progestins and oestrogens but also anti-androgens bind to mutant receptors and act as agonists[56]. Mutations in the LBD of ER however, are moreover associated with constitutive activity of the mutant receptors, driving ER transcription in absence of a ligand[93]. In prostate cancer the androgen receptor splice variants (AR-V) AR-V3, -V4, -V7 and -V17 have been shown to be constitutively active and a potential explanation for the resistance to first and second-generation AR-targeted therapies. In particular, AR-V7 is the most clinically relevant variant as it is the only reproducibly detectable and the most abundant variant in clinical specimens[94,95].

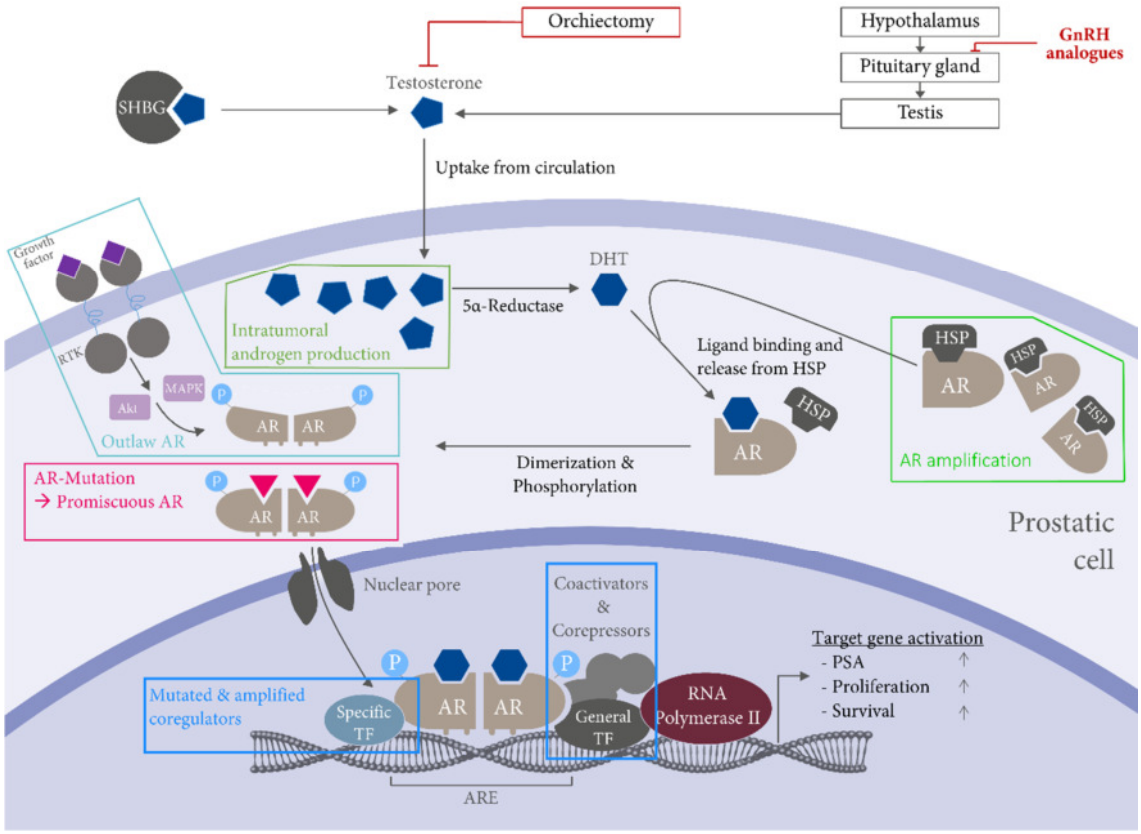


**Fig. 1-7** Overview of resistance mechanisms to hormone therapy in PCa. Approaches to decrease androgen receptor (AR) activity for instance through surgical or medical castration can be circumvented by intratumoural androgen production, AR amplification as well as AR mutations in the LBD of the receptor, leading to decrease in receptor specificity and activation by other steroids and antiandrogens (pink triangle). Growth factors can activate the kinase activity of receptor tyrosine kinases (RTK) such as HER2, and mediate through downstream serine/threonine kinases of the AKT or MAPK pathway phosphorylation and activation of the AR, creating an outlaw receptor which is active independent from a ligand. Transactivation of the AR can furthermore be influenced by mutations and increased expression of AR coregulators, like TF, coactivators and corepreressors. Figure is taken and modified in collaboration with Christoph Raschdorf from FELDMAN & FELDMAN[56]. GnRHSHBG, sex hormone binding protein; DHT, dihydrotestosterone; P, phosphate; TF, transcription factor; PSA, prostate-specific antigen.

A third mechanism leading to hormone resistance includes the upregulation of alternative signalling pathways as the HER2/MAPK pathway or the PI3K/AKT/mTOR pathway[56,96]. Thus, overexpression of the HER2 receptor, which has a tyrosine kinase activity, is associated with phosphorylation and activation of AR and ER in the absence of their steroidal ligands. Moreover, the phosphorylation of the androgen receptors has been shown to be mediated through HER downstream mitogen activated protein kinase pathway (MAPK), attaching importance to the serine threonine kinases of the MAPK kinase pathway in the creation of an outlaw receptor, leading to hormone-independent growth of prostate and breast cancer cells[56]. Furthermore, it has been demonstrated

that the serine/threonine kinases of the PI3K/AKT/mTOR pathways mediate properties of hormone-independent growth[56,96,97]. Activated AKT, for instance, has been shown to phosphorylate the AR at Serine (Ser) 213 and Ser791 in prostate cancer, while on the other hand the ER at Ser167 lead in both cases to activation of AR and ER in the absence of their steroidal ligands, promoting cell survival and growth[97,98]. To add more complexity to the resistance mechanisms, complementary or alternative signalling pathways may also contribute to the development of resistances independent from hormone receptor signalling. Hence, survival inhibiting conditions can be bypassed through expression of oncogenes like *BCL-2* gene, which is known for its apoptosis blocking function and that has been shown to be frequently expressed in CRPC, but not in normal secretory prostatic cells[99,100]. The presented selection of possible mechanisms that contribute to hormone therapy resistance (Fig. 1-7), shows not only the progress of research which has led to development of more efficient drugs but also the need to identify the resistance mechanisms of individual patients in order to tailor medical decisions based on their predicted response or risk of disease.

## 1.7 The concept of Liquid Biopsy for clinical management of cancer patients

Current therapeutic decision making for metastatic BrCa is based on the molecular features of the primary tumour[96]. The initial response of metastatic BrCa and PCa patients to treatment supports the hypothesis of several studies suggesting that the metastatic characteristics in regard to growth and response to treatment are determined by the primary seeding cancer cell[7,101]. The development of resistance to e.g. hormone deprivation therapies however is considered to be an evolutionary process that can involve multiple convergent events in different metastases. Thus, in the majority of cases, aberrations in AR signalling have been observed to occur after metastatic spread[101]. With increased appreciation of these changes and their effect on disease management, repeated biopsies have been suggested for the reassessment of advanced disease[96]. Due to invasiveness of the procedure and difficulties in the assessment of metastatic tissue, rebiopsies are not routine practice in most hospitals[101]. To overcome these limitations of tissue biopsy, liquid biopsy is as a promising alternative or additional approach that relies on a small amount of patients' blood that can be drawn easily and repeated frequently[102,103]. It is capable to improve therapeutic strategies in cancer patients as a powerful and reliable minimal invasive clinical tool for individual molecular profiling of patients in real time. The liquid biopsy approach includes the analysis of CTCs, circulating tumour DNA (ctDNA) and other components shed from the primary tumour or the metastatic site into the blood of the patient[104].

The presence of CTCs was first described in 1869 by Thomas Ashworth, who microscopically observed cells in the blood system of a deceased man with metastatic cancer that were identical with those of the cancer itself[105]. Today, CTCs can be isolated from blood samples with either marker dependent techniques or techniques that are based on distinct physical properties of the cells. Marker dependent approaches use for instance antibodies to target the epithelial cell adhesion molecule (EpCAM) or tumour-associated surface proteins, such as HER2 or EGFR, before isolating the cells from remaining components of the blood by positive selection[106,107]. To isolate the phenotypically very heterogeneous CTCs independent on their protein expression, techniques were developed separating the CTCs from the non-malignant blood cells based on their differences in size, density, deformability and electric charge[107]. The enriched CTCs are subsequently identified with immunocytologic assays by staining with antibodies against epithelial, mesenchymal, tissue or tumour-associated markers. Furthermore, molecular technologies such as quantitative reverse transcription PCR (qRT-PCR), RNA sequencing and in situ RNA hybridization can be used for the purpose of identification, but also for further CTC characterisation. In addition to transcriptome analysis, it is possible to study the genome and proteome of isolated CTCs or to use them for generation of xenograft model systems[107]

The clinical utility of CTC enumeration as prognostic marker has been shown in several studies including non-metastatic or metastatic breast and prostate cancer in which presence of CTC is associated with impaired clinical outcome[108–110]. Furthermore, CTCs enumeration and molecular characterisation can be used as predictive marker for overall survival, disease free survival/disease recurrence and therapy outcome. It has been suggested that CTC analysis could help to identify diverse intra- and interpatient molecular mechanisms of endocrine therapy resistance in ER-positive breast cancer patients[104]. The prognostic value of CTCs has also been shown for the metastatic prostate cancer, while correlation in CTC count and clinical outcome in the localized PCa still remains under investigation[107,110].

In breast cancer, heterogeneous ER expression has detected in CTCs of fulvestrant resistant, metastatic BrCa patients, suggesting insufficient dosage or evolved resistance mechanisms[111]. PAOLLILO et al. have furthermore demonstrated that it is possible to detect activating ER gene (ERS1) mutations on single CTC level, showing a great potential of CTC analysis to improve therapeutic decisions[112]. In addition, CTCs lack frequently ER expression in metastatic breast cancer patients with ER-positive primary tumours and show a considerable intra-patient heterogeneity, which may reflect a mechanism to escape endocrine therapy[113].

In prostate cancer, a well-recognized study, analysing the expression of the AR splice variant 7 (AR-V7) in CTCs has shown that positive AR-V7 expression in metastatic CRPC patients treated with enzalutamide or abiraterone is associated with resistance to treatment manifested by shorter

PSA progression-free survival (PFS), clinical or radiographic PFS, and overall survival[114]. A fundamental study on the AR-V7 expression has moreover shown that clinical outcomes of CRPC patients with AR-V7-positive CTCs are superior to taxane based chemotherapy than to enzalutamide or abiraterone therapy, while the results in AR-V7-negative men did not differ according to the type of treatment[115]. These results demonstrate how molecular characterisation of CTCs could contribute to the improvement of cancer disease management, beyond a mere CTC enumeration.

The molecular analysis of cell free ctDNA from patients' plasma is the second pillar of liquid biopsy and its clinical utility has so far been demonstrated by three FDA- approved cfDNA-based tests, which were either designed to detect *EGFR* mutations in lung cancer patients, *PIK3CA* mutations in advanced, hormone therapy resistant BrCa or to assess the methylation status of the *SEPT9* promoter in plasma cfDNA from patients undergoing screening for colorectal cancer (CRC). While the methylation status is assigned as an effective blood-based marker for CRC detection, the mutation analysis of the first two assays assist in decision-making on the administration of RTK inhibitors or the PI3K inhibitor alpelisib for treatment of the indicated cancer entities, emphasising the potential of liquid biopsy approaches[116,117]

## 1.8 Retinoic acid-induced protein 2

Loss of RAI2 expression in hormone-dependent breast tumours is a novel genetic determinant especially associated with early metastatic spread to the bone[118]. The human gene encoding for retinoic-acid induced protein 2 (RAI2) was first identified and characterized by Walpole in 1999 in search of genes that might play a role in X-chromosomal related diseases. The 2.5-kb transcripts of the *RAI2* gene that is located in in the Xp22.2 region were found in fetal tissue such as the heart, lung, brain and kidney and beyond that in the placenta, skeletal muscle, pancreas and retina of the adult organism. Due to a 94% homology with a murine retinoic acid induced gene that has been described as being involved into early embryonal development, the researches were suggesting a developmental role for *RAI2*[119,120].

The association of *RAI2* with cancer was first identified at the Institute of Tumour Biology (ITB) and described in a Cancer Discovery paper in 2015[118]. In particular, low RAI2 expression in primary tumour samples was identified to be significantly associated with the presence of DTC in the bone marrow of early-stage breast cancer patients, assigning a particular role of RAI2 for early dissemination. Moreover, analysis of published large breast cancer data sets has shown, that low RAI2 expression is an independent prognostic factor for poor overall survival and associated with less differentiated and more aggressive breast tumours. Furthermore, clinical correlation analysis

revealed a highly significant correlation of *RAI2* mRNA expression with the ERα status and the luminal differentiation. In concordance with these findings, RAI2 protein expression was most abundantly expressed in ERα-positive cell lines corresponding to the luminal subtype. Downregulation of RAI2 protein in those cells resulted in dedifferentiation characterized by a downregulation of ERα, FOXA1 and GATA3 along with increased invasiveness and activation of the AKT signalling[118]. These observations lead to the hypothesis that RAI2 expression is important to keep the integrity of luminal cells by maintaining the ER signalling and might have an impact on the progression to hormone-independent disease. Also, other researchers have previously reported that integration of viral mouse mammary tumour virus (MMTV) into the RAI2 gene locus is associated with the emergence of recurrent and hormone-independent breast tumours[121,122], emphasizing a particular role for RAI2 depletion in the progression from hormone-dependent to hormone-independent tumours. Besides, further data from our working group has shown a predominant RAI2 expression in hormone-dependent LNCaP and VCaP prostate cancer cell lines, compared to hormone-independent growing and metastatic PC-3 and DU145 cells. Together with an increased hormone response in VCaP cells after RAI2-depletion, these findings reinforce a particular role of RAI2 in hormone-dependent cancer.

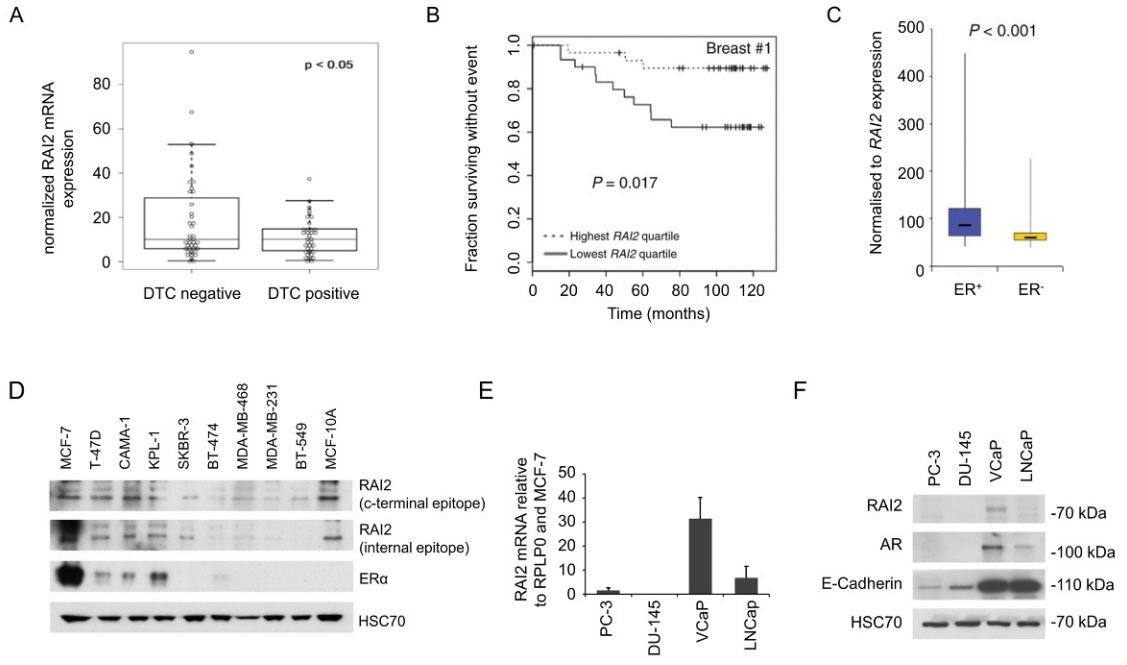


**Fig. 1-8** Preliminary analysis of RAI2 expression in breast cancer and prostate cancer cell lines. **A**, Low *RAI2* mRNA expression has been shown to be associated with positive DTC status in patients with early stage-breast cancer[118]. **B**, Furthermore, lower RAI2 expression has been associated with shortened survival in published breast cancer[118]. **C**, Additional analysis of published datasets revealed a significant correlation of *RAI2* mRNA expression with the ERα status of breast cancer tissue[118]. **D**, RAI2 expression evaluated in a panel of breast cancer cell lines indicated predominant expression of RAI2 in ERα protein expressing cell

lines [118].**E+F**, In four analysed prostate cancer cell lines, RAI2 mRNA (E) and protein expression was highest in cell lines expressing the AR protein and high levels of E-cadherin (F)[123].

Functional analysis showed molecular interaction between RAI2 and the C-terminal binding proteins (CtBP) 1 and 2 that is mediated through two ALDLS binding motives on the RAI2 protein[118]. CTBP proteins are described as oncogenic transcriptional coregulators that are overexpressed in many cancer types, where they are negatively regulating the expression of tumour repressor genes and activating genes that reduce cell death or promote proliferation, invasion and metastasis[124]. The 530 amino acid long RAI2 protein with a predicted mass of 57.2 kDa furthermore contains a nuclear localisation signal and has been shown to co-localize with CtBP proteins in nuclear speckles of so far unknown function[118]. Besides, recent work at the ITB revealed that RAI2 depletion is associated with chromosomal instability, assigning RAI2 a role as a guardian of genomic stability by maintaining DNA damage response[125].

Interestingly, the prognostic relevance of RAI2 expression is not restricted to breast cancer. This was also demonstrated in published datasets of other cancer entities, including two lung cancer patient cohorts as well as one colon and one ovarian patient cohort[118]. Furthermore, YAN et al. have recently shown that downregualtion of RAI2 expression in colorectal cancer (CRC) is mediated by promoter methylation. Furthermore, methylation of RAI2 promoter region is an independent prognostic factor in CRC, which is significantly associated with poor 5-year overall survival and relapse-free survival. In colorectal cancer cell lines, RAI2 moreover suppressed cell proliferation, migration and invasion. In addition, RAI2 was shown to inhibit AKT signalling and to induce cell apoptosis in CRC cells[126]. However, despite the data presented, the biological function of RAI2 and especially its implication for hormone-dependent malignancies remains largely unclear.

## 1.9 Objectives of this study

Based on previously published data on the tumour suppressor function of RAI2 and the association of the RAI2 protein with positive ER and AR receptor status in breast and prostate cancer cell lines, the work pursues four overall objectives. Besides the (1) analysis of the prognostic relevance of the RAI2 protein on prostate cancer and (2) the investigation of a functional relationship between RAI2 and the hormone receptors, (3) the influence of RAI2 on the aggressiveness of breast and prostate cancer cell lines should be assessed. Furthermore, a major goal of this study

was to (4) establish a liquid biopsy approach that allows detection and analysis of the RAI2 expression status of prostate tumours from tumour-derived material circulating in the patients' blood.

(1) In order to get a first impression of a possible prognostic relevance of RAI2 gene expression on prostate cancer progression, the RAI2 mRNA expression should first be evaluated in publicly available GEO datasets.

(2) To investigate the potential of a functional link between RAI2 and the growth promoting hormone receptor in breast and prostate cancer cells, the mutual effect of RAI2 and ER or AR depletion on each other's protein expression should be analysed using RNAi technology followed by Western blot analysis. Furthermore, the influence of approved ER and AR inhibitors on the expression of both proteins should be tested. Moreover, it should be clarified whether RAI2 expression has an impact on the regulation of the hormone response in prostate cancer cell lines by analysing the expression of AR-target genes following RAI2 depletion and by determining a possible interaction of RAI2 with the AR and the CtBP proteins.

(3) Cell lines with modified RAI2 expression should be established and used to analyse the influence of RAI2 on the progression of hormone-dependentant cancer cell lines. In line with the hallmarks of cancer, the ability of these cells to sustain proliferation, anchorage-independent growth and to induce cell migration should be examined *in vitro* and validated *in vivo* in case of significant effects.

(4) In the translational part of this study, a major aim was to establish a liquid biopsy method that would allow information on the RAI2 expression of prostate tumours to be obtained from patients' blood. More specifically, based on the results of YAN et al, one objective was to assess the promoter methylation status of RAI2 at the ctDNA level. In addition, another assay for the detection of RAI2 expression was to be established and tested on a small cohort of patients with metastatic PCa.

# 2 Material and Methods

## 2.1 Material

### 2.1.1 Laboratory equipment

Tab. 2-1 List of Laboratory equipment used in this study

| Device designation | Manufacturer | Company headquarters |
|---|---|---|
| AdnaMag-L | Quiagen | Hilden, DE |
| AdnaMag-S | Quiagen | Hilden, DE |
| Analytic balance BP610 | Sartorius | Göttingen, DE |
| Analytic balance BP6100 | Sartorius | Göttingen, DE |
| Analytic balance CP224S-OCE | Sartorius | Göttingen, DE |
| BioPhotometer | Eppendorf | Hamburg, DE |
| Centrifuge 5417R | Eppendorf | Hamburg, DE |
| Centrifuge 5417R | Eppendorf | Hamburg, DE |
| Centrifuge Heraeus Megafuge 8 | Thermo Fisher Scientific | Waltham, MA, US |
| Centrifuge Multifuge 3 S-R | Heraeus | Hanau, DE |
| Centrifuge Rotofix 32A | Hettich | Tuttlingen, DE |
| DNA Engine PTC-200 | MJ Research | Waltham, MA, US |
| Epson perfection V750 Pro | SEIKO Epson | Suwa, JP |
| Fluorometer Qubit 2.0 | Life Technologies | Carlsbad, CA, US |
| Gel chamber EasyPhor | Biozyme Scientific | Hessisch Oldendorf, DE |
| Gel documentation system GeneGenius | Syngene | Cambridge, UK |
| GloMax® Luminometer | Turner BioSystems | Sunnyvale, CA, US |
| Hoefer SE250 | GE Healthcare | Chalfont St Giles, GB |
| Hoefer™ Dual Gel Caster System | GE Healthcare | Chalfont St Giles, GB |
| Incubator Hera Cell 150 | Thermo Fisher Scientific | Waltham, MA, US |
| Laminar flow cabinet Herasafe™ KS 12 | Heraeus Kendro | Langenselbold, DE |
| Magnetic stirrer MR 3001 | Heidolph Instruments | Schwabach, DE |

| Device designation | Manufacturer | Company headquarters |
|---|---|---|
| Multipette M4 | Eppendorf | Hamburg, DE |
| Nanodrop ND100 spectrometer | PeqLab | Erlangen, DE |
| Neubauer improved counting chamber | Paul Marienfeld | Lauda-Königshofen, DE |
| PamStation®12 | PamGene | Hertogenbosch, NLD |
| Parsotix® System | Angle PLC | Surrey, UK |
| pH Meter inoLab™ | WTW™ | Heidelberg, DE |
| Platereader NanoQuant infinite M200Pro | Tecan | Männedorf, CH |
| Platform shaker Titramex 100 | VWR International | Radnor, PA, US |
| Power Pac Basic | Bio-Rad Laboratories | Hercules, CA, US |
| Power Pac HC | Bio-Rad Laboratories | Hercules, CA, US |
| Power supply Consort E143 | Sigma Aldrich | St-Louis, MI, US |
| Roller mixer Stuart SRT1 | Bibby Sterilin | Staffordshire, UK |
| Hoefer™ Mighty Small™ II Mini Vertical electrophoresis system | Thermo Fischer Scientific | Waltham, MA, US |
| Thermal Printer DPU | Eppendorf | Hamburg, DE |
| Thermocycler peqSTAR PeqLab 96 | PeqLab | Erlangen, DE |
| Thermocyler C1000 Touch CFX96 | Bio-Rad Laboratories | Hercules, CA, US |
| Thermomixer Comfort | Eppendorf | Hamburg, DE |
| Thermoshaker PHMT | Grant-Bio | Cambridge, UK |
| Tilt/Roll RS-TR 5 | Phoenix Instrument | Garbsen, DE |
| Transblot DS semidry transfer cell | Bio-Rad Laboratories | Hercules, CA, US |
| Ultrasound homogenisator | Hielscher Ultrasonics | Teltow, DE |
| Vortex Genie 2 | Scientific Industries | New York, NY, US |
| Water bath GFL 1002 | GFL | Burgwedel, DE |
| X-ray film processor Curix 60 | AGFA Health Care | Bonn, DE |

Tab. 2-2 List of microscopes used

| **Device designation** | **Manufacturer** | **Company headquarters** |
|---|---|---|
| Axioplan 2 imaging fluorescence microscope, AxioCam MRm with light source HXP 120 V | Carl Zeiss | Oberkochen, DE |
| Axiovert 200 inverse microscope, AxioCam MRc | Carl Zeiss | Oberkochen, DE |
| Axiovert 25 transmitted light microscope, AxioCam MRc | Carl Zeiss | Oberkochen, DE |
| DM IL inverted laboratory microscope | Leica | Wetzlar, DE |
| Primovert transmitted light microscope | Carl Zeiss | Oberkochen, DE |
| TCS SP5 confocal laser scanning microscope | Leica | Wetzlar, DE |

### 2.1.2 Software

Tab. 2-3 List of softwares used for data acquisition, analysis and image editing

| **TabSoftware designation** | **Manufacturer** | **Company headquarters** |
|---|---|---|
| AxioVision SE64 Rel. 4.9 | Carl Zeiss | Oberkochen, DE |
| BioNavigator | PamGene | HH's-Hertogenbosch, NLD |
| Bio-Rad CFXTM Manager 3.1 | Bio-Rad Laboratories | Hercules, CA, US |
| FinchTV 1.4.0 | Geospiza Inc. | Seattle, WA, US |
| Genesnap | Syngene | Cambridge, UK |
| GenEx Ver. 7.1.1.118 | MultiD Analyses | Göteborg, SWE |
| GloMax SIS V.1.10.0 | Turner BioSystems | Sunnyvale, CA, US |
| Graphpad 8.0.1 | Graphpad Software Inc. | San Diego, CA, DE |
| Image J 1.49v | Wayne Rasband, NIH | Bethesda, MD, US |
| Image StudioTM Lite Ver. 5.2 | LI-COR Biosciences | Lincoln, NE, US |
| Leica LAS AF | Leica | Wetzlar, DE |
| XcytoViewTM 1.0.98.0 | ChemoMetec | Lillerød, DNK |

### 2.1.3 Consumables

Tab. 2-4 List of consumables used

| **Consumable** | **Manufacturer** | **Company headquarters** |
|---|---|---|
| 6-well plate | Sarstedt | Nürnbrecht, DE |
| 96-well microtiter plate | Eppendorf | Hamburg, DE |
| Cell scraper | Biowisstec | Schaffhausen, CH |
| Culture slides 80426 | Ibidi | Planegg, DE |
| Falcon™ 4-well cell culture slides | Thermo Fisher Scientific | Waltham, MA, US |
| K2E (EDTA) Plus blood collection tube | BD Vacutainer | Wokingham, UK |
| Micro tube, 1.5 mL Safe Seal | Sarstedt | Nürnbrecht, DE |
| Micro tube, 2 mL Safe Seal | Sarstedt | Nürnbrecht, DE |
| Millex HV 0.45 µM PVDF filter | Merck Millipore | Darmstadt DE |
| Multiply®- µ Strip Pro 8-strip | Sarstedt | Nürnbrecht, DE |
| Pipettes tips | Sarstedt | Nürnbrecht, DE |
| Protran BA 85, pore size 0.45 µm | GE Healthcare | Chalfont St Giles, UK |
| Serological pipettes | Sarstedt | Nürnbrecht, DE |
| S-Monovette 7.5 mL K3E | Sarstedt | Nürnbrecht, DE |
| STK PamChip® Array | PamGene | Hertogenbosch, NLD |
| Super RX films | Fujifilm | Minato, JP |
| SuperFrost® Microscope slides | R. Langenbrinck | Emmendingen, DE |
| T175 cell culture flask | Sarstedt | Nürnbrecht, DE |
| T25 cell culture flask | Sarstedt | Nürnbrecht, DE |
| T75 cell culture flask | Sarstedt | Nürnbrecht, DE |
| Tubes 15 mL, PP, conical bottom | Greiner Bio-One | Frickenhausen, DE |
| Tubes 50 mL, PP, conical bottom | Greiner Bio-One | Frickenhausen, DE |

### 2.1.4 Chemicals and reagents

Tab. 2-5 List of chemicals and reagents used

| **Consumable** | **Manufacturer** | **Company headquarters** |
|---|---|---|
| Absolute ethanol | Merck | Darmstadt, DE |
| Acetic acid | J.T. Baker | Deventer,NL |
| Acrylamid (40%) | Carl Roth | Karlsruhe, DE |
| Agarose LE | Genaxxon Bioscience | Ulm, DE |
| Ammonium persulfate (APS) | AppliChem | Darmstadt, DE |
| Aqua | B. Braun Melsungen | Melsungen, DE |
| Bromophenol blue | Merck | Darmstadt, DE |
| BSA Fraction V | Biomol | Hamburg, DE |
| cOmplete™ mini proteinase inhibitor | Roche Diagnostics | Basel, CHE |
| DAPI | Carl Roth | Karlsruhe, DE |
| Difco™ Agar Noble | BD Bioscience | Franklin Lakes, NJ, US |
| DM2100 50bp Ladder | Smobio | Hsinchu City, TWN |
| DMEM medium | PAN Biotech | Aidenbach, DE |
| DMSO | Serva | Heidelberg, DE |
| dNTPs Set | Roche Diagnostics | Mannheim, DE |
| DTT | Sigma-Aldrich | St. Louis, MO, US |
| FCS | PAA Laboratories | Pasching, A |
| Ficoll-Paque Plus™ | Amersham Bioscience | Buckinghamshire |
| GeneRuler 1kb DNA Ladder | Thermo Fisher Scientific | Waltham, MA, US |
| Glycine | Carl Roth | Karlsruhe, DE |
| Halt™ Protease Inhibitor Cocktail, EDTA free | Thermo Fischer Scientific | Waltham, MA, US |
| Halt™ Phosphatase Inhibitor Cocktail | Thermo Fischer Scientific | Waltham, MA, US |
| Hydrochloric acid (HCl) | Carl Roth | Karlsruhe, DE |
| Hydrogen peroxide ($H_2O_2$) | Merck | Darmstadt, DE |
| Isopropanol | Carl Roth | Karlsruhe, DE |
| L-glutamine | PAA Laboratories | Pasching, A |

| Consumable | Manufacturer | Company headquarters |
|---|---|---|
| Lipofectamine 2000 Transfection Reagent | Thermo Fisher Scientific | Waltham, MA, US |
| Luminol | Sigma-Aldrich | St. Louis, Mo, US |
| Matrigel® Basement Membrane Matrix | Corning Inc. | Corning, NY, US |
| Methanol | J.T. Baker | Deventer, NL |
| Milk powder | Carl Roth | Karlsruhe, DE |
| Mowiol | Merck | Darmstadt, DE |
| M-PER Mammalian Extraction Buffer | Thermo Fischer Scientific | Waltham, MA, US |
| MTT | Sigma-Aldrich | St. Louis, MO, US |
| Normal Goat Serum | DAKO | Glostrup, DK |
| Nuclease free water | Qiagen | Hilden, DE |
| OptiMEM Medium | Gibco | Eggenstein, DE |
| Orange G | Waldeck | Münster, DE |
| Page Ruler Protein Ladder 10- 180 kDa | Thermo Fischer Scientific | Waltham, MA, US |
| p-Coumaric acid | Sigma-Aldrich | St. Louis, MO, US |
| PFA (Paraformaldehyde) | Merck | Darmstadt, DE |
| PhosSTop™ phosphatase inhibitor | Roche Diagnostics | Basel, CHE |
| Polybrene (hexadimethrine bromide) | Thermo Fischer Scientific | Waltham, MA, US |
| RPMI 1640 medium | PAN Biotech | Aidenbach, DE |
| SDS solution 20% (Sodium dodecyl sulfate) | AppliChem | Darmstadt, DE |
| Sodium chloride (NaCl) | Carl Roth | Karlsruhe, DE |
| Sodium deoxyycholate | Sigma-Aldrich | St. Louis, MO, US |
| Sodium hydroxide (NaOH) | Merck | Darmstadt, DE |
| TEMED (Tetramethylethylenediamine) | Thermo Fischer Scientific | Waltham, MA, US |
| Tris Acetate | Sigma-Aldrich | St. Louis, MO, US |
| Tris-EDTA | Sigma-Aldrich | St. Louis, MO, US |
| Trition X-100 | Sigma-Aldrich | St. Louis, MO, US |
| Trizma base | Sigma-Aldrich | St. Louis, MO, US |
| Trypan blue | Sigma-Aldrich | St. Louis, MO, US |

| Consumable | Manufacturer | Company headquarters |
|---|---|---|
| Trypsin-EDTA solution 0.25% (w/v) | Gibco | Eggenstein, DE |
| Tween-20 | Thermo Fischer Scientific | Waltham, MA, US |
| β-Mercaptoethanol | Merck | Darmstadt, DE |

### 2.1.5 Buffer and media

Tab. 2-6 Composition of buffer and media

| Description | Composition |
|---|---|
| 1x Laemmli buffer | 19.2 mM Glycine<br>0.01% SDS<br>2.5 mMTris-base<br>ad. dd$H_2O$ |
| 2x SDS lysis buffer | 10% Glycerol<br>2% SDS<br>62.5 mM Tris/HCL, pH 6.8<br>ad. dd$H_2O$ |
| 50x TAE buffer, pH 8.0 | 40 mM Tris-base<br>20 mM Acetic acid<br>50 mM EDTA, pH 8.0<br>ad. dd$H_2O$ |
| DMEM complete growth medium | 500 mL DMEM medium<br>10% FCS<br>1% L-Glutamine |
| DMEM hormone depleted (HD) | 500 mL DMEM medium (w/o phenol-red)<br>10% charcoal stripped FCS, one Shot™<br>1% L-Glutamine |
| ECL-Solution,<br>(Solution A and B, 1:1) | *Solution A*:<br>2.5 mM Luminol<br>0.4 mM Cumaric acid<br>100 mM Tris/HCL, pH8.5<br>ad. dd$H_2O$<br>*Solution B*:<br>0.018% $H_2O_2$<br>100 mM Tris/HCl, pH8.5<br>ad. dd$H_2O$ |
| RPMI complete growth medium | 500 mL RPMI medium<br>10% FCS<br>2 mM L-glutamine |

| Description | Composition |
|---|---|
| RPMI hormone depleted (HD) | 500 mL RPMI medium (w/o phenol-red)<br>10% charcoal stripped FCS, one Shot™<br>2 mM L-glutamine |
| TBS-T, pH 7.6 | 150 mM NaCl<br>50 mM Tris-base<br>0.05% Tween 20<br>ad. $ddH_2O$ |
| Transfer buffer | 39 mM Glycine<br>48 mM Tris-base<br>20% Methanol<br>0.0037% SDS<br>ad. $ddH_20$ |

### 2.1.6 Commercial Kits

Tab. 2-7 Commercial Kits used

| Kit | Manufacturer | Company headquarters |
|---|---|---|
| AdnaTest ProstateCancerDetect™ | Qiagen | Hilden, DE |
| AdnaTest ProstateCancerSelect™ | Qiagen | Hilden, DE |
| AmpliTaq Gold™ Polymerase and Buffer I | Thermo Fischer Scientific | Waltham, MA, US |
| First Strand cDNA Synthesis Kit | Thermo Fischer Scientific | Waltham, MA, US |
| GrandPerformance® Assay | TATAA | Götteborg, SW |
| Internal Control Calibrator | TATAA | Götteborg, SW |
| InviMag® Bisulfite Conversion KIT/IG | Invitek Molecular | Berlin, DE |
| Maxima SYBR Green/ROX qPCR Master Mix | Thermo Fisher Scientific | Waltham, MA, US |
| NucleoSpin Gel and PCR-Clean-up | Macherey-Nagel | Düren, DE |
| NucleoSpin RNA | Macherey-Nagel | Düren, DE |
| NucleoSpin RNA Plus | Macherey-Nagel | Düren, DE |
| NucleoSpin Tissue | Macherey-Nagel | Düren, DE |
| Pierce™ BCA Protein Assay | ThermoFischer Scientific | Waltham, MA, US |
| Probe GrandMaster® Mix | TATAA | Götteborg, SW |
| Sensiscript RT | Qiagen | Hilden, DE |

| Kit | Manufacturer | Company headquarters |
|---|---|---|
| SYBR® GrandMaster® Mix | TATAA | Götteborg, SW |
| ValidPrime® Assay | TATAA | Götteborg, SW |
| Venor GeM Classic Mycoplasma detection | Minerva Biolabs | Berlin, DE |

### 2.1.7 Hormones, Inhibitors and Cytostatics used in cell culture experiments

Tab. 2-8 Hormoones, inhibitors and cytostatics used in this study

| Reagent | Function | Manufacturer | Headquarter |
|---|---|---|---|
| Bicalutamide (CDX) | Androgen receptor antagonist, 1st generation | Selleckchem | Houston, TX, US |
| Dihydrotestosternone (DHT) | Testosterone, ligand for androgen receptor | Sigma Aldrich | St.Louis, MI, US |
| Docetaxel | Inhibition of mitotic cell division by stabilizing microtubule assembly | Fluka (Thermo Fisher Scientific) | Waltham, MA, US |
| Enzalutamide (MDV3100) | Androgen receptor antagonist, 2nd generation | Selleckchem | Houston, TX, US |
| Fulvestrant (ICI) | Selective oestrogen receptor degrader (SERD) | Sigma Aldrich | St.Louis, MI, US |
| MK2206 | Akt1/2/3 inhibitor | Selleckchem | Houston, TX, US |
| Paclitaxel | Inhibitor of mitotic spindle degradation, cytostatic | Cell signaling | Danver, MA, US |
| RAD-001 | mTOR inhibitor | Sigma Aldrich | St.Louis, MI, US |
| Tamoxifen (TAM) | Selective oestrogen receptor modulator (SERM) | Sigma Aldrich | St.Louis, MI, US |

### 2.1.8 Vectors and Expression plasmids

Tab. 2-9 List of vector and expression plasmids used

| Vector/Expression plasmids | Source |
|---|---|
| phCMV3-RAI2 OE | Dr. Stefan Werner, ITB, UKE |
| phCMV3-vector | Dr. Stefan Werner, ITB, UKE, Genlantis |

| Vector/Expression plasmids | Source |
|---|---|
| pLKO.1 non-target | Dr. Stefan Werner, ITB, UKE, Sigma Aldrich |
| pLKO.1-AR shRNA | Dr. Stefan Werner, ITB, UKE, Sigma Aldrich |
| pLKO.1-ER shRNA | Dr. Stefan Werner, ITB, UKE, Sigma Aldrich |
| pLKO.1-RAI2 shRNA1 | Dr. Stefan Werner, ITB, UKE, Sigma Aldrich |
| pMD2.G (envelope plasmid) | Addgene #12259, Cambridge, MA, US |
| psPAX2 (packaging plasmid) | Addgene #12259, Cambridge, MA, US |
| pSpCas9(BB)-2A-GFP-Guide | Addgene #48138, modified by Dr. Stefan Werner, ITB, UKE |

For the depletion of RAI2, ER or AR hormone receptor expression, lentiviral pLKO.1 shRNA vectors targeting either human RAI2 (shRNA1, TRCN0000139927), ER (TRCN0000003300) or AR (TRCN0000003718) as well as the scrambled non-targeting control shRNA were obtained from the RNAi Consortium (https://www.broadinstitute.org/rnai-consortium/rnai-consortium-shrna-library).

### 2.1.9 Oligonucleotides

Tab. 2-10 Oligonucleotides used for quantitative Real-Time -PCR

| Description | Target | Primer-Sequence | Annealling-Temperature [°C] |
|---|---|---|---|
| AR-f | AR | TTGGAGACTGCCAGGGAC | 59 |
| AR-r | AR | TCAGGGGCGAAGTAGAGC | 59 |
| ERBB2-f | ERBB2 | TGCCTGTCCCTACAACTACC | 59 |
| ERBB2-r | ERBB2 | CAGACCATAGACCACTCGG | 59 |
| ERBB3-f | ERBB3 | CAAGTTCCCTTGAGGAGCTG | 59 |
| ERBB3-r | ERBB3 | CATCTCGTTGCCGATTCATA | 59 |
| MME-f | MME | CCGAACCTACAAGGAGTCCA | 59 |
| MME-r | MME | GCAAATGCTGCTTCCACATA | 59 |
| PSA-f | PSA | GGCAGGTGCTTGTGGCCTCTC | 59 |
| PSA-r | PSA | CACCCGAGCAGGTGCTTTTGC | 59 |

| Description | Target | Primer-Sequence | Annealling-Temperature [°C] |
|---|---|---|---|
| RAI2-f | RAI2 | GGCGAAGTCAAGGCTGAAAA | 59 |
| RAI2-r | RAI2 | TCCCCTTGGCTGTTGATGTC | 59 |
| RPLPO-f | RPLPO | TGAGGTCCTCCTTGGTGAACA | 59 |
| RPLPO-r | RPLPO | CCCAGCTCTGGAGAAACTGC | 59 |
| SGK1-f | SGK-1 | TGCTGCTGAAATAGCCAGTG | 59 |
| SGK1-r | SGK-1 | CTCCTTGCAGAGTCCGAAGT | 59 |

Tab. 2-11 Oligonucleotides used for DNA amplification by PCR

| Description | Target | Primer-Sequence | Annealling-Temperature [°C] |
|---|---|---|---|
| BSSQ-RAI2-f | *RAI2* promotor | GGGTTTTTTGTTATGTTAGGTAT | 53 |
| BSSQ-RAI2-r | *RAI2* promotor | ATAAAATACCATTTCCCCACC | 53 |
| RAI2-seq-f | *RAI2* | CAAGTGGCATCAGAGAG | 52 |
| RAI2-seq-f | *RAI2* | TTTCTTGGAAAAAAGGTGGCCAGC | 52 |

The BSSQ-RAI2-f/r primer-sequences were taken from YAN et al.[126], while all other oligonucleotides were designed with the Primer Blaster Tool from NCBI (https://www.ncbi.nlm.nih.gov/tools/primer-blast/). The synthesis of oligonucleotides was carried out by Eurofins, Germany.

### 2.1.10 Antibodies

Tab. 2-12 Primary antibodies used for Western blot and Immunofluorescence staining

| Antigen | Host | Dilution | Specificity | Manufacturer | Cat. # |
|---|---|---|---|---|---|
| AR | rabbit | 1:7000 | monoclonal | Santa Cruz | sc-812 |
| CtBP1 | mouse | 1:2000 | monoclonal | BD Biosciences | 612042 |
| ERα | mouse | 1:7000 | monoclonal | Santa Cruz | 8002 |
| HSC70 | mouse | 1:2000000 | monoclonal | Santa Cruz | 7298 |
| RAI2 | rabbit | 1:2000 | monoclonal | Cell Signaling | 97857 |

Tab. 2-13 Fluorophore-conjugated primary antibodies

| Antigen | Clone | Conjugate | Host | Dilution | Manufacturer | Cat. # |
|---|---|---|---|---|---|---|
| EpCAM | 9C4 | AlexaFluor®-488 | mouse | 1:50 | Biolegend | 324210 |
| Pan-Cytokeratin | AE1/AE3 | AlexaFluor®-488 | mouse | 1:200 | eBioscience | 53-9003-82 |
| Murine CD45 | 30-F11 | APC | rat | 1:100 | BD Pharmingen | 559864 |

Tab. 2-14 Fluorophore- and HRP-conjugated secondary antibodies

| Reactivity | Conjugate | Host | Dilution | Manufacturer | Cat. # |
|---|---|---|---|---|---|
| mouse-IgG | HRP | horse | 1:2000 | Cell signaling | 7076 |
| mouse-IgG | IRDye®800CW | goat | 1:7500 | Li-Cor | 925-32210 |
| rabbit-IgG | HRP | mouse | 1:2000 | Cell signaling | 7074 |
| rabbit-IgG | IRDye®680RD | goat | 1:7500 | Li-Cor | 925-68071 |
| mouse-IgG | AlexaFluor-A488 | goat | 1:500 | ThermoFischer Scientific | A21121 |
| mouse-IgG | AlexaFluor-A546 | goat | 1:500 | ThermoFischer Scientific | A11030 |
| rabbit-IgG | AlexaFluor-A488 | goat | 1:500 | ThermoFischer Scientific | A11008 |
| rabbit-IgG | AlexaFluor-A546 | goat | 1:500 | ThermoFischer Scientific | A21428 |

### 2.1.11 Human cell lines

Tab. 2-15 Human cell lines

| Cell line | Tissue origin | Medium | Source |
|---|---|---|---|
| LNCaP | Prostate cancer, lymph node metastasis | RPMI | Institute of Anatomy and Experimental Morphology, UKE |
| VCaP | Prostate cancer, vertebral metastasis | DMEM | Institute of Anatomy and Experimental Morphology, UKE |
| PC-3 | Prostate cancer, Lumbar metastasis | RPMI | Institute of Anatomy and Experimental Morphology, UKE |
| DU-145 | Prostate cancer, Central nervous system metastasis | RPMI | Institute of Anatomy and Experimental Morphology, UKE |
| MCF-7 | Breast cancer, Pleura effusion | DMEM | ITB, UKE |
| KPL-1 | Breast carcinoma, Pleural effusion | DMEM | ITB, UKE |
| HEK 293T | Embryonic kidney cells | DMEM | ATCC, CRL-3216 |

| Cell line | Tissue origin | Medium | Source |
|---|---|---|---|
| Phoenix-ampho | Kidney, 2nd generation retrovirus producer cell | DMEM | Dr. Volker Assmann, ITB, UKE |
| VCaP RAI2-KO | Prostate cancer, vertebral metastasis, RAI2 gene knockout | DMEM | Alexandra Weglarz, ITB, UKE |
| MCF-7 RAI2-KO | Breast cancer, Pleura effusion, RAI2 gene knockout | DMEM | Stefan Werner, ITB, UKE |

### 2.1.12 Mouse material

Male immunosuppressed Pfp/Rag$^{-/-}$ double knockout mice were used from a breeding colony at University Medical Center Hamburg-Eppendorf. In collaboration with Prof. Tobias Lange's laboratory, animals were inspected daily and maintained under pathogen-free conditions in individually ventilated cages and fed with sterile standard food and water *ad libitum*. Blood was taken by cardiocentesis while animals were narcotized with lethal concentration of Ketamine/Rompun solution, whereas brain-, lung-, tumour tissue and bone marrow were isolated from mice after additional cervical dislocation. All procedures were performed with the approval of the local Animal Experiment Committee.

### 2.1.13 Patient material

A total of 36 late stage prostate cancer patients were recruited from June 2018 to September 2019 at the Center of Oncology, Medical Center Hamburg-Eppendorf in Germany in cooperation with Prof. Dr. Gunhild von Amsberg. A written informed consent was obtained from all patients before enrolment and blood was drawn in accordance with the Helsinki Declaration. The study was approved by the Ethics Committee Hamburg .Furthermore, blood from ten healthy donors was obtained as negative control from the Institute of Transfusion Medicine, Medical Center Hamburg-Eppendorf.

## 2.2 Cell culture methods

Before starting the cell culture work, media, PBS and Trypsin-EDTA were preheated to 37 °C in a water bath, containing 2 mL of AQUA-STABIL per 1 L water. In order to avoid contaminations and to ensure sterile working condition, all material and work surfaces were disinfected with Fermacidal D2® before and after work has been performed. All work steps that exposed the cells to

the outside environment were carried out under a vertical laminar flow cabinet using sterile, disposable tips and pipettes. The personal protective equipment included sterile gloves, laboratory coat and additionally a protective mask as soon as S2-conditions were met. To detect and prevent mycoplasma contaminations, cell lines were tested routinely every month and prior to cryopreservation with the PCR-based "Venor GeM Classic Mycoplasma Detection" Kit.

### 2.2.1 Resuscitation of frozen cells

For re-cultivation of cells, cryopreserved cells were transported at low temperature from -80 °C storage freezer and placed immediately into a 37 °C water bath for a maximum of 5 minutes. After thawing, cells were taken up in 5 mL of pre-warmed culture medium and centrifuged at 1200 rpm for 2 min. Supernatant, including residual DMSO, was removed and cells were resuspended with fresh culture media and transferred into a culture flask at high density.

### 2.2.2 Cultivation of cells

Cells were grown as monolayers according to standard conditions in their respective culture medium (see tab. 2-15) supplemented with 10% FBS and 2 mM L-Glutamine at 37 °C in a humidified atmosphere containing 10% $CO_2$ or 5% $CO_2$. After cells have reached a confluent state, they were sub cultivated to allow further growth. Therefore, growth media was removed and cells were washed with PBS before they were incubated at 37 °C with 1 mL Trypsin-EDTA, which cleaves peptides on the C-terminal side of lysine and arginine residues, resulting in detachment of adherent cells from culture surface. The enzymatic reaction was stopped with 5 mL growth media and dislodged cells were centrifuged for 2 min at 1200 rpm. After suspending the cells with fresh growth media they were fractionized into new culture flask according to table.

### 2.2.3 Cryopreservation of cell lines

For the cryopreservation of cell lines, cells which were optimally in log phase were detached from their culture surface (see 2.2.2) and centrifuged at 1200 rpm for 2 min. After resuspending the cell pellet in freezing media, composed of growth medium and 10% DMSO, 1 mL of cell suspension was aliquoted into cryogenic storage vials and stored for not longer than 5 min in 4 °C refrigerator. To achieve slow freezing of cells, vials were placed in an isolated box in a -80 °C freezer, where they were kept for short time storage. For long time storage vials were transferred to liquid nitrogen storage containers.

### 2.2.4 Cell number determination

The reproducibility and comparability of experiments as well as the majority of cell line manipulations depend on quantification of cells prior to use. For this purpose cells were harvested according to 2.2.2 and counted using a Neubauer chamber. Briefly, 10 µL cell suspension was mixed with 10 µL of 0.5% trypan blue solution, which enables distinguishing between viable and dead cells. From this dilution, 10 µL were applied near the edge of the coverslip of the assembled Neubauer chamber, allowing the suspension to enter the chamber by capillary flow. Viable, bright cells were counted in four large squares under an inverted phase microscope using x10 magnification. Cell number per mL was calculated as follows:

$$\left(\frac{Live\ cell\ number\ counted}{Number\ of\ large\ squares\ counted}\right) * 2 * 10^4 = Viable\ cells\ per\ milliliter$$

### 2.2.5 Cell line authentication

The authentication and determination of the purity of VCaP and LNCaP cell line was carried out on isolated DNA (see 2.4.1) by the company Multiplexion (Friedrichshafen, DE) based on Single Nucleotide Polymorphism (SNP) typing.

### 2.2.6 Retroviral gene transfer for overexpression of *RAI2* gene in cell lines

Retroviral vectors are used to enable the incorporation of a gene of interest into the genome of mitotically active host cell, resulting in a stable expression of the selected gene product. To establish human cell lines with constitutive expression of RAI2 wildtype protein, first retroviral particles had to be produced containing the pMXs-IP-RAI2 plasmid[118]. For this purpose the amphotropic retroviruses producing Phoenix–ampho cells were plated into T25 culture flask 24 h prior to transfection. At a confluency of 80% cells were transfected using Lipofectamine 2000®. More precisely, 20 µL Lipofectamine 2000® diluted in 250 µL Opti-MEM were added in a 1:1 ratio to 5 µg of the pMXs-IP-RAI2 plasmid diluted in 250 µL Opti-MEM. After 5 min of incubation at room temperature the DNA-lipid complex was added to the cells. On the next day, medium was replaced carefully in order not to detach any cells. Cell culture supernatant was collected in a 10 mL syringe after 48 h and filtrated through a Millex-HV 0.45 µM filter unit to purify viral particles from cells. The resulting filtrate, containing viral particles, was used directly or stored in 1 mL Aliquots at -80 °C. Same procedure was performed to produce viral particles packaging the empty pMXs-IP plasmid as a control. For the transduction of LNCaP and PC-3 cells, cells were exposed to media composed of 2 mL viral supernatant, 2 mL growth media and 5 µg/mL polybrene for

24h before it was replaced by fresh growth media. Besides a HA-tag for the target gene, the pMXs-IP plasmid encodes a puromycin resistance gene, that allows the selection of effectively transduced cells by adding 3 µg/mL puromycin to growth media for several passages. Stable expression of RAI2 protein was verified by Western blot, targeting RAI2 or the HA-protein with primary antibodies.

### 2.2.7 Lentiviral gene transfer for downregulation of gene expression in cell lines

The RNA interference technology of the cell is used to downregulate or knockdown selectively the expression of a target gene. Main components of this process are double-stranded short hairpin RNAs (shRNAs), which bind complementary to their target mRNA leading to its degradation and thus to the silencing of the gene. For the depletion of RAI2, ER or AR hormone receptor expression, lentiviral pLKO.1 shRNA vectors targeting either human RAI2 (shRNA1 TRCN0000139927), ER (TRCN0000003300) or AR (TRCN0000003718) were obtained from the RNAi Consortium. A pLKO.1 vector harbouring a scrambled non-targeting shRNA sequence served as a negative control. For lentiviral production, HEK293T cells were plated into T25-flask 24 h before transfection. At the late afternoon of the next day, a cocktail of 5 µg pLKO.1 lentiviral vector, 3.75 µg psPAX2 packaging plasmid, 1.25 µg pMD2.G envelope plasmid, diluted in 500 µL Opti-MEM and 20 µL Lipofectamine 2000® was prepared. After 5 min of incubation, it was subjected to cell culture medium and remained for 12-15 h on the cells before it was replaced with fresh growth media. Two days later supernatant was collected, filtered through a Millex-HV 0.45 µM filter unit, aliquoted into 2 mL Eppendorf tubes and stored at -80 °C. For knockdown of selected genes, 80% confluent target cells (exceptional, 50% confluent VCaP cells) were infected with respective recombinant lentiviral stock in a 1:10 ratio with growth media and 5 µg/mL polybrene for 12-15 h. Cells recovered 32 h in growth media previous to second transduction. Effective gene knockdown was verified by Western blot. Due to recovery of RAI2 expression, assays were performed within 10 days after first transfection.

### 2.2.8 CRISPR/Cas-9 genome editing to knockout RAI2 expression in LNCaP cell line

To establish cells with a somatic RAI2 knockout CRISPR-Cas9 technology was used following the protocol of RAN et al.[127]. In brief, a RAI2 specific 20-nt guide sequence 5'-GGCTCAGCTGATCACCACCG-3' was cloned into the Cas9 expression plasmid pSpCas9(BB)-2A-GFP (PX458) using *BbsI* restriction sites. Insertion of the guide sequence was verified by sequencing, before transfecting the 2.5 µg plasmid with Lipofectamine 2000® into parental cell lines, according to manufacturer's protocol. After 5 days single GFP-positive cells were

isolated using fluorescence activated cell sorting and clonally expanded. Successful RAI2 knock-out was verified by Western blot (see 2.5.4) and Sanger sequencing (see 2.4.2)of individual clones. A pool of five RAI2-negative LNCaP clones were used for further experiments, whereas one single clone was picked for the VCaP, KPL-1 or MCF-7 cell line.

## 2.3 Functional assays to analyse the hallmarks of cancer

The techniques introduced in this section were used to assess possible malignant transformation and progression of cells after RAI2 manipulation. In line with the hallmarks of cancer the ability to sustain proliferation, anchorage independent growth and the induction of cell migration was examined. Unless otherwise stated, statistical analyses were carried out using the Student T-test, considered a p-value below 0.05 as significant.

### 2.3.1 MTT assay

The MTT-Assay is a method that enables measurement of cellular proliferation of human cancer cells, which is defined by intracellular metabolic activity of viable cells. In order to compare the cell viability of parental and RAI2-modified cells, $0.5\times10^3$ LNCaP, $1x10^4$ VCaP, 1x103 PC-3 or $1\times10^3$ MCF-7-cells were seeded per well into two 96-well plates and incubated for 24 h at 37°C. Absorbance of one plate was measured at this as “day zero” referred time point for later normalization. In the second plate growth media was replaced with either standard medium, hormone deprived medium or medium containing DMSO serving as solvent for hormone receptor inhibitors, AKT-pathway inhibitors and cytostatics. The exact compounds as well as the final treatment concentrations are described in result sections 3.7.1-3.7.3. The respective medium was refreshed on fifth day and cell viability was assessed after 10 days of treatment. For this, 20 µL of a 5 mg/mL MTT (3-(4,5-dimethylthiazol-2-yl)-2,5-diphenyltetrazolium bromide) solution were added to the media and incubated for 3 h. During this time MTT was intercellular reduced to formazan, which was subsequently solubilized in 100 µL DMSO. The absorbance was measured at 540 nm with a reference at 650 nm and normalized by subtracting the absorbance of day 0 from day 10 using a plate reader. The average normalized absorbance was calculated from three (LNCaP, VCaP) or four (PC-3, MCF-7) independent experiments.

### 2.3.2 Colony formation assay

To analyse the clonogenic potential of individual RAI2 modified cells, single cell solutions were prepared and $2\times10^3$ LNCaP or $1x10^3$ PC-3 cells were seeded per well into 6-well plates. Cells were

allowed to adhere for 24 h at 37 °C and treated as indicated in result sections 3.7.1-3.7.3 for 14 days. Medium was changed every fifth day. To analyse colony formation, medium was removed, colonies were fixed with 4% (w/v) PFA in PBS, washed with PBS and stained with 0.5% crystal violet solution for 20 minutes. Subsequently, plates were washed with $H_2O$, scanned and evaluated using the ColonyArea plugin for ImageJ[128]. Results are expressed as the average percentage of covered area from five (LNCaP) or three (PC-3) independent experiments.

### 2.3.3 Transwell migration assay

The migratory capacity of cells was analysed by seeding $5\times10^4$ LNCaP or PC-3 cells in serum-free RPMI media in the upper well of a Boyden double chamber. To trigger chemotaxis, the lower chamber was filled with RPMI media containing 10% FCS. Plates were incubated at 37°C under standard conditions, and vertical migration through a 8.0 µm porous membrane was allowed to proceed for 24 h. Non migrated cells in the upper chambers were removed with cotton swabs, and the remaining cells were fixed in 4% paraformaldehyde and stained with crystal violet. To quantify the migratory response, cells in four squares were counted under an inverted phase microscope with a 20x magnification. Results are shown as average total number of migrated cells of four (PC-3) and five (LNCaP) independent replicates. Statistical evaluation was performed using the Mann-Whitney-U-Test, whereas values below a p-value of 0.05 were considered as significant.

### 2.3.4 Soft agar assay

To monitor anchorage-independent proliferation, $4x10^3$ LNCaP or $2x10^3$ PC-3 cells were grown in soft agar, composed of RPMI medium and 0.33% agarose, on a solidify 0.5% agarose bottom layer in a 6-well plate. 250 µL growth medium were added weekly and after 14 (LNCaP) or 10 days (PC-3) colonies were visualized by adding 200 µL of 1 mg/mL nitroblue tetrazolium chloride solution per well and incubating over night at 37 °C [129]. Plates were scanned with resolution of 2400 dpi and colonies of > 100 nm were counted using the Cell Colony Edge macro for ImageJ[130]. The macro was adjusted to our conditions by setting the "number of pixel" to 0.095 pixel/µm, the "Rolling Rall radius" to 50 and the "Gaussian Blur-sigma" to 2. In order to count only tumour spheres equal or bigger than 100 µm the "minimal size" of the "Analyse Particles" was set to 7854 $µn^3$ and the roundness value (Analyze Particles-Min circ) to 0.5. Furthermore, the macro was allowed to subtract background and to separate overlapping objects by activating the Watershed option. Results are expressed as averaged relative quantities, relative to the colony count of the respective parental cell line, from three (PC-3) and five (LNCaP) independent experiments. In order to obtain a standard deviation for the parental measurements, parental colony counts of

each biological replicate were averaged and relative quantities were calculated relative to the mean for each single replicate.

## 2.4 Molecular biologic Methods

Molecular biological work was carried out in the designated work areas of the laboratory which, in exception of the RNA area, were disinfected with antifect® N liquid before and after completion of work. When working with RNA, it was ensured that the work surface as well as utensils such as pipettes and racks were decontaminated from RNAse and nucleic acids with RNaseZap™. For additional protection of the samples and for self-protection, laboratory coat and gloves were worn.

### 2.4.1 Genomic DNA isolation from human cell lines

Genomic DNA (gDNA) isolation was performed with the "NucleoSpin Tissue" Kit from Macherey-Nagel GmbH & Co. Cells which were grown in 6-well or T25 culture flasks were washed with PBS and scraped down from their culture surface in the presence of 1 mL PBS before gDNA isolation was performed according to the manufacturer's specifications for cultured cells. Samples were eluted in 50 µL Buffer BE and stored at -20°C.

### 2.4.2 Sequencing

To determine the nucleotide sequence of a DNA molecule, the DNA fragment of interest was first amplified from genomic DNA (see 2.4.1) by PCR (see 2.4.6) and the specific amplicon was verified by an agarose gel (see 2.4.7). Subsequently, the PCR product was either purified from reaction components like primers, Taq polymerase and DMSO, or extracted from TAE-Agarose gel using the NucleoSpin® Gel and PCR Clean-up kit, according to the manufacturer's instructions. Samples were eluted in 20 µL NE buffer and used directly or stored at -20 °C. For sequencing, a total volume of 17 µL was premixed from 15 µL of purified DNA, consisting of 1 ng/µL, and 2 µL primer with a concentration of 10 pmol/µL and sent to the TubeSeq Service of Eurofins in a TubeSeq labelled 1.5 mL safe lock tube. The obtained sequence was opened using the FinchTV chromatogram viewer and analysed using the NCBI Blast function or compared with expected sequences using sequence alignment tolls from EMBL-EBI (www.ebi.ac.uk).

### 2.4.3 Quantity and quality measurement of nucleic acids

In order to determine concentration and quality of nucleic acid, samples were measured with the Nanodrop ND-1000 spectrophotometer. Before starting the sample measurements, the device was initialized with water and a reference spectrum was measured by loading the elution buffer. After blank measurement, 1 µL of sample was pipetted likewise directly onto the measurement pedestal, the sampling arm was lowered and spectral measurement using the Nanodrop software was started. Between sample measurements upper and lower pedestals were cleaned with clean, dry lint-free lab wipe. Beside the concentration, purity ratios were measured as indicators for sample quality. Nucleic acids with a 260/280 ratio of ~1.8 for DNA and ~2.0 for RNA were accepted as pure from proteins, phenol or other at 260 nm absorbing contaminants, whereas the 260/230 ratio values between 1.8 and 2.2 proved them free from e.g. guanidine, carbohydrates.

### 2.4.4 RNA isolation from human cancer cell lines

For total RNA isolation, cultured cells were washed with PBS and scraped from culture surface in the presence of 350 µL RA1 lysis buffer of the "NucleoSpin® RNA" or "NucleoSpin® RNA Plus" Kit. The following isolation was performed according the user manual. Elution of RNA was done with 50 µL RNAse-free $H_2O$. After determination of the concentration (see 2.4.3), RNA was used for reverse transcription (see 2.4.5) or stored at -80 °C.

### 2.4.5 Complementary DNA (cDNA) synthesis by reverse transcription of RNA

Total RNA from cell lines was reverse transcribed to cDNA by using the "First Strand cDNA Synthesis" Kit. Deviating from the manufacturer's instructions, 500 ng of total RNA (see 2.4.3) were transcribed in a 10 µL reaction mixture following the protocol for Oligo$(dT)_{20}$ primers. The product was used for or quantitative PCR (qPCR, see 2.4.8) stored at -20 °C.

### 2.4.6 Polymerase-chain-reaction (PCR) with AmpliTaq Gold® polymerase

To amplify a specific DNA fragment, primer pairs were first designed with the Primer-BLAST tool from NCBI (https://www.ncbi.nlm.nih.gov/tools/primer-blast/) and tested for specificity and optimum annealing temperature by gradient PCR. The primer sequences and annealing temperatures used are summarized in table 2-11. In a total volume of 25 µL, the in table 2-16 listed components were combined for the enzymatic reaction.

Tab. 2-16 PCR components for a 25 µL reaction mixture

| **Component** | **25-µL rxn** | **Final Concentration** |
|---|---|---|
| 10X PCR Buffer I | 2.5 µL | 1X |
| 10 mM dNTP mix | 2 µL | 0.2 mM |
| 10 µM forward Primer | 0.5 µL | 0.2 µM |
| 10 µM reverse Primer | 0.5 µL | 0.2 µM |
| Template DNA | varies | 25 ng |
| AmpliTaq Gold DNA Polymerase (5 U/ µL) | 0.125 µL | 0.625 U |
| Autoclaved, distilled water | to 25 µL | - |

Subsequently, qPCR was performed in the Thermocycler peqSTAR PeqLAb 96 as follows: denaturation at 95 °C for 5 min, followed by 35-40 Cycles of 95 °C for 30 s, annealing temperature (Tab. 2-11) or temperature gradient for 30 sec, and 72 °C for 40 sec. The program was completed with a final elongation at 72 °C for 5 min. Amplification products were held at 4 °C , before being analysed using an agarose gel (see 2.4.7) and used for sequencing (see 2.4.2)

### 2.4.7 Agarose gel electrophoresis

Agarose gel electrophoresis was used either for analytic purpose after amplification of DNA by PCR (see 2.4.6) or as a preparative technique before DNA sequencing (see 2.4.2). Therefore, agarose was add to 1x TAE electrophoresis buffer, boiled up in a microwave and mixed with ethidium bromide (1:10000) before it was poured into "EasyPhor" gel chamber for polymerization. As the running behaviour and the optimal separation of DNA fragments is determined by the amount of agarose, fragments bigger in size than 300 bp were analysed with a 1% agarose matrix, while 2% agarose was chosen for smaller ones. Each DNA sample was loaded together with 6x loading Dye in a separate well and separated for one hour at an electric tension of 100 V. The "GeneGenius2" documentation system was used together with the Genesnap software to visualize the DNA intercalating ethidum bromide at a wavelength of 254 nm. A commercial DNA size marker, such as the "GeneRuler 1kb DNA Ladder"or the "SMOBIO DM2100 50bp Ladder", passing the gel parallel to the samples allowed for sizing.

### 2.4.8 Quantitative real time-PCR (qRT-PCR)

Quantitative real time PCR allows gene expression analysis of specific target genes by a PCR-based relative quantification of messenger RNA (mRNA), which has previously been converted to cDNA (see 2.4.5). The real time cDNA amplification measurement is achieved by adding a dsDNA incorporating fluorescent dye into the PCR-reaction mix and measuring the fluorescent signal, which will increase directly proportional to the amount of dsDNA, after each amplification cycle. In this study, the SYBR Green fluorescent dye was used as a component of the Master mix of the "Maxima SYBR Green" kit. A 10 µL reaction mix was prepared consisting of 0.2 µL of the target specific reverse and forward primer and 5 µL of Master mix which included, additionally to SYBR Green dye, dNTPS, and Maxima Hot Start Taq polymerase in the reaction buffer. The reaction mix was dispensed into a 96- well plate and 150 ng cDNA were added to each well before amplification was started in the "Bio-Rad C1000 Touch CFX96" thermocycler using the program listed in table 2-17. Primer sequences were designed to amplify at an annealing temperature of 59 °C. Analyses were performed in triplicates and the Bio-Rad CFX Manager 3.1 software was used to assign a Cq value, which is defined as the cycle number at which the measured fluorescent signal was significantly exceeding the background fluorescence, for each measured sample. Subsequently, mean Cq value was calculated for each gene and data was analysed by applying the ΔΔCq-method using RPLP0 as reference gene for normalization. First, the ΔCq-value was calculated by subtracting the reference Cq-value from the Cq-value of the gene of interest:

$$\Delta\mathrm{Cq} = \mathrm{Cq}\ (\text{gene of interest}) - \mathrm{Cq}\ (\text{reference gen})$$

To compare the mRNA expression of genes between samples, e.g. a treated or genetically modified sample A and control sample B, the ΔΔCq- value was calculated as follows:

$$\Delta\Delta\mathrm{Cq} = \Delta\mathrm{Cq}(\text{sample A}) - \Delta\mathrm{Cq}(\text{sample B})$$

Relative expression of target genes compared to the specified control sample was calculated for each gene in the following manner:

$$Fold\ change = 2^{(-\Delta\Delta Cq)}$$

Tab. 2-17 Cycling program for qPCR

| PCR Steps | Temperature [°C] | Time [min] | Cycle |
|---|---|---|---|
| **Initial denaturation** | **95 °C** | **5** | **1** |
| **Denaturation** | **95 °C** | **0:15** | **40** |
| **Annealing** | **58 °C** | **0:30** | |
| **Extension** | **72° C** | **0:30** | |
| | **Plate read** | | |
| **Melting gradient** | **60 °C – 95 °C** | **20 min** | |

## 2.5 Protein biochemical methods

Several protein analysis techniques were used to analyse and quantify the expression of selected proteins (see 2.5.4), to determine their distribution within the cell (see 2.5.6) or to monitor the activities of kinases (see 2.5.5).

### 2.5.1 Cellular extract preparation

To isolate total cellular extract from cultured cell lines for Western blot analysis, cells were washed with PBS before they were dislodged in the presence of 1 mL PBS by scraping. Cell suspension was transferred into 1.5 mL tube and centrifuged for 3 min at 750 rcf at 4 °C. Supernatant was withdrawn to the lowest volume and pellet was lysed with 50-300 µl 2x SDS lysis buffer, containing one tablet each of "PhosSTOP™" phosphatase inhibitor and "cOmplete™" proteinase inhibitor per 10 mL lysis buffer. Genomic DNA was fragmented by sonification using an ultrasound homogenisator. Subsequently, samples were either used directly for determination of protein concentration (see 2.5.2) or frozen at -20 °C.

### 2.5.2 BCA assay

The protein concentration was determined by the "Pierce™ BCA Protein Assay" kit according to manufacturer's instructions. A standard series of 0 µg/µL, 5 µg/µL, 10 µg/µL and 20 µg/µL was prepared with the enclosed bovine serum albumin. Absorbance at 562 nm was measured for the standard series and all the samples with the "Biophotometer" spectrophotometer within 10

minutes. Protein concentration was calculated using the equation of the standard curve. Samples were used for gel-electrophoresis (see 2.5.3) or frozen at –20 °C.

### 2.5.3 SDS-polyacrylamide gel-electrophoresis

The SDS-polyacrylamide gel-electrophoresis was used to separate proteins vertically by their relative mass. This is enabled by the SDS (Sodium Dodecyl Sulphate) as a component of the lysis buffer and the SDS-polyacrylamide gel (SDS-PAGE). The SDS binds to polypeptide chains and leads to linearization and a proportional to mass, negative charge of the polypeptides. The SDS-PAGE is composed of an upper stacking gel and a lower resolving gel, which were prepared according to table 2-18 using the "Hoefer™ Dual Gel Caster" system. The amount of acrylamide in the resolving gel varied from 6% to 8%, depending on the mass of the proteins of interest. Each sample was supplemented with 1 µL saturated bromophenol blue solution and denaturated at 95 °C for 5 min, chilled on ice and load parallel to the "PageRuler™ Prestained Protein Ladder" into the gel pockets. Electrophoresis was performed in 1x Laemmli buffer at a constant electrical current of 0.025 A for 60 min for each gel. Afterwards, gel was prepared for Western bot analysis (see 2.5.4)

Tab. 2-18 Components for preparation of stacking and separation gel

| **Component** | **Stacking gel** | **6% Separating gel** | **8% Separating gel** |
|---|---|---|---|
| H2O | 1.46 mL | 2.3 mL | 2.1 mL |
| 40% Acrylamide | 0.3 mL | 0.6 mL | 0.8 mL |
| 1.0 M Tris (pH 6.8) | 0.3 mL | - | - |
| 1.5 M Tris (pH 8.8) | - | 1.0 mL | 1.0 mL |
| 10% SDS | 0.02 mL | 0.04 mL | 0.04 mL |
| 10% APS | 0.02 mL | 0.04 mL | 0.04 mL |
| TEMED | 0.002 mL | 0.004 mL | 0.004 mL |

### 2.5.4. Western blot analysis

For the specific detection of selected proteins, the proteins separated according to section 2.5.3 were transferred to a membrane and visualized by immunodetection. In detail, gel was removed from electrophoresis unit and the stacking gel was separated. The separation gel was placed in the "Trans-Blot SD semi-dry transfer cell" on top of two layers of Whatman paper and a nitrocellulose

membrane (NC-membrane) and covered with two additional layers of Whatman paper. Whatman paper and NC-membrane were previously cut to 5.3 cm x 8.3 cm and saturated with transfer buffer. The semidry eletro-transfer was performed at a constant current of 0.04 A for each gel for 120 min. Subsequently, Membrane was washed with 1x TBS-T for 5 min and free binding sites were blocked with 5% milk powder in 1x TBST for 30 min. For the detection of proteins, which are bound to the membrane by hydrophobic interactions, a primary antibody specific for the target protein was diluted in 5% BSA or 5% milk powder and incubated over night at 4°C. On the next day, membrane was washed 5 times for 5 min with 1x TBS-T and incubated for 60 min with HRP- or IRDye®-conjugated secondary antibody, diluted in 5% BSA in TBS-T. For the detection of HRP-labelled proteins, membrane was soaked for 1 min in a self-made ECL solution before photons emitted during the enzymatic degradation of luminol were captured by an X-ray film and visualized with the "Curix 60 Processor". IRDye®-labelled proteins were detected using the Odyseey® Clx Imaging System and the Image Studio™ lite Ver 5.2 acquisition software. Same software was used for protein quantification. Results are shown as average fold change of protein expression normalized to HSC70 and respective control protein expression in three independent experiments.

### 2.5.5 PamStation

PamStation® 12 instrument from PamGene was used to analyse activity of serine-threonine kinases (STK) in human cell line cells in a fully automated manner. Therefore in collaboration with Priv.-Doz. Dr. Malte Kriegs, whole cell lysates were analysed in triplicates with the STK PamChip® Array, consisting of 140 ser/thr containing peptides and 4 phosphorylated peptides as positive controls. Actively phosphorylated peptides were detected with a primary antibody cocktail and a secondary FITC-conjugated antibody. Phosphorylation signals were quantified and analysed with the data analysis software BioNavigator by our collaborator. For the preparation of cell lysate from cultured cells, a lysis buffer was prepared by diluting "Halt Phosphatase Inhibitor Cocktail" and "Halt Protease Inhibitor Cocktail, EDTA free" 1:100 in "M-PER Mammalian Extraction Buffer" and placed on ice. Culture medium was removed from T25 flask and 70% confluent cells were washed twice with ice cold PBS before and lysed with 70 µL Lysis buffer by incubating for 15 min on ice. Lysate was centrifuged for 15 min at 16,000 rcf at 4 °C and supernatant was aliquoted into labelled, on dry ice pre-cooled tubes. One aliquot was used for Protein quantification using the BCA assay (2.5.2), while remaining aliquoted samples were snap-frozen in liquid nitrogen before they were stored in a – 80 °C freezer. Protein lysates with a concertation above 1 µg/µl indicated a successful lysis. 5 ng from each sample were applied in a volume of 1-10 µL per array and measured in technical triplicates.

### 2.5.6 Immunofluorescence staining of cultured cells

Immunofluorescence staining of cultured cells allows the analysis of protein expression and –distribution on a single cell level. Furthermore, targeting two proteins with specific primary antibodies and their visualisation by species specific secondary conjugated to distinctive fluorophores can give first hints on a possible protein interaction in case of co-localizing fluorescent signals. Before staining, $5x10^5$ cells were seeded in a Falcon™ 4-well cell culture slide and grown until a cell confluence of 70-80% was reached. Next, medium was removed and cells were washed twice with PBS and fixed with 4% PFA for 15 min at RT. PFA was removed from the cells by washing two times with PBS before cell membranes were permeabilised with 0.2% Triton X-100 for 15 min at RT. After three washing steps with PBS for 5 min cells, were blocked for 30 min at RT with 250 µL of blocking solution (1% BSA inPBS). Primary antibodies directed against specific target antigens were added at a dilution of 1:500 to the blocking solution and incubated over night at 4 °C. On the next day, cells were washed 5 times à 5 min with PBS before AlexaFluor™-488- and/or AlexaFluor-456™-conjugated secondary antibodies against the primary antibody, diluted 1:500 in blocking solution, were added to the cells. After 90 min of incubation at RT in the dark, secondary antibodies were washed from cells two times for 5 min each with PBS. Nuclei were stained with 1µl DAPI/PBS-solution (1:10,000) at RT for 5 min. Cells were covered with 25 µL Mowiol inclusion agent per camber and a cover slip, which was sealed with nail polish. Samples were kept at 4 °C in the dark until they were visualized with either the "Axioplan 2 imaging fluorescence microscope" or the "TCS SP5 confocal laser scanning microscope" (UKE Microscopy Imaging Facility) on the next day.

## 2.6 Xenograft experiment

Male immunosuppressed Pfp/$Rag^{-/-}$ double knockout mice were used from a breeding colony at University Medical Center Hamburg-Eppendorf. Animals were maintained under pathogen-free conditions in individually ventilated cages and fed with sterile standard food and water *ad libitum*. This animal experiment was approved by local animal experiment approval committee. 3 x $10^6$ parental or RAI2-knockout LNCaP cells were suspended in 200 µL PBS with 50% Corning® Matrigel® Basement Membrane Matrix (Corning Incorporated) and injected subcutaneously above the right scapula of the mouse. Before application of the tumour cells, the animals were briefly anesthetized with $CO_2/O_2$. Animals were killed when the tumours exceeded a size of 1000 $mm^3$. Complete blood was drawn by cardiocentesis into an EDTA tube and circulating tumour cells (CTCs) were enriched using the Parsotix™ device (see 2.6.1). Additionally bone marrow and was

isolated (see 2.6.2) for subsequent DTC detection by *Alu*-PCR analysis (see 2.6.4) or Immunofluorescence staining (see 2.6.3). Furthermore, half of a lung was snap-frozen per animal in nitrogen and examined for the presence of CTCs by *Alu*-PCR analysis.

### 2.6.1 Enrichment of CTC from murine EDTA-blood by the Parsotix™ system

To isolate CTCs from mouse blood, the Parsotix™ Cell Separation Sytem (Angle Plc, Guildford, UK) was used. To ensure a size and deformability-based separation of cells a disposable cassette with a final gap of 6.5 µm was used in combination with the separation program S23A, according to the manufacturer's protocol. Cells which were caught in the cassette were eluted onto an object slide, centrifuged and dried overnight. Slides were packed in aluminium foil and kept at -80°C until direct immunofluorescence staining (see 2.6.3).

### 2.6.2 Isolation and processing of murine bone marrow cells

For the isolation of murine bone marrow cells, left femur and tibia were removed with a scalpel from skin and muscles and separated at the knee joint. Epiphyses of the bones were cut off and bone marrow cells were flushed with 1 mL PBS from both bone ends using a 25-gauge needle and a 2 mL syringe until whitening of the bones. Subsequently, cells were centrifuged for 5-10 min at 13,000 rpm and erythrocytes in the cell pellet were lysed for 2 min with 500 µL Ery-Lysis buffer. The collection tube was filled up with PBS and cells were centrifuged for 5 min at 13,000 rpm, before supernatant was removed. For cell count determination, cells were transferred into a 15 mL Falcon tube, diluted with PBS and counted using a Neubauer hemocytometer slide (see 2.2.4). $5x10^5$ to $7.5x10^5$ cells each were cyto-centrifuged onto a glass slide for 4 min at 244 x g, dried overnight and frozen at -80 °C until cytospins were used for DTC detection (see 2.6.3).

### 2.6.3 Immunofluorescence staining for the detection of CTCs and DTC

To identify human circulating or disseminated LNCaP tumour cells in murine blood or bone marrow, cells enriched by Parsotix™ system (2.6.1) and cytospins from 2.6.2 were stained with fluorophore-conjugated antibodies targeting the human epithelial marker EpCAM and Cytokeratin. Murine CD45 staining was used as an exclusion marker for contaminating leukocytes. Briefly, cells on object slides were fixed with 4% PFA for 10 minutes, permeabilized with 0.1% Triton™ X-100 (Sigma-Aldrich) for 10 minutes and blocked by incubating with 5% Normal Goat Serum (NGS) (DAKO) for one hour. Subsequently, cells were stained in 2% NGS with antibodies targeting EpCAM (Alexa488, clone 9C4, 1:50), pan-cytokeratin (Alexa488, clone AE1/AE3, 1:200)

and murine CD45 (APC, clone30-F11, 1:100). Additionally, cell nuclei were stained with DAPI (100µg/mL). For the detection and enumeration of CTC, slides were automatically scanned by the Xcyto® 10 Quantitative Cell Imager (Chemometec). The associated XcytoView™ software was used for standardized identification of CTCs and DTCs. Due to different contaminating population gaiting were set differently for the CTC and DTC detection in a blinded fashion.

### 2.6.4 *Alu*-PCR for DTC detection in murine organs

DNA isolation and *Alu*-PCR-based quantification of DTC load in bone marrow have been performed by our collaboration partner as previously described[131].

## 2.7 Enrichment and detection of CTC from peripheral blood of prostate cancer patients

A total of 40 late stage prostate cancer patients were recruited from June 2018 to September 2019 at the Centre of Oncology, University Medical Centre Hamburg-Eppendorf in Germany. From each patient, 7.5 mL blood were drawn into an ethylenediaminetetraacetic acid (EDTA) collection tube. Additionally blood from ten healthy donors was obtained as negative control from the Institute of Transfusion medicine, Medical Center Hamburg-Eppendorf. Blood reached the laboratory within 30 minutes, where it was placed at +4°C for a maximum of two hours before CTCs were isolated marker dependent by the AdnaTest (see 2.7.3) and analysed for the expression of 15 target genes (see 2.7.5).

### 2.7.1 Ficoll density gradient for isolation of PBMCs from healthy donors

Peripheral Blood Mononuclear Cells (PBMCs) were isolated by Ficoll density gradient centrifuge. First plasma was removed from EDTA blood by centrifugation at 500 rcf for 10 min. Remaining lower layer of blood was diluted to 30 mL with PBS. Subsequently, 20 mL Ficoll were filled into a 50 mL collection tube and layered carefully with the diluted blood. Mononuclear cell fraction was separated from erythrocytes and other blood components by centrifuging at 400 rcf for 30 min at RT with slow acceleration and without break. The mononuclear cells were washed by diluting them with 50 mL PBS and centrifuging at 400 rcf for 10 min. In case of contaminations with erythrocytes, cell pellet was lysed with 1 mL Ery-Lysis buffer for 3 min. The isolated PBMCs were diluted to 5 mL with PBS and quantified using a Neubauer haemocytometer (see 2.2.4) or were directly used for isolation of genomic DNA (see 2.4.1).

### 2.7.2 Bisulfide conversion

Automated DNA denaturation and bisulfide conversion of genomic DNA, isolated from PBMCs from peripheral blood of healthy donors (see 2.7.1 and 2.4.1) was performed according the "InviMag® Bisulfite Conversion KiT/IG" using the "InViGenius® PLUS" system. Deviating from user's manual additional 200 µL of Solution BS were added to "SolutionBS/IG" tube. Samples were eluted in 50 µL elution buffer and frozen at -80 °C. RAI2 methylation status of leucocytes from healthy donors was determined by sequencing (see 2.4.2) the RAI2 promotor region after PCR-based amplification (see 2.4.6) with bisulfide-specific sequencing primers (BSSQ-primer, see tab. 2-11)

### 2.7.3 CTC enrichment from PCa-patients by "AdnaTest ProstateCancer"-kit

For the isolation of CTC from peripheral blood of late stage prostate cancer patients 7.5 mL blood were drawn into an EDTA blood collection tube at the Center of Oncology, Medical Center Hamburg-Eppendorf. For CTC from 5 mL peripheral blood of prostate cancer patients were enriched immunomagnetically by AdnaTest ProstateCancerSelect™, by targeting the epithelial and tumour-associated cell surface epitopes EpCAM, ERBB2 and EGFR as described by the manufacturer's instructions. Subsequently RNA was isolated and reverse-transcribed to cDNA using the $Oligo(dt)_{25}$ primer and Sensiscript Reverse Transcriptase (Sensiscript RT Kit, Cat No./ID:205211) according to the AdnaTest ProstateCancerDetect Kit™ (all from QIAGEN, Hilden, Germany) instructions. Blood from healthy donors was exposed to same procedure. The resulting cDNA was further preamplified before used for qRT-PCR analysis.

### 2.7.4 Preamplification

For PCR-based preamplification 5 µL of cDNA were mixed in a 50 µL reaction with TATAA SYBR® GrandMaster® Mix and 15 TATAA GrandPerformance Assays, containing the forward and reverse primers (50 nM final concentration, respectively) of each specific target gene as well as the ValidPrime® Assay, to test for presence of gDNA in the samples. The CFX™ Real Time System (Bio-Rad Laboratories) was set to the following preamplification program: initial denaturation at 95°C for 3 min, followed by 18 cycles of denaturation at 95°C for 15 sec, annealing at 60°C for 2 min and elongation at 72°C for 1 min. Samples were further kept for a maximum of four minutes at 72°C until they were snap frozen on dry ice and stored at -80°C.

### 2.7.5 Expression analysis qRT-QPCR and data analysis

Preamplified cDNA (see, 2.7.5) was diluted 8x in nuclease-free-water during thawing before 5 µL were subjected to RT-qPCR. TATAA GrandPerformance® Assays were used to analyse each sample for the expression of *AR*, *ARv7*, *PSMA*, *PSA*, *HOXB13*, *RAI2*, *EGFR*, *EPCAM*, *KRT19*, *MRP1*, *PI3KCA*, *CD45* and the reference genes *ACTB*, *GAPDH*, *HPRT1*. For this purpose, 2x TATAA Probe GrandMaster® Mix was mixed with respective "TATAA GrandPerformance® Assay, containing target specific primer and FAM-probe (400 nM and 200 nM, final concentration) and the preamplified cDNA. Furthermore, ValidPrime® was used as control assay for human genomic background and three technical replicates of the "TATAA Internal Control Calibrator" were included in all qPCR runs. RT-qPCR was performed in the "CFX™ Real time System" as follows: pre-amplification at 95°C for 3 min, 40 Cycles of denaturation at 95°C for 10 sec, annealing at 60°C for 30 sec and elongation at 72°C for 30sec. The "CFX™ Manager" software was used to obtain the Cq-values which were first compensated for variations between instrument runs and corrected for the presence of genomic DNA using Excel. Subsequently, the "GenEx" software was applied to process and analyze the data. Missing data from the reference gene measurements (GAPDH value for PCa-24 and ACTB value for PCa-17) was replaced using the "impute" option of "GenEx", leading to an interpolation of missing values using information from all samples. Remaining missing data was replaced with a Cq-value of 36. GAPDH was identified by NormFinder (algorithm included in GenEx), accounting for intergroup variations, as the most stably expressed gene and was used for ΔCq calculation. For multivariate analysis ΔCq-values were converted for each gene separately into relative quantities, relative to the sample with the maximum Cq (lowest expression) and transformed into logarithmic scale using base $2^{132}$. Data was mean-centred and analysed by dendogram, heat map and PCA. Furthermore Pearson's correlation and Spearman's rank correlation coefficient were calculated and Scatterplots were created with the appropriate GenEx function.

## 2.8 In Silico analyses

*RAI2* mRNA expression was analysed in two publicly available gene expression GEO datasets (GDS2546 and GDS3289). Expression values from GEO data sets were retrieved from NCBI server and samples were grouped according to the indicated parameters. P-values were calculated by Student's T-test.

# 3 Results

## 3.1 In Silico Analysis of RAI2 expression in Prostate Cancer

It was previously described that low *RAI2* gene expression in primary breast tumours is associated with the presence of DTCs in the bone marrow and is correlated with poor patient overall survival[118]. To investigate the prognostic relevance of *RAI2* gene expression in prostate cancer progression, the *RAI2* mRNA expression was evaluated in two publicly available GEO datasets. In the analysed data sets, *RAI2* mRNA expression was significantly lower expressed in metastatic prostate tumours compared to localized prostate tumours and either normal tissue or benign intraepithelial neoplasia (Fig. 3-1).

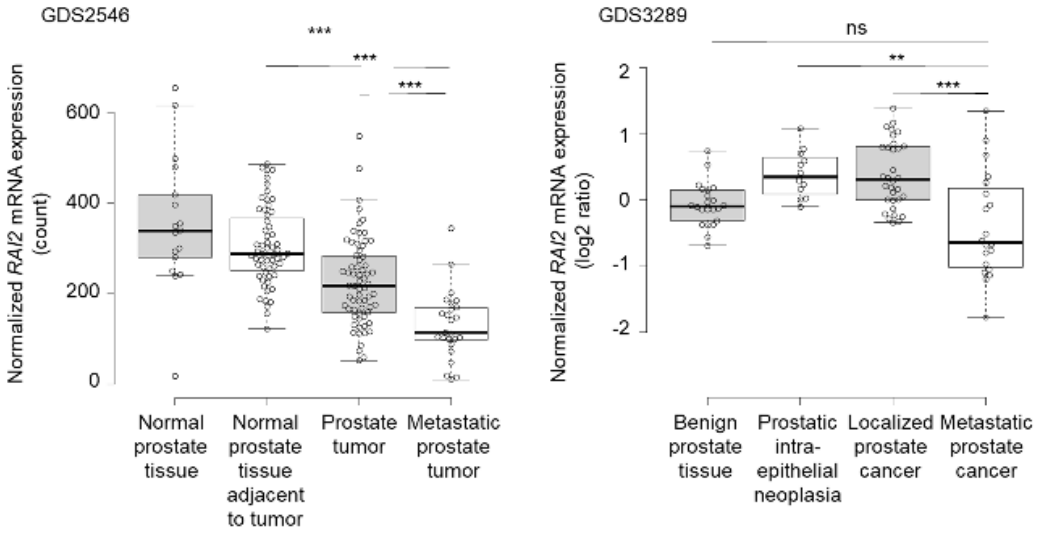


**Fig. 3-1** *RAI2* mRNA expression in publicly available GEO-datasets. Normalized *RAI2* mRNA expression values were obtained from GDS2546 and GDS3289 (GEO database) and grouped to the specified parameters. P-values were calculated using Student's T-test. **p < 0.01, ***p < 0.001; ns, not significant

## 3.2 Analysis of the relationship between RAI2 and Hormone receptors

Due to the observed correlation of RAI2 expression with the ERα status in human breast cancer tissue and the elevated RAI2 expression in hormone-dependent growing ERα-positive breast and AR-positive prostate cancer cells, the question whether there is a functional link between RAI2 and the respective growth promoting hormone receptor has been raised[118,123]. To address this

question RNAi technology was used to deplete the protein expression of RAI2 and either ERα in breast cancer cells or AR in prostate cancer cell lines. Western blot analysis was performed to determine the mutual effect of depletion on each other's protein expression.

### 3.2.1 Analysis of the relationship between RAI2 and the Oestrogen Receptor

To find out if there is a functional relationship between RAI2 and the ERα protein in breast cancer cells, the ERα positive KPL-1 and MCF-7 breast cancer cell lines were transduced with lentiviral particles harbouring shRNA against the *RAI2* or *ERα* mRNA to achieve a knockdown of respective protein expression. After successful RAI2 knockdown (RAI2-KD) in KPL-1 and MCF-7 cell lines, Western blot signals at the expected molecular weight of the ERα protein showed a 0.72 ± 0.12 fold (p-value= 0.011) and a 0.75 ± 0.09 fold (p-value= 0.012) weaker protein expression than in the respective NT-control (Fig. 3-2, A). On the other hand ERα knockdown (ERα-KD) led to an up to 3.04 ± 1.16 –fold (p-value= 0.0018) and 1.77 ± 0.71 (p-value= 0.079) fold induction of the RAI2 protein expression in KPL-1 and MCF-7 cells (Fig.3-2, B).

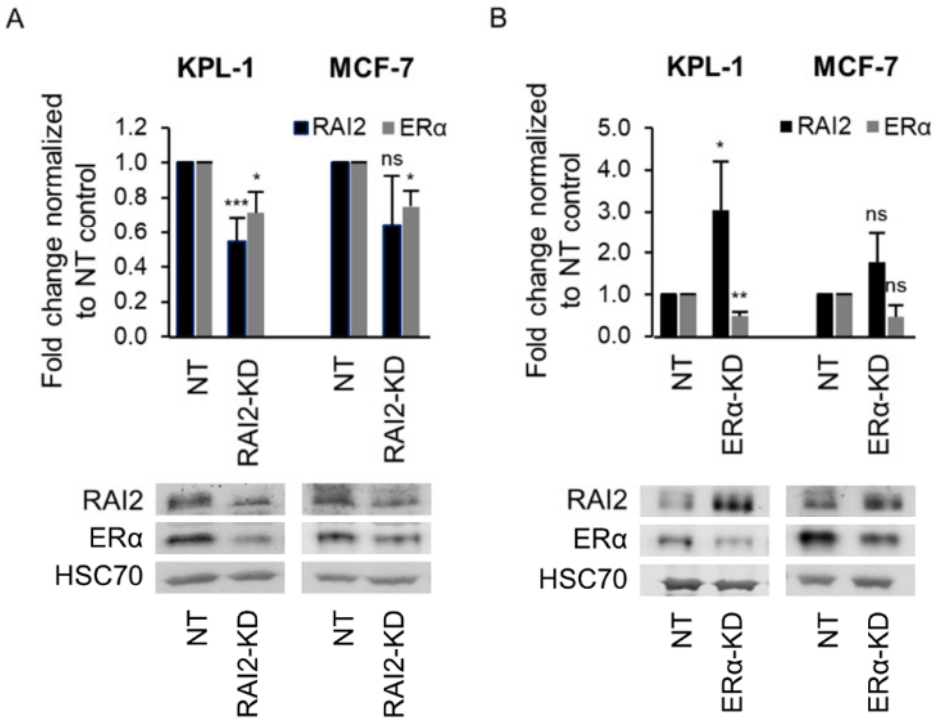


**Fig. 3-2** Western blot analysis after shRNA-mediated knockdown (KD) of *RAI2* and *ERα* mRNA in BrCa-cells. **A**, Analysis of RAI2 and ERα protein expression after RAI2 knockdown in KPL-1 and MCF-7 breast cancer cells. **B**, RAI2 and ERα protein expression after selective knockdown of the ERα protein in KPL-1 and MCF-7 cells. HSC70 protein expression was used as loading control. Relative protein expression was

determined by normalizing to HSC70 and the NT-protein expression using the Image Studio Lite software (Li-Cor). Columns show the average fold change and standard deviation of four (MCF-7) and three (KPL-1) independent experiments. P value were calculated using the one sample *t*-test. *p < 0.05, **p < 0.01, ***p < 0.001; ns, not significant; NT, non-target shRNA

### 3.2.2 Analysis of relationship between RAI2 and Androgen Receptor

An shRNA-mediated knockdown of RAI2 or AR expression was performed to examine a possible functional link between both proteins. In LNCaP and VCaP prostate cancer cell lines, RAI2 depletion caused a 0.54 ± 0.25-fold (p-value= 0.085) and 0.66 ± 0.14 fold (p-value= 0.02) downregulation of AR in LNCaP and VCaP cells, respectively, when compared to cells transduced with control shRNA (NT) (Fig. 3-3, A). In contrast, AR knockdown resulted in a 3.34 ± 1.52 -fold (p-value= 0.055) and 2.14 ± 0.15 –fold (p-value= 0.006) increased RAI2 protein expression in LNCaP and VCaP cells (Fig. 3.3, B).

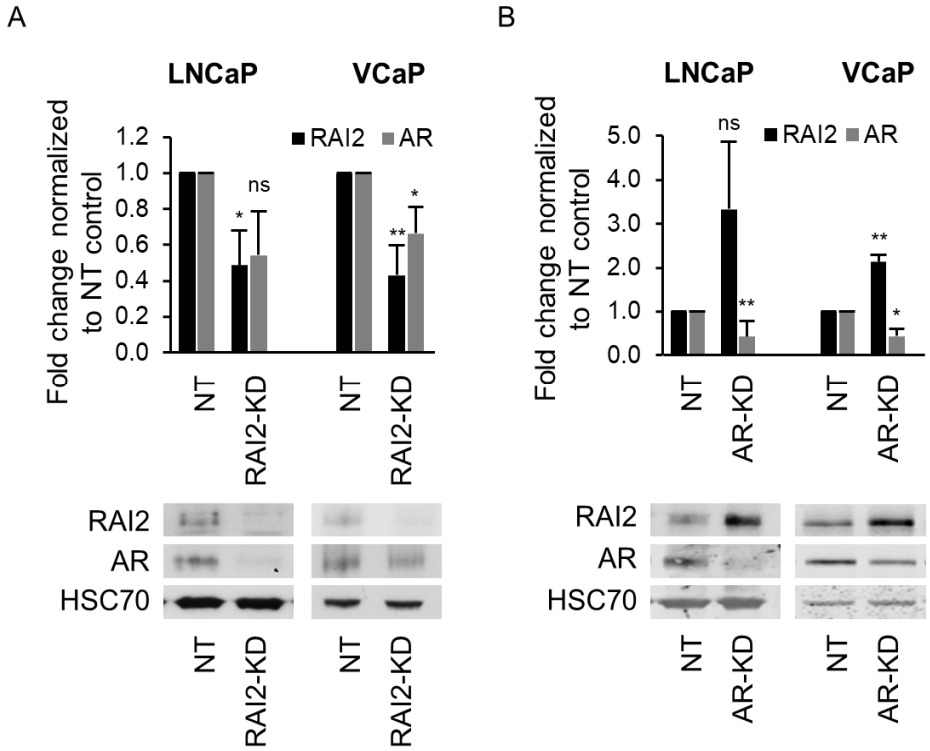


**Fig. 3-3** Western blot analysis after shRNA-mediated knockdown (KD) of RAI2 and AR mRNA in PCa-cell lines**. A**, RAI2 and AR protein expression in LNCaP (n= 3) and VCaP (n= 4) prostate cancer cells, following shRNA-mediated knock-down of RAI2 protein. **B**, Expression of RAI2 and AR protein determined after knockdown of AR in LnCap (n= 4) and VCaP (n= 3) cells. Relative protein expression was determined by normalizing to HSC70 loading c and the NT-protein expression using the Image Studio Lite

software (Li-Cor). Columns show the average fold change and standard deviation of respective number of independent experiments. P values were calculated using the one sample *t*-test. *p < 0.05, **p < 0.01, ns: not significant; NT, non-target shRNA

The combined results of both breast and prostate cancer cell line experiments showed that RAI2 knockdown causes a down-regulation of hormone receptor expression, while inhibition of each hormone receptor induces RAI2 expression in all tested cell lines, implying that there is an inter-dependent regulation of RAI2 and the respective hormone receptor.

## 3.3. Effects of hormone receptor inhibition on RAI2 expression

In order to further investigate the relationship of the expression of RAI2 and the hormone receptors, ERα and AR positive breast and prostate cancer cells were treated with hormone receptor specific inhibitors, used in the clinic. Western blot analysis was performed to analyse whether pharmacological inhibition of ERα and AR activity affects RAI2 protein levels.

### 3.3.1 Inhibition of ERα activity in human breast cancer cells lines

Inhibition of ERα activity was achieved by either depleting the complete hormones from growth media (HD) or by adding the selective oestrogen receptor down-regulator (SERD) fulvestrant to standard growth medium (DMEM). After 10 day of cultivation, KPL-1 and MCF-7 cells showed a significant 0.48 (p=0.008) and 0.16 fold (p= 0.006) decreased ERα protein expression after inhibition with ICI, while complete hormone deprivation increased (1.77 fold change, p= 0.026) the ERα protein level in KPL-1 and decreased (0.77 fold change, p= 0.018) the same in MCF-7 cells. Even though an increase in RAI2 protein expression could been observed und ER inhibitory conditions in both breast cancer cell lines, the difference did not reach the significance threshold of $p \leq 0.05$ (Fig. 3-4).

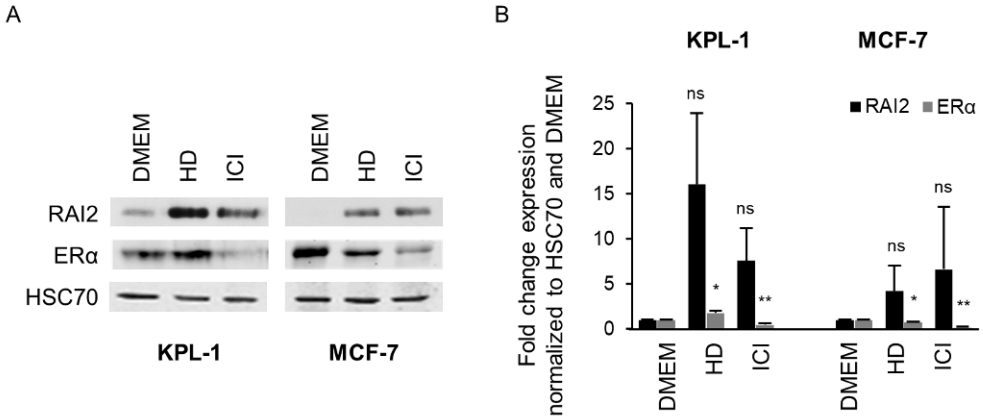


**Fig. 3-4** RAI2 and ERα protein expression after inhibition of oestrogen receptor activity**. A**, KPL-1 and MCF-7 cells were grown in hormone deprived medium (HD) or treated with 1 μM fulvestrant (ICI) or 3 μM for 10 days. **B**, Relative protein expression was determined by normalizing to HSC70 loading control and DMEM protein expression using the Image Studio Lite software (Li-Cor). Columns show the average fold change and standard deviation of three independent experiments. P values were calculated using the one sample *t*-test. *p < 0.05, **p < 0.01, ns: not significant

### 3.3.2 Inhibition of AR activity in human prostate cancer cells

To analyse the effects of AR signalling inhibition on RAI2 protein expression in prostate cancer cell lines, parental LNCaP and VCaP cells were grown for 10 days under hormone deprivation or treated with the antiandrogens bicalutamide (BIC) and enzalutamide (ENZ). Quantification of four independent Western blot analysis revealed no significant changes for RAI2 and AR protein expression in LNCaP cells after AR inhibition. For VCaP cells, however, a significant 2.14.fold (p= 0.008) and a 1.53 fold (p= 0.014) induction of RAI2 and AR protein was observed after hormone deprivation. A similar picture was obtained after enzalutamide treatment, although only the 2.10-fold induction of AR protein expression resulted in a significant (p= 0.002) difference. A significant change was furthermore observed for RAI2 expression after bicalutamide treatment, which resulted in a 0.79 fold (p=0.005) decreased protein expression compared to control condition (DMEM) (Fig. 3-5).

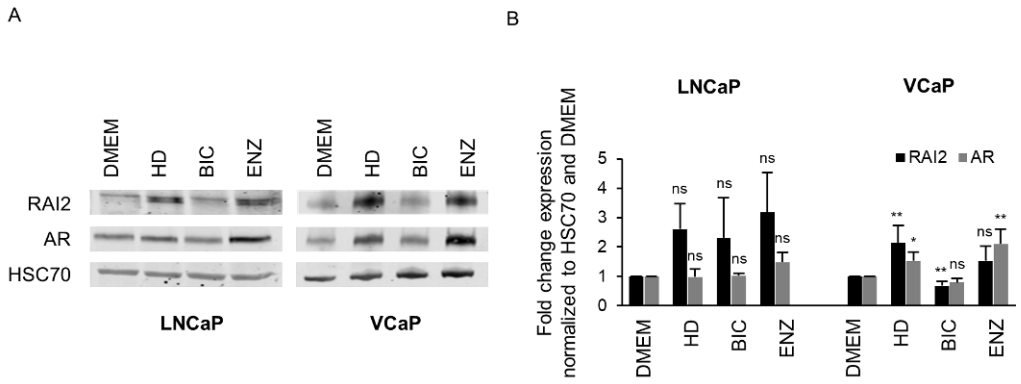


**Fig. 3-5** RAI2 and AR protein expression after inhibition of androgen receptor activity**. A**, LNCaP and VCaP cells were grown in hormone deprived medium (HD) or treated with either 3 µM bicalutamide (BIC) or 3 µM enzalutamide (ENZ) for 10 days. **B**, Relative protein expression was determined by normalizing to HSC70 loading control and protein expression in respective standard growth medium using the Image Studio Lite software (Li-Cor). Columns show the average fold change and standard deviation of four independent experiments. P values were calculated using the one sample *t*-test. *p < 0.05, ns: not significant

## 3.4 Analysis of possible interaction partners of RAI2 protein in prostate cancer cells

Previous studies at our institute have shown the co-localisation of RAI2 protein with CtBP1 and CTBP2 proteins in nuclear speckles in the nuclei of RAI2 protein overexpressing MCF-7 breast cancer cells. Furthermore, coimmunoprecipitation analysis verified a direct molecular interaction that is mediated via the non-consensus bipartite ALDLS binding domain of RAI2 protein[118]. Here, microscopic analysis was used to analyse the possible interaction of either RAI2 and the CtBP1 protein or RAI2 and the androgen receptor in prostate cancer cell lines. Due to low basal expression of RAI2 in LNCaP cells, cells were transduced with a RAI2 overexpression vector. After verification of increased RAI2 protein expression by Western blot analysis (Fig. 3-6, A), distribution of RAI2 and the AR was analysed by immunofluorescence staining with two distinct fluorophore coupled antibodies against the RAI2 and AR protein. Figure 3-6 B, shows a clear distribution of both proteins in the nucleus of LNCaP cells, however signals were not overlapping, indicating that there is no direct interaction of both proteins in prostate cancer cells under normal growth conditions. Nevertheless, co-localisation of endogenous RAI2 protein and CtBP1 protein in nuclear speckles could be confirmed for untransfected VCaP cells, after RAI2 stimulation with enzalutamide (Fig. 3-6, C)

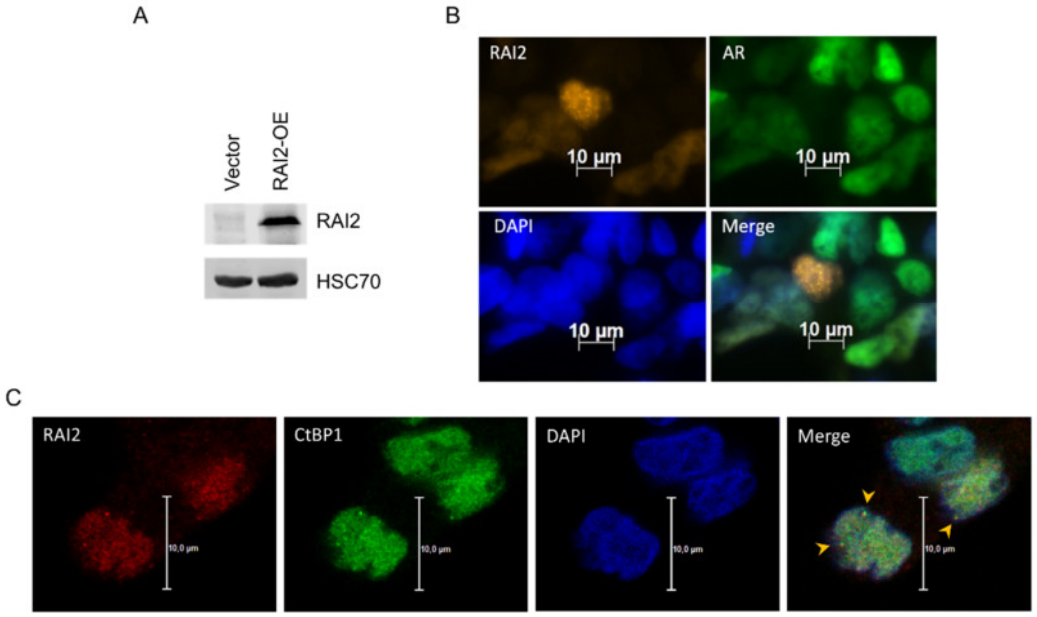


**Fig. 3-6** Distribution of fluorescent labelled RAI2, AR and CtBP1 protein in prostate cancer cell lines. **A**, Western blot analysis of RAI2 protein expression after retroviral transduction of LNCaP cell with the RAI2 expression vector pMXs-IP-RAI2 or the empty vector. HSC70 protein was detected as loading control. Representative pictures of RAI2-OE cells after staining against RAI2 (orange), AR (green) protein and the cells nuclei (blue). **B**, Immunofluorescence staining of RAI2 (red) and CtBP1 (green) protein in VCaP cells, treated with 10 µM enzalutamide for 10 days. Nuclei were stained with DAPI (blue). Merge shows overlap of all channels.

## 3.5 Establishment of a *RAI2*-gene knockout in human LNCaP cell line by CRISPR-Cas9 editing

Due to a rapid recovery of RAI2 expression in human breast and prostate cancer cells, it was of interest to establish cell lines with a stable RAI2 knockout in order to enable long term experiments. For this purpose a RNA-guided Cas9 nuclease from the microbial clustered regularly interspaced short palindrome repeats (CRISPR) adaptive immune system of *S. pyogenes* was used to edit the RAI2 gene following the protocol of Ran et al.[127]. In brief, a specific 20-nt sequence targeting the first exon of *RAI2* was cloned by Dr. Stefan Werner into the Cas9 guide RNA of pSpCas9(BB)-2A-GFP (PX458) expression plasmid before transfecting it into parental LNCaP cells. The GFP reporter gene within the plasmid allowed Fluorescence-activated cell sorting (FACS) of single GFP positive cells. After clonal expansion of five single cells, the *RAI2* gene editing was analysed by sequencing, showing either one base pair deletion in cells of Clone 1, 2 and 4 or an insertion of one base pair in Clone 5. Sequence of Clone 3 showed a base pair insertion and a base pair exchange (Fig. 3-7, A). Indel mutations within the coding sequence resulted in a

frameshift and creation of a premature stop codon leading to knockout of *RAI2* gene. Complete loss of RAI2 protein expression was verified via Western blot analysis in all tested clones (Fig. 3-7, B). For further characterization of the LNCaP RAI2-knockout cell, a pool consisting of equal amounts of each clone was created and is further referred to as LNCaP RAI2-KO cell line.

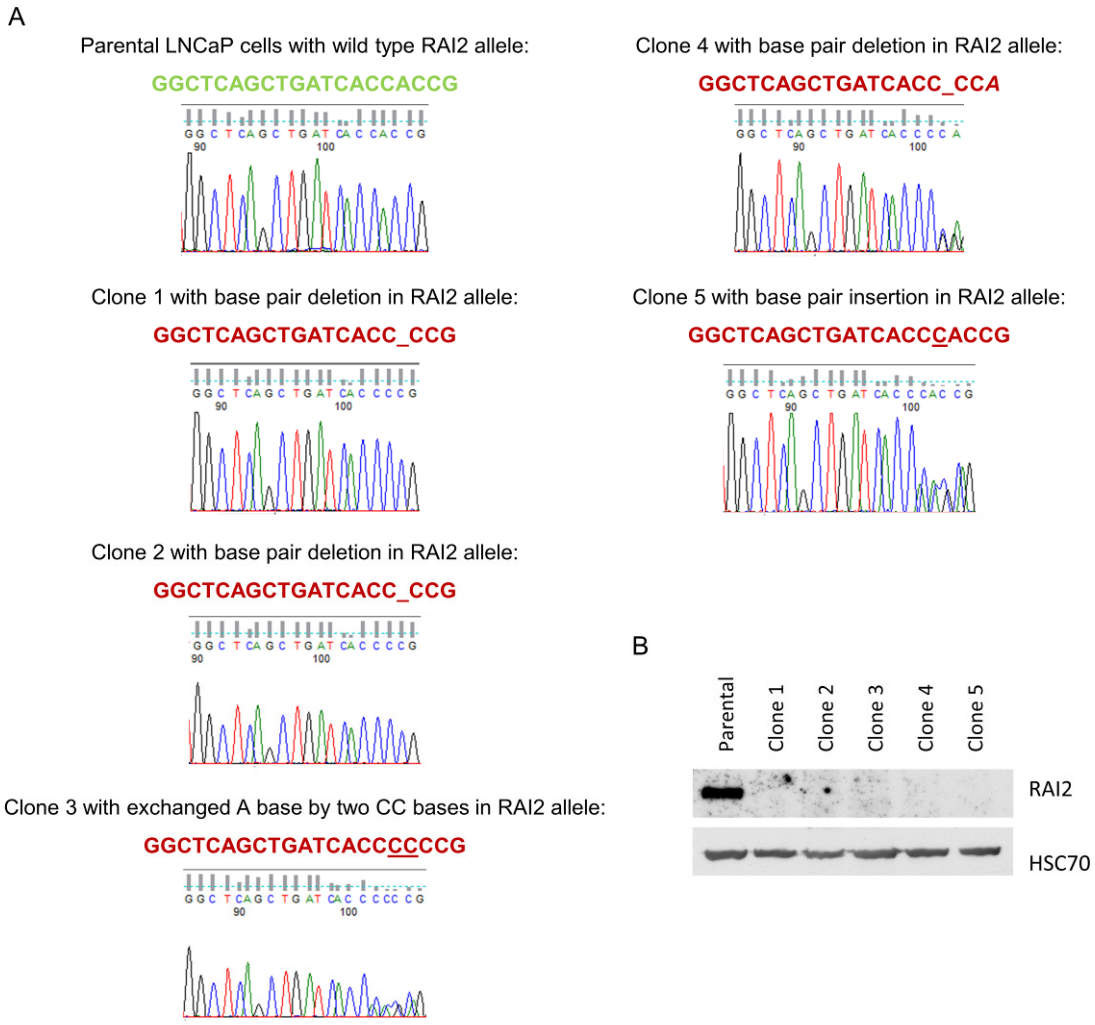


**Fig. 3-7** Validation of a LNCaP cell line with RAI2 knockout. **A**, Sequencing of a 20 bp region(+ to bp downstream of) of the first exon of *RAI2* gene, which is targeted by the Cas9 nuclease. Wildtyp sequence of parental LNCaP cells is shown in green, while mutated sequences of the Clone 1-5 are highlighted in red. Underline indicates a change in the sequence. Letter marked in italics in the sequence of Clone 4 , shows poor sequencing quality. **B**, RAI2 protein expression determined by Western blot in parental and CRISPR/Cas9 modified cells (Clone 1-5). To stimulate RAI2 expression, cells were grown in hormone free culture medium for 10 days before whole cell extracts were prepared. HSC70 was detected as loading control.

## 3.6 Androgen response in RAI2-depleted LNCaP cells

Due to suspected link between RAI2 and hormone receptor, Alexandra Weglarz has previously analysed the influence of shRNA-mediated RAI2-knockdown on the expression of androgen receptor target in VCaP cells genes using RT$^2$ PCR Arrays and identified the induction of several genes, especially the serine/threonine-protein kinase *SGK-1* and the membrane metallo-endopeptidase (*MME*)[123]. To investigate, whether the previous identified changes in mRNA expression of AR target genes could be validated in LNCaP cells, parental and RAI2-KO cells were grown in hormone deprived medium (HD) to reduce the AR-activity before stimulating the AR with dihydrotestosterone (DHT) for 24 h. RNA from cells of both conditions was reverse transcribed into cDNA and expression of the selected targets *PSA*, *SGK-1* and *MME* was analysed by quantitative PCR. Additionally, differential transcription of those genes was assessed under normal growth conditions in RPMI medium. Fold change relative to parental gene expression in RPMI medium was calculated by $2^{(-\Delta\Delta CT)}$-method after normalization to RPLP0. The knockout of RAI2 resulted in a significant induction of *PSA* and *SGK-1* mRNA in RPMI growth medium. In addition *PSA* mRNA expression was significantly reduced after hormone deprivation and recovered to significantly higher levels after stimulation with DHT in parental and RAI2-knockout cells. However, neither other could significant differences be observed between parental and RAI2-knockout cells nor between the different growth conditions for *MME* and *SGK-1* expression (Fig. 3-8). To summarize, complete RAI2 depletion in LNCaP cells did not show the same effect on AR target gene expression as for VCaP cells after partial reduction of RAI2 .

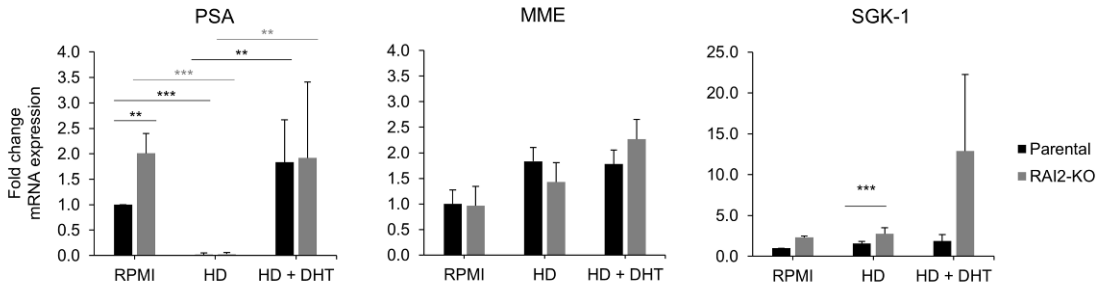


**Fig. 3-8** Gene expression analysis of *PSA*; *MME* and *SGK*-1 gene in parental and RAI2-KO LNCaP cells in normal growth medium (RPMI), in hormone-free medium (HD) and after AR-stimulation with 3 µM DHT. Fold change relative to parental expression in RPMI medium was calculated by $2^{(-\Delta\Delta CT)}$-method after normalization to the reference gene RPLP0.

## 3.7 Viability of RAI2 modified prostate cancer cells

Tumorigenesis is a multi-step process that converts normal cells through sequential accumulation of mutations and phenotypic changes into malignant cancer cells. The most essential phenotypic characteristics required for neoplasia formation and progression are described by HANAHAN and WEINBERG in the hallmarks of cancers[6]. One main hallmark of cancer cells is to sustain proliferation signalling and evade growth suppression. The maintenance of cell proliferation and viability over time is measured *in vitro* based on biochemical events specific to living cells[133]. To study proliferation as a function of the RAI2 protein, viable cells were defined based on their metabolic activity and ability to reduce the MTT-tetrazolium dye into purple coloured, water insoluble formazan. Optical density of formazan was measured with a plate reader after dissolving it with DMSO. The MTT-assay was performed with MCF-7 breast cancer cells or the VCaP and LNCaP prostate cancer cells with a somatic knockout of RAI2 protein, which was either established prior to this study or within (see 3.5). Furthermore the effect of RAI2 overexpression was analysed in PC-3 prostate cancer cells after retroviral transduction of the cells with the pMXs-IP-RAI2 vector. The successful modification of cells was verified by Western blot, analysing RAI2 protein expression under normal or RAI2 inducing growth conditions, see figure 3-9.

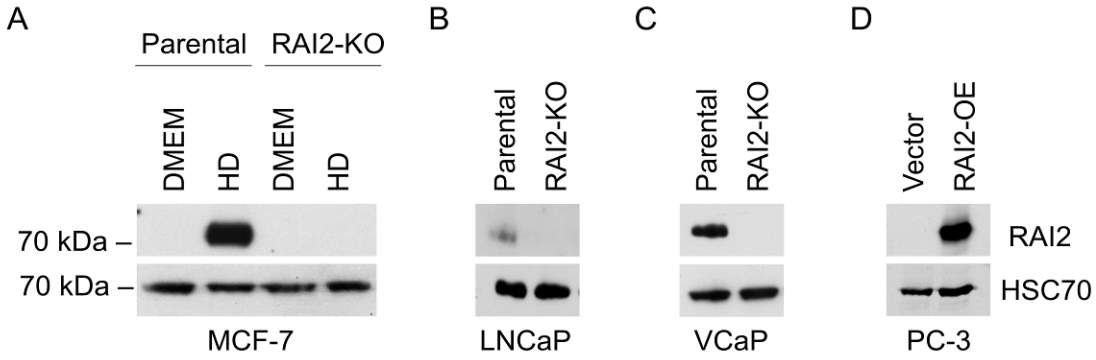


**Fig. 3-9** Western blot analysis of RAI2- modified cell lines used in this study. **A**, RAI2 knockout verification in MCF-7 cells after CRISPR/Cas9 genome editing. Cells were grown in hormone deprived (HD) medium for induction of RAI2 protein. Western blot analysis was performed by Jana Jensen[134]. **B**, RAI2 protein expression in LNCaP parental and LNCAP RAI2-KO cells line, introduced in section 3.4. **C**, RAI2 protein expression in parental VCaP cells and cells with RAI2-knockout, which were established by Alexandra Weglarz using CRISPR/Cas9 method. **D**, Overexpression of RAI2 protein in PC-3 prostate cancer cell line after transduction of parental cell with the pMXs-IP-RAI2 or the empty vector for control purposes.

### 3.7.1 Cell viability of MCF-7 breast cancer cells with RAI2-KO

Prior work at our institute demonstrated that loss of RAI2 protein contributed to an increased viability of KPL-1 breast cancer cells under ER inhibiting conditions. To test this observation in a second ERα positive breast cancer cell lines, the viability of MCF-7 cells with complete RAI2 depletion was tested in standard DMEM growth media or under growth suppressing conditions, either in hormone deprived growth medium or medium supplemented with the ERα-specific inhibitors tamoxifen (TAM) and fulvestrant (ICI). Additionally, our research group has shown that shRNA-mediated depletion of RAI2 leads to the activation of the proliferation activating Akt-kinase in KPL-1 and MCF-7 cells[118]. These results the reason for studying whether the inhibition of the Akt kinase and the downstream mTOR kinase will directly affect the viability of RAI2-knockout cells. Interestingly, RAI2-KO cells showed a significantly increased viability under complete hormone free conditions ($p = 0.0007$), but no proliferative differences compared to parental cells after specific inhibition of the oestrogen receptor by TAM and ICI. On the other hand, inhibition of the Akt/mTOR axis lead, to a decreased viability of RAI2-KO cells, reaching significant changes after mTOR kinase inhibition with RAD001 ($p = 0.04$; MK2206, $p = 0.055$). The drug solvent DMSO was added to DMEM growth medium as a control for specific effect of the used inhibitors and should be comparable to cell viability in DMEM medium, which was increased in RAI2-KO cells, but didn't hit significance as in DMSO supplemented medium (Fig. 3-10).

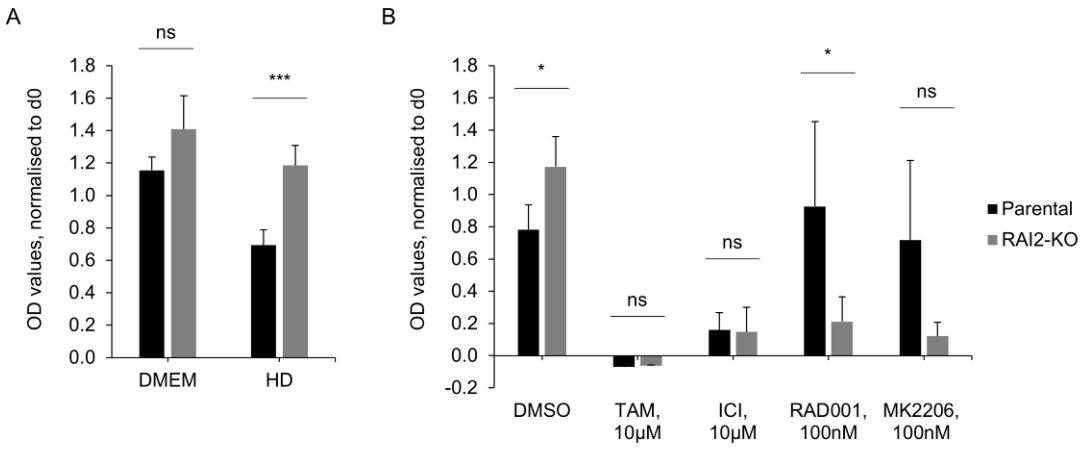


**Fig. 3-10** Cell viability of RAI2 depleted MCF-7 cells after inhibition of the ER or the Akt/mTOR proliferation pathway. **A**, MTT-assay was used to compare cell viability of parental and RAI2-knockout (RAI2-KO) under standard growth conditions (DMEM) as well as complete hormone withdrawal (HD). **B**, Likewise, impact of ER inhibitors, tamoxifen (TAM), fulvestrant (ICI) or the Akt/mTOR inhibitors RAD001and MK2206 was analysed by supplementing the inhibitors into growth medium at the indicated concentrations. DMSO was used as a diluent for the substances and thus served as a control for specific inhibition. Cells were grown in quadruplicates for 10 days before they were analysed. *P* values were calculated with a two sided Student *t* test. *$p < 0.05$, ***$p < 0.001$, ns: not significant

### 3.7.2 Cell viability of LNCaP and VCaP prostate cancer cells after RAI2-KO

The viability of LNCaP and VCaP cells with RAI2 complete depletion was tested in standard RPMI or DMEM growth media or under growth suppressing conditions. Thus, similar to the MCF-7 breast cancer cell line, cells were grown in hormone deprived growth medium or medium supplemented with the AR specific inhibitors bicalutamide (BIC) and enzalutamide (ENZ) or the Akt and mTOR kinase inhibitors MK2206 and RAD001. Additionally, the cell growth of RAI2 KO cells under treatment with taxane-based cytotoxic drugs docetaxel and paclitaxel was investigated. The knockout of the RAI2 gene significantly increased LNCaP cell viability under normal and DMSO control condition (p= 0.013, and p= 0.012, respectively) (Fig. 3-11, A and B). Furthermore, a significantly higher viability of RAI2-KO cells was maintained under the suppressive action of all tested inhibitors with the exception of enzalutamide (Fig. 3-11, B). In contrast, RAI2-knockout in VCaP cells did not lead to any significant changes in cell viability under normal or most of the tested, growth inhibiting conditions (Fig. 3-11, C and D). Moreover, RAI2 loss resulted in a higher sensitivity to BIC and RAD001 treatment, as shown by significantly decreased viability compared to parental VCaP cells (Fig. 3-11, D).

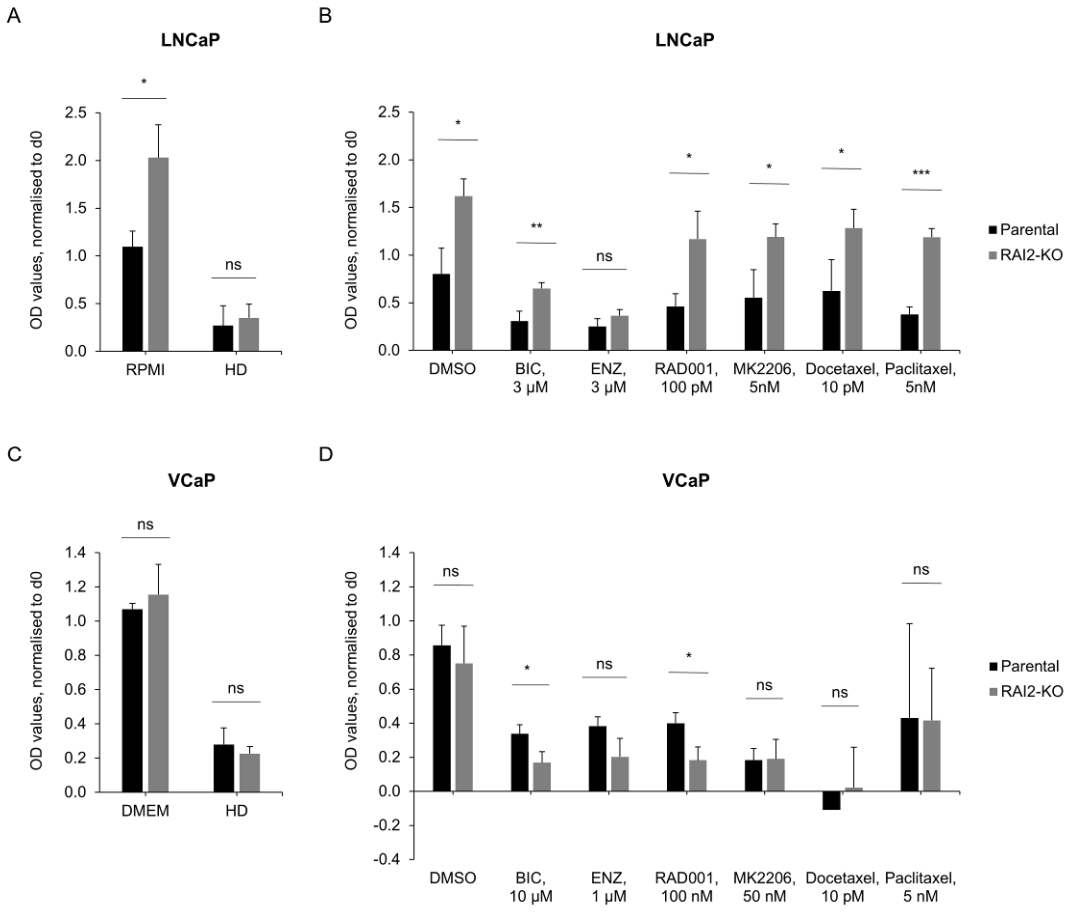


**Fig. 3-11**. Cell viability of RAI2 depleted PCa-cells after inhibition of the AR or the Akt/mTOR proliferation pathway and the cell cycle. **A,C**, MTT-assay was used to compare viability of parental LNCaP and VCaP

cells with the corresponding RAI2-knockout cells (RAI2-KO) under standard growth conditions (RPMI or DMEM, respectively) or complete hormone depletion (HD). **B**, Furthermore, impact of the AR inhibitors bicalutamide (BIC) and enzalutamide (ENZ), the Akt/mTOR inhibitors RAD001and MK2206 and the cytostatic drugs docetaxel and paclitaxel on cell viability was analysed by supplementing the inhibitors into growth medium at the indicated concentrations. DMSO was used as a control for specific inhibition. Cells were grown in quadruplicates for 10 days before they were analysed. *P* values were calculated with a two sided Student *t* test. *p < 0.05, **p < 0.01, ***p < 0.001, ns: not significant

### 3.7.3 Cell viability of PC-3 prostate cancer cells with RAI2 overexpression

Parental PC-3 prostate cancer cells, expressing low protein levels of RAI2, were transduced with retroviral particles harbouring either the pMXs-IP-RAI2 or the empty vector to generate RAI2 overexpressing (RAI2-OE) cell line or its control counterpart (Fig. 3-9, D). MTT assay was performed to test whether elevated levels of the RAI2 protein are able to make the aggressive PC-3 cell line more susceptible to the prior introduced Akt/mTOR inhibitors or to the taxane-based chemotherapeutics. Figure 3-12 shows that the RAI2 protein introduction did not affect the cell viability of PC-3 cells, which was tested in four independent experiments. The anti-androgens BIC and ENZ were tested only in one experiment and were excluded due to failing inhibition of cell viability under saturated concentrations, verifying hormone-independent growth of this cell line even after RAI2 overexpression.

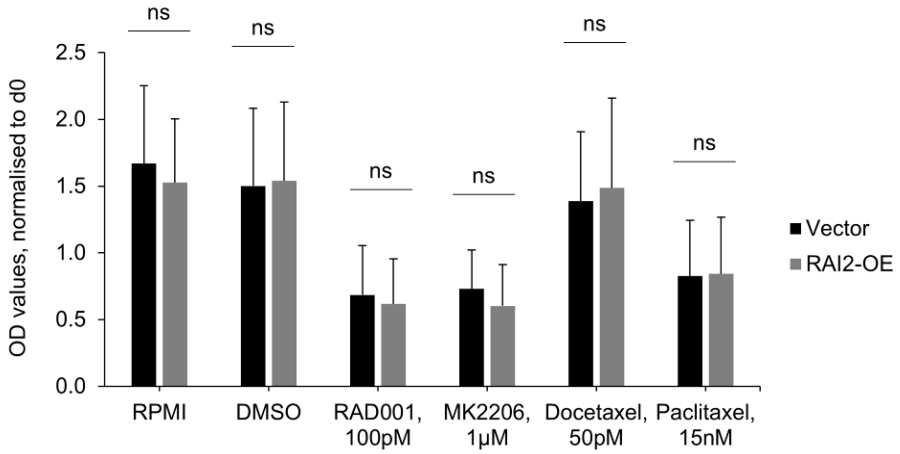


**Fig. 3-12** Cell viability of RAI2 overexpressing PC-3 cells after inhibition of the Akt/mTOR pathway and the cell cycle. Parental cells were infected with lentiviral particles, harbouring RAI2 coding sequences or an empty control vector to establish a RAI2 overexpressing (RAI2-OE) or control (Vector) PC-3 cell line. Cells were either grown in RPMI growth medium or treated for 5 days with the Akt and mTOR inhibitors RAD001 and MK2206 or the cytostatic drugs docetaxel and paclitaxel before cell viability was assessed by MTT assay. Concentrations used are shown in the figure. An appropriate volume of DMSO was used as control. *P* values were calculated with a two sided Student *t* test. ns: not significant

## 3.8 Colony formation ability of RAI2 modified cells

Another common *in vitro* assay to test the survival of cells is the colony formation assay. As the name suggests, the assay tests the ability of individual cells to undergo sufficient proliferation to form colonies[135]. While the MTT-assay as a short term, high-throughput assay is measuring early functional changes, the colony formation assay is a more robust long term assay that provides information on overall toxicity of treatment. Thus, it is recommended to use both assays for the assessment of cellular sensitivity to cytotoxic treatments[136]. For the colony formation assay, RAI2 modified LNCaP or PC-3 prostate cancer cells were dissociated into single cell suspension and plated at low density prior to treatment with the in section 3.7 introduced inhibitors and cytostatic drugs. After 14 or 7 days, LNCaP and PC-3 colonies were stained with crystal violet and area covered by the colonies was determined using Image J[128]. Multiple washing steps and low attachment of VCaP cells to culture surface made it impossible to assess reliable results for this cell line.

### 3.8.1 Clonogenic ability of LNCaP cells with RAI2-knockout

The ability of LNCaP cells to form colonies under normal and control condition as well as under treatment with both androgen receptor inhibitors, bicalutamide(BIC) and enzalutamide (ENZ), was significantly increased after RAI2 loss ($p= 0.009$, and $p=0.041$). Furthermore the knockout of the RAI2 protein led to a significantly decreased sensitivity of LNCaP cells to the cytostatic drugs docetaxel ($p= 0.011$) and paclitaxel ($p= 0.032$). After five independent experiments, no significant changes in clonogenicity of parental and RAI2-KO cells were observed after complete hormone deprivation and inhibition of the Akt/mTOR signalling (Fig. 3-13).

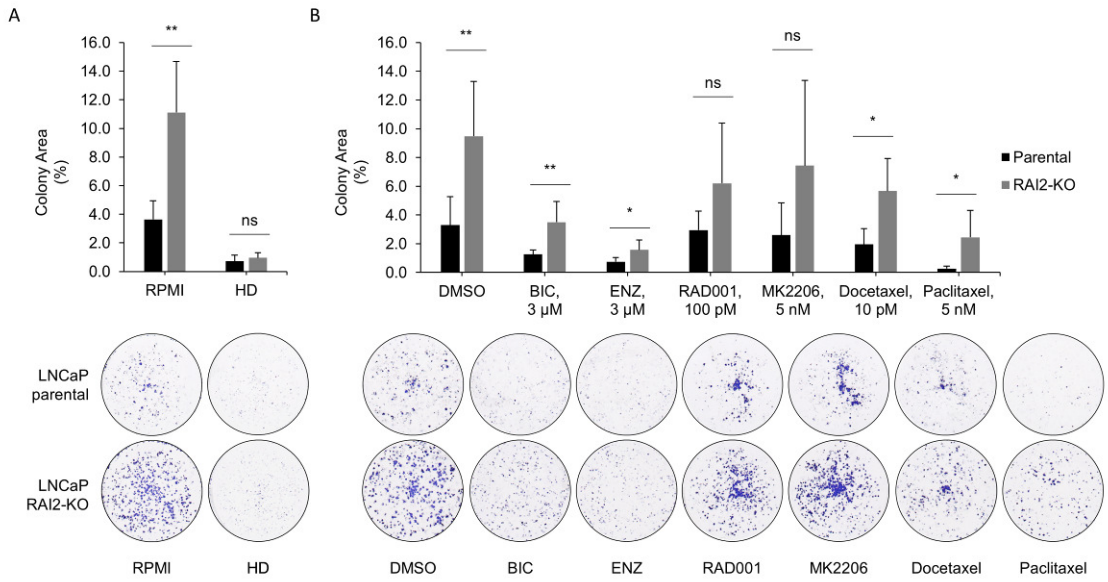


**Fig. 3-13** Colony formation of LNCaP cells after inhibition of proliferation controlling processes. **A**, To compare the clonogenicity of parental and RAI2- knockout (RAI2-KO) cells in RPMI growth medium and hormone free-medium, the colony formation assay was used. **B**, Clonogenic capacity of parental and RAI2-KO cells was further measured after treating the cells with indicated concentrations of the AR-Inhibitors bicalutamide (BIC) and enzalutamide (ENZ), the Akt/mTOR inhibitors RAD001and MK2206 and the cytostatic drugs docetaxel and paclitaxel. As a control for specific inhibition the drug solvent DMSO was used. For both partial images cells were grown for 14 days in 6-well plates and colonies were stained with crystal violet, as shown in corresponding well images in lower figure panel. Image J was used to determine the percentage area covered by the colonies. Average was calculated out of five independent experiments and statistical significance was tested with a two sided Student *t* test. *p < 0.05, **p < 0.01, ***p < 0.001, ns: not significant

### 3.8.2 Clonogenic ability of PC-3 prostate cancer cells overexpressing RAI2

The clonogenicity of RAI2 overexpressing PC-3 cells (Fig. 3-9) and its vector control cells was assessed after 7 days of growth in RPMI growth medium and in the presence of the Akt and mTOR inhibitors MK2206 and RAD001 or the cytostatic drugs docetaxel and paclitaxel. No significant differences were observed between the tested cells in either growth condition (Fig. 3-14).

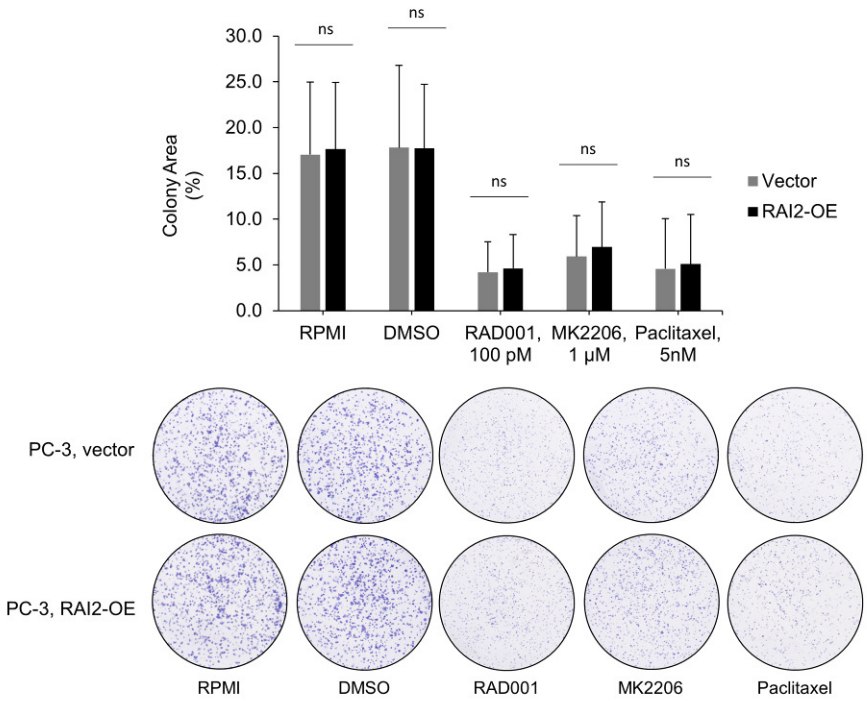


**Fig. 3-14** Colony formation of PC-3 cells overexpressing RAI2. Clonogenic capacity of PC-3 cells, that were retroviral transduced to obtain a RAI2 overexpressing (RAI2-OE) and a control (Vector) cell line, was analysed with the colony formation assay. Cells were grown either in RPMI growth medium or medium supplemented with 5 nM paclitaxel or the solvent DMSO as a control for 7 days in 6-well plates before colonies were stained with crystal violet, as shown in corresponding well images in lower figure panel. Image J was used to determine the percentage area covered by the colonies. Average was calculated out of three independent experiments and statistical significance was tested with a two sided Student *t* test. ns: not significant

### 3.8.3 Analysing LNCaP cell recovery after reintroduction of RAI2 protein into RAI2-KO cells

In order to test whether the reintroduction of RAI2 protein expression into RAI2 knockout cells might decrease the clonogenic capability of those cells back towards the parental level, RAI2-KO cells were retroviral transduced with the RAI2 expression plasmid, pMXs-IP-RAI2 or infected with the empty vector as control. After 14 days growing in RPMI growth medium colonies were stained and average area covered by colonies from three independent experiments was calculated. Increased clonogenicity of RAI2-KO cells, as described in chapter 3.7.2, could be confirmed within this experiment. However, overexpression of RAI2 protein did not lead to a change in clonogenic ability of RAI2-KO cells, and thus to no recovery of the cells from complete RAI2 depletion after RAI2 restoration (Fig. 3-15).

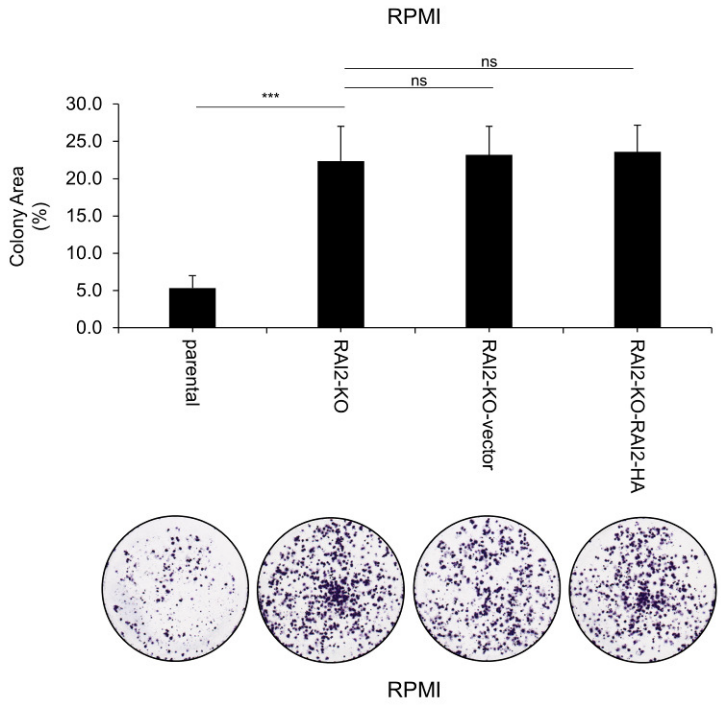


**Fig. 3-15** Colony formation of LNCaP cells with a RAI2 knockout after reintroduction of RAI2 protein expression. **A**, RAI2 protein overexpression (RAI2-OE) in LNCaP cells with RAI2 complete loss (RAI2-KO) was verified by Western blot. **B**, Colony formation assay was performed to compare the clonogenicity of RAI2-KO cells and RAI2-KO cells with RAI2-overexpression (RAI2-KO/RAI2-OE) under normal growth conditions in RPMI medium. Parental cells and RAI2-KO cells transduced with empty vector served as control. Cells were grown for 4 days in 6-well plates before colonies were stained with crystal violet, as shown in corresponding well images in lower figure panel. Image J was used to determine the percentage area covered by the colonies. Average was calculated out of three independent experiments and statistical significance was tested with a two sided Student *t* test. ***$p < 0.001$, ns: not significant

## 3.9 Anchorage independent growth of RAI2 modified cells

As normal cells undergo a particular type of apoptotic death, called anoikis, when they detach from the extracellular matrix, the soft agar assay is used to determine anchorage independent proliferation, as a hallmark of tumorigenesis[137]. Furthermore, the soft agar assay is considered as the most rigorous assay to test and confirm tumour suppressive function of signalling proteins *in vitro* and is often predictive of tumorigenicity *in vivo*[129,133]. To test weather RAI2 loss in LNCaP or its overexpression in PC-3 prostate cancer cell line changes the cells capability to grow and proliferate without binding to a surface, single cells were grown in a layer of soft agar mixed with growth medium on top of a lower layer with denser agar. Figure 3-16, A shows that loss of the RAI2 protein enabled significantly more LNCaP cells to form colonies in an anchorage independent manner ($p = 0.033$), suggesting them to be more tumorigenic than the parental cells. However,

the overexpression of the RAI2 protein in PC-3 cells did not lead to any significant changes in growth and cell division under this environment.

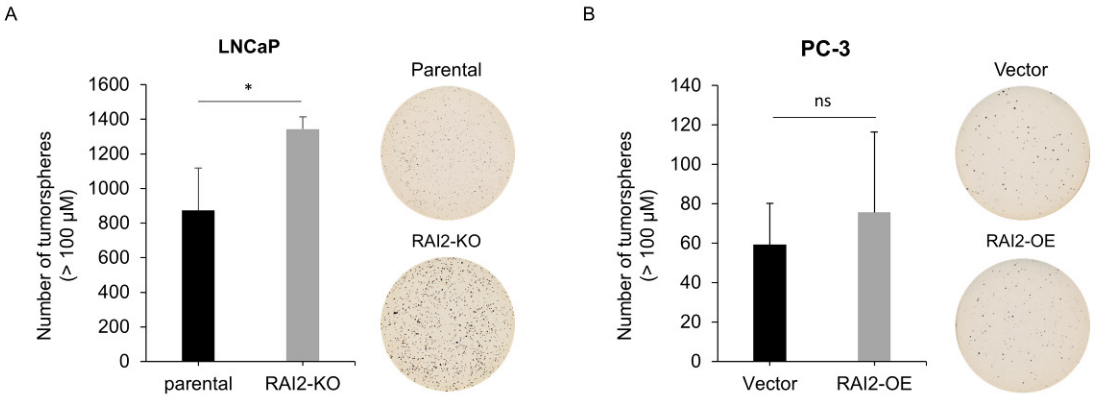


**Fig. 3-16** Anchorage independent growth of RAI2 modified LNCaP and PC-3 prostate cancer cells. **A**, Soft agar assay was performed with parental and RAI2-knockout (RAI2-KO) LNCaP cells in three independent experiments. **B**, Effect of RAI2 overexpression on anchorage independent growth of PC-3 cells was examined in four independent runs. Images from individual wells of one representative experiment each are shown. Columns represent the average number of tumour spheres, which were determined with Image J. Statistical significance was calculated with two sided Student *t* test. *p < 0.05, ns: not significant

## 3.10 Cell motility of RAI2 modified cells

The activation of metastasis was monitored as the next hallmark of cancer with the transwell migration assay which allows to analyse the migratory capacity of cells. Migration is hereby defined as the vertically directed movement of cells through a 8.0 µm porous membrane along a chemotaxic gradient within 24 hours. Migrated cells were visualized with crystal violet and counted under an inverse microscope. Significantly increased cell migration was observed in LNCaP cells after the knockout of RAI2 expression (p= 0.008) (Fig. 3-17, A). Correspondingly constitutive RAI2 overexpression in PC-3 cells reduced cell migration compared to the control cells (p= 0.114) (Fig. 3-17, B), suggesting a possible role of RAI2 in metastasis formation.

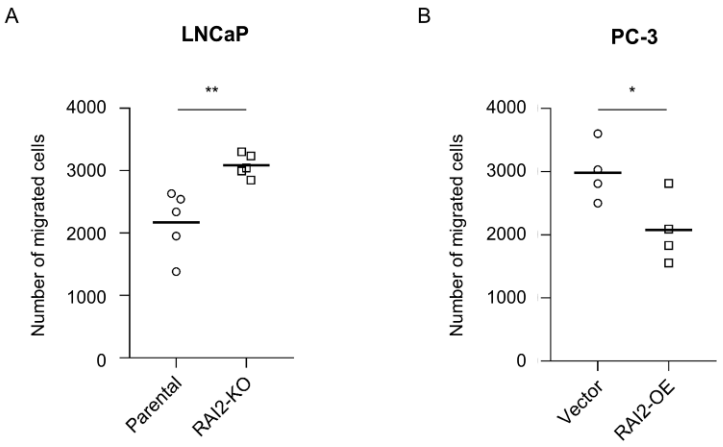


**Fig. 3-17** Cell migration of RAI2 modified LNCaP and PC-3 prostate cancer cells. **A**, Transwell migration assay was performed to analyse cell migration of parental and RAI2-knockout (RAI2-KO) LNCaP cells in four independent experiments. **B**, The effect of RAI2 overexpression (RAI2-OE) on PC-3 cell migration was analysed in five independent experiments. Scatterplots show the counts for each replicate and the data mean is shown in form of a line. Statistical significance was tested with the Mann-Whitney U Test. *$p < 0.05$, **$p < 0.01$

## 3.11 Serine/threonine kinase activity after RAI2-knockout

Viability and colony formation analysis from this study have shown an increased viability and survival of RAI2-depleted MCF-7 and LNCaP cells under specific hormone receptor inhibiting conditions, suggesting a progression toward hormone-independent disease after RAI2 loss. Additionally, parallel analyses carried out by our former master student Christina Zill showed an increased growth of KPL-1 cells in fulvestrant supplemented media, supporting the observation for a second breast cancer cell line. One mechanism of hormone-dependent growing cancer cells to maintain cell proliferation under hormone receptor (HR) inactivating conditions, is to restore HR-signalling by the activation of receptor tyrosine kinases, leading to phosphorylation of HR by downstream activated serine/threonine kinases, resulting in an ligand independent activation of the receptor[56]. To analyse if RAI2 knockout is capable to increase the activity of serine/threonine kinases under hormone receptor repressive condition, parental and RAI2 depleted KPL-1 and LNCaP cells were treated for 10 days with the anti-oestrogen fulvestrant or the anti-androgen bicalutamide before peptide based, functional kinomic profiling was performed with whole cell lysates. Incubation of the STK PamChip array consisting of 140 ser/thr containing peptides, revealed in phosphorylation of several peptides shown in the respective heat maps in the appendix section A. Three peptides showed significantly increased phosphorylation in KPL-1 RAI2-KO cells, whereas one peptide showed significant higher phosphorylation in the parental cells (Fig. 3-

18, A). The analysis of upstream kinases identified increased activation of 8 kinases (ERK2, ERK1, CDK2, caMLCK, MAPK14, MAPK13,CDK6 and CDK3) in the lysates of RAI2-KO KPL-1 breast cancer cells (Fig. 3-18, B).

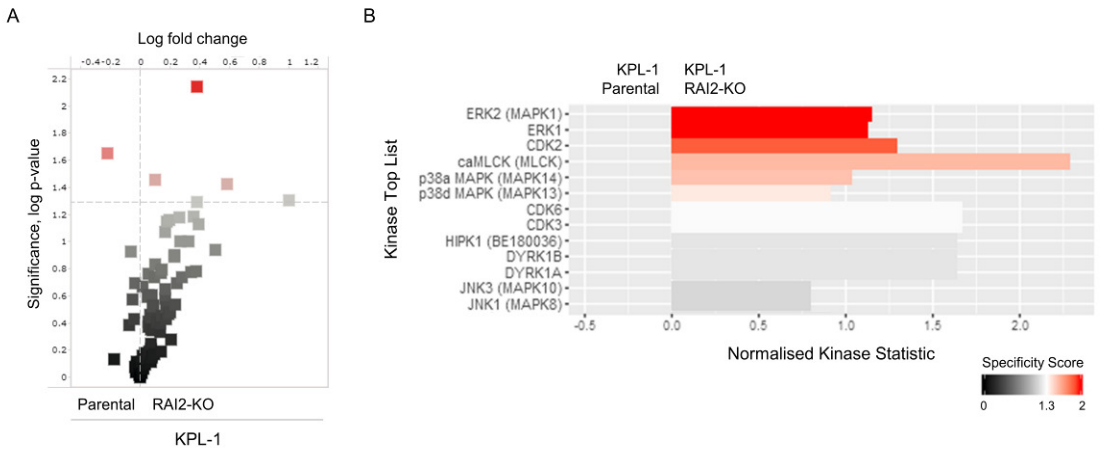


**Fig. 3-18** Comparison of serine/threonine kinase activity in parental and RAI2-knockout KPL-1 cells, treated with 1 µM fulvestrant. **A**, Two-group comparison of parental and RAI2 knockout (RAI2-KO) LNCaP cells shown as a volcano plot. Logarithm of fold change to base 2 >0 represents increased peptide phosphorylation in RAI2-KO cells. Statistically significant changes were identified at a log p-value greater than 1.3, as indicated by the dotted line. **B**, Top 13 differentially activated kinases between parental and RAI2-KO cells are shown after kinase analysis. Normalized kinase statistic >0 reflects a higher kinase activity in KPL-1 RAI2-KO cells. A specificity score >1.3 (white to red bars) assigns statistically significant changes.

The kinomic profiling of parental and RAI2-KO LNCaP cells, revealed only one significantly, differentially phosphorylated peptide after incubation with the lysates of parental cells (Fig. 3-19, A). Upstream kinase analysis showed a significant increased activation of the DCAMKL3, CDKL2 and SgK085 kinases as a result of a RAI2-knockout in LNCaP prostate cancer cells (Fig. 3-19, B).

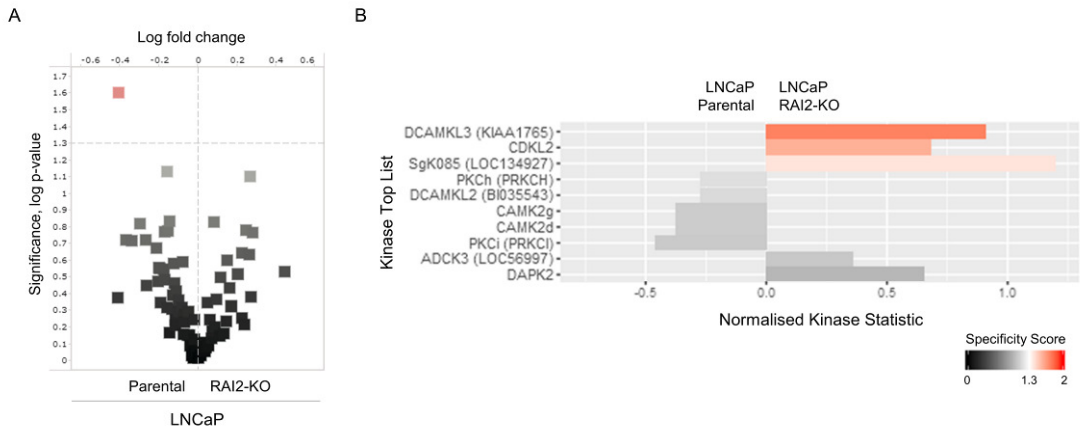


**Fig. 3-19** Comparison of serine/threonine kinase activity in parental and RAI2-knockout LNCaP cells, treated with 3 µM bicalutamide. **A**, Volcano plot of two group comparison of peptide phosphorylation between parental LNCaP cells and cells with a somatic RAI2 knockout (RAI2-KO). Logarithm of fold change to base 2 >0 represents increased peptide phosphorylation in RAI2-KO cells. Statistically significant changes were identified at a log p-value greater than 1.3, as indicated by the dotted line. **B**, Top 10 differentially activated Kinases between parental and RAI2-KO cells are shown after Kinase analysis. Normalized kinase statistic >0 reflects a higher Kinase activity in LNCaP RAI2-KO cells. Specificity score >1.3 (white to red bars) assigns statistically significant changes.

## 3.12 Analysis of tumour progression in a xenograft model

According to the results from section 3.7-3.10, complete depletion of the RAI2 protein leads to increased cell viability and increased capacity to form colonies even under proliferation suppressing conditions, anchorage independent growth as well as an increased migration of LNCaP prostate cancer cells *in vitro*, suggesting a higher tumourigenicity of those cells. To test weather RAI2 loss is also able to promote tumour growth and metastasis formation *in vivo*, either parental or RAI2-KO LNCaP cells were subcutaneously injected into male immunodeficient mice, lacking functional B-and T-lymphocytes and NK-cells due to a double knockout of the recombination activating gene (rag2) and the perforin gene (pfp)[138]. The pfp/rag2$^{-/-}$ mice were killed when the tumours exceeded a size of 1000 mm$^3$. Complete blood was drawn and the Parsotix$^{TM}$ device was used for label-independent enrichment of circulating tumour cells (CTCs) prior to detection by immunofluorescence staining. Additionally, the dissemination of tumour cells into distant organs was analysed using immunofluorescence staining and *Alu*-PCR analysis (performed at the Department of Anatomy by members of AG Lange).

### 3.12.1 Survival Analysis of LNCAP RAI2-KO inoculated

After subcutaneously injection of parental and RAI2-knockout LNCaP cells in to 13 or 16 male pfp/rag2$^{-/-}$ mice, tumour growth was monitored daily for a total follow up period of 232 days. Animals were killed when they were reaching a primary tumour size of 1000mm$^3$, which was the case for 10 and 15 mice inoculated with either the parental or RAI2.KO cells, respectively. Three mice from the parental xenograft group and one mouse from the RAI2-KO group did not reach the event of death within the follow up time. Survival analysis were performed according to Kaplan Meyer estimation in order to analyse the effect of RAI2 expression on the overall survival. Statistical analysis applying the log rank test showed no significant difference in the overall survival between both tested groups (Fig. 3-20).

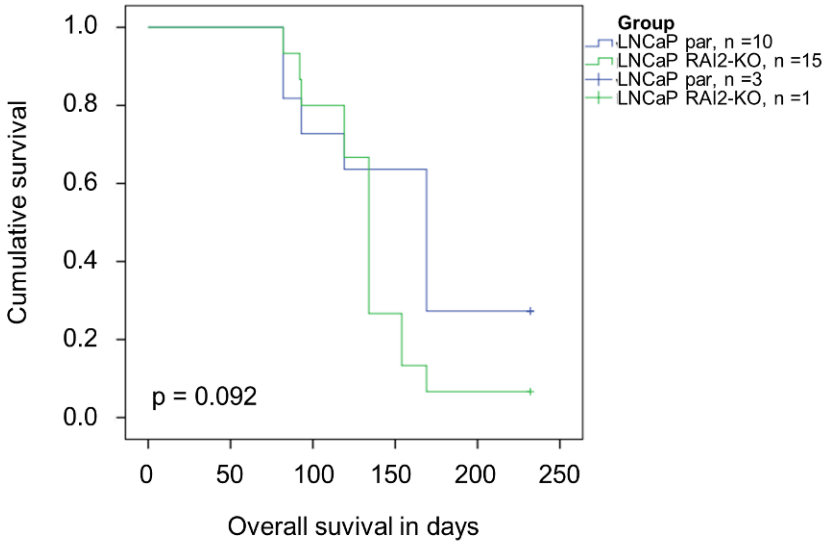


**Fig. 3-20** Kaplan Meyer survival analysis of pfp/rag2$^{-/-}$ mice injected with LNCaP RAI2-KO cells. Comparison of the overall survival of mice harbouring either parental LNCaP cells or cells with somatic RAI2-knockout (RAI2-KO) based on log-rank test. Three mice injected with parental and one mouse with RAI2-KO cells didn't experience the event of death until the termination of the experiment. P-value was calculated by Chi square log rank Test

### 3.12.2 Detection of cell dissemination by IF staining and *Alu*-PCR

In order to find out whether inactivation of RAI2 affects tumour dissemination, whole blood and the bone marrow of sacrificed mice were analysed for the presence of CTC or DTC, respectively. For the enrichment of CTC the Parsotix® system was used, which captures CTCs in a microfluidic cassette, due to their larger size and lower compressibility than other blood cells[139]. Harvested on an objective slide, CTCs were identified by a positive staining for the epithelial markers EpCAM

and pan-keratin and a negative staining for the CD45 leucocyte marker. Due to high degree of cell damage after the enrichment procedure, only three samples per group could be analysed. Figure 3-21 is showing a representative CTC (A) and the number of CTCs detected in 500 µl blood per sample of each group (B). With an average count of 8.3 and 9.3 CTCs, no significant difference was found between the LNCaP parental and RAI2-KO injected mice. Similarly, the analysis of DTCs from the bone marrow revealed no significant difference in the presence of disseminated parental or RAI2-KO LNCaP cells.

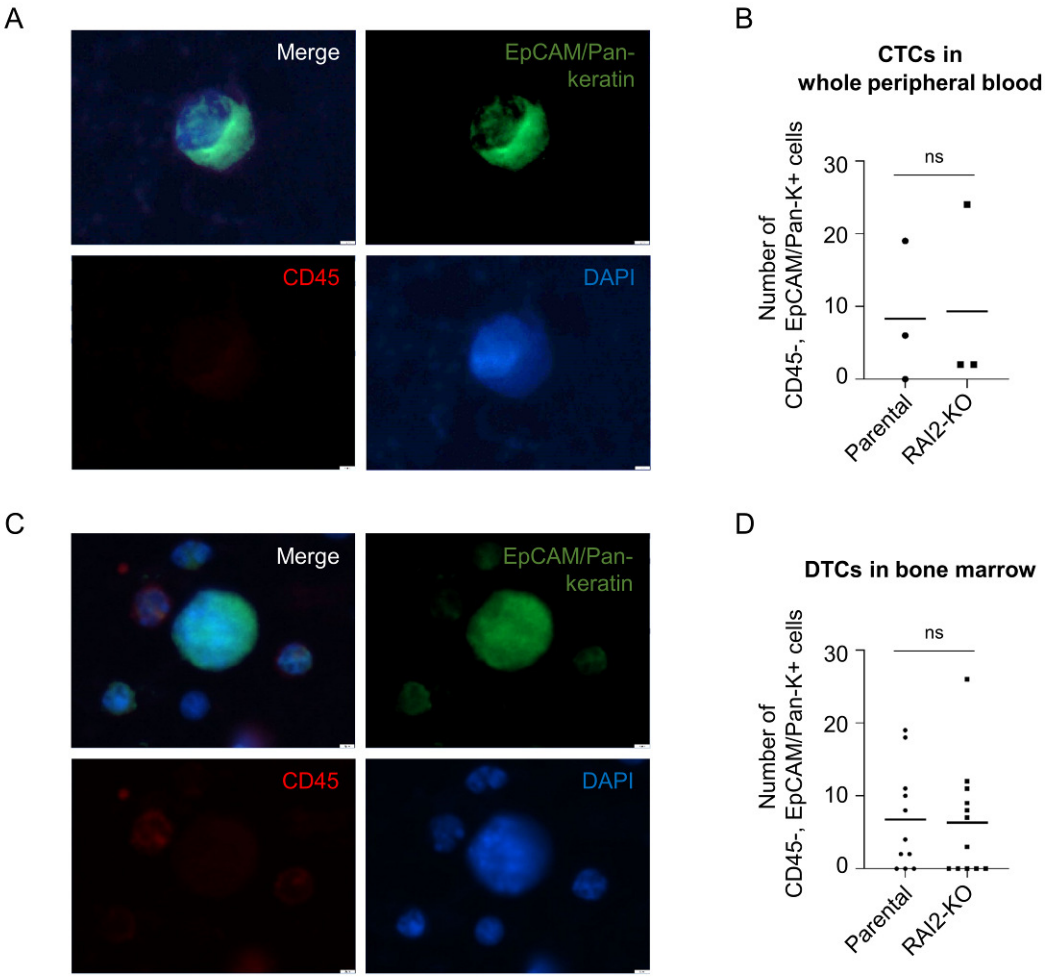


**Fig. 3-21** Detection of CTCs and DTCs in pfp/rag2$^{-/-}$ mice injected with parental or RAI2-KO LNCaP cells. **A**, Representative picture of a CD45-, EpCAM/Pan-K+ CTC. Scale bar in lower right corner of the pictures: 3 µm. **B**, Scatter box plot representing the number of CD45-, EpCAM/Pan-K+ cells counted in three animals per group. **C**, Representative picture of a CD45-, EpCAM/Pan-K+ DTC and surrounding CD45+ leucocytes. Scale bar in lower right corner of the pictures: 3 µm. **D**, Scatter box plot representing the number of CD45-, EpCAM/Pan-K+ cells counted in 11 LNCaP parental or 12 RAI2-KO injected animals. Black line is showing the mean. Statistical significance was calculated with the Mann-Whitney U test. ns: not significant. Scale bar in lower right corner of the pictures: 3 µm.

In collaboration with Prof. Dr. Lange, metastatic spread of parental and RAI2-KO LNCaP cells to the lung and the bone marrow of injected mice was furthermore analysis by a PCR-based detection of human-specific *Alu*-sequences in 60 ng DNA, isolated from the site of interest. The quantity and the mean number of detected DTCs are shown in fig. 3-22, depicting no difference in the DTC amount found in the lung of both groups (A). However, a slightly not significant increased presence of human DTCs could be detected above the detection limit of the assay in the RAI2-KO cells bearing mice group (4/14) than in the group injected with parental cells (1/11) (p= 0.098), implementing that RAI2 night have a role in the homing of cells to the bone marrow.

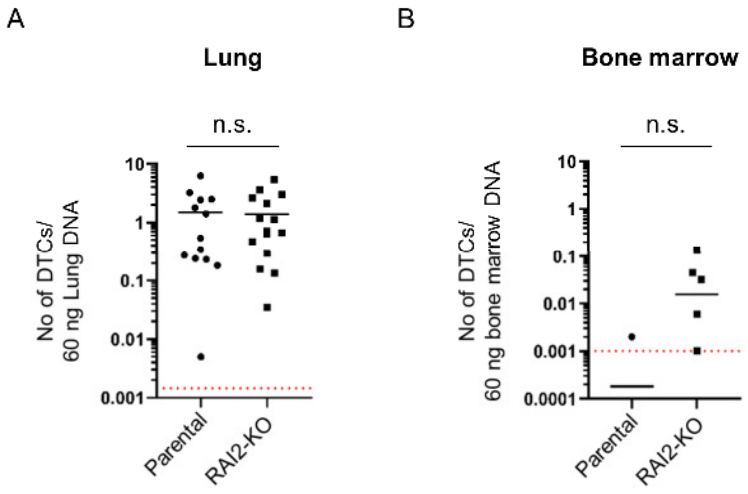


**Fig. 3-22** Metastatic spread of parental and RAI2-KO LNCaP cells to distant organs detected by *Alu*-PCR A, Number of DTCs present in 60 ng lung DNA of 13 parental or 16 RAI2-KO cells injected mice. B, Calculated number of DTCs in 60 ng bone marrow DNA of 11 parental or 14 RAI2-KO cells injected mice. The red dotted line indicated the detection limit for human sequences in murine background as quantified by *Alu*-PCR using standard dilution series. Statistical significance was calculated with the Mann-Whitney U Test. ns: not significant

## 3.13 Establishment of a liquid biopsy test to detect RAI2 expression status in patients

Liquid biopsy can provide molecular details of the cancer phenotype by analysing circulating tumour cells (CTCs), circulating cell free tumour DNA (ctDNA) and other components shed from the primary or metastatic tumours into the patients' blood[107]. One major goal of this study was to establish a liquid biopsy approach, which allows to detect and analyse the RAI2 expression status in existing tumours and to evaluate if RAI2 could be used as a novel liquid biopsy marker for prognostic evaluation of disease progression or therapeutic response.

### 3.13.1 First establishment steps for RAI2 promoter methylation status analysis on ctDNA level

YAN et al. have shown that methylation of RAI2 specific promoter region is associated with loss or reduction of RAI2 expression in colorectal cancer (CRC) cell lines and patients samples. Furthermore, methylation of RAI2 was correlated with poor overall survival in patients with colorectal cancer and increased cell proliferation, invasion and metastasis of CRC cell lines[126]. In order to measure the RAI2 promoter methylation status of ctDNA isolated from blood samples of breast and prostate cancer patients, the methylation of peripheral blood mononuclear cells (PBMCs) had to be excluded first. Therefore PBMCs, which are considered to shed the major amount of cell free DNA into the blood, were enriched from three male (HD 1-3) and two female (HD 4-5) healthy donors before their DNA was isolated and bisulfide converted[107]. During bisulfite conversion unmethylated cytosines are converted to uracil, whereas unmethylated remained unchanged[140]. In subsequent bisulfite specific PCR, primer from YAN et al. were used to amplify a 212 bp CpG island downstream of RAI2 transcription site, resulting in a replacement of all uracil bases by thymine[126,140]. Figure 3-23 is showing the methylation profile of the tested healthy donors, restricted to a CpG fragment used to define the RAI2 methylation status by methylation specific PCR (MSP) in the study of YAN et al. Alignment with the unconverted sequence revealed methylation in the primer region which would lead to amplification with methylation specific primers. Since the methylation of the analysed RAI2 promoter region is not only restricted to malignant cells, the published primers are not suitable for methylation analysis on ctDNA level.

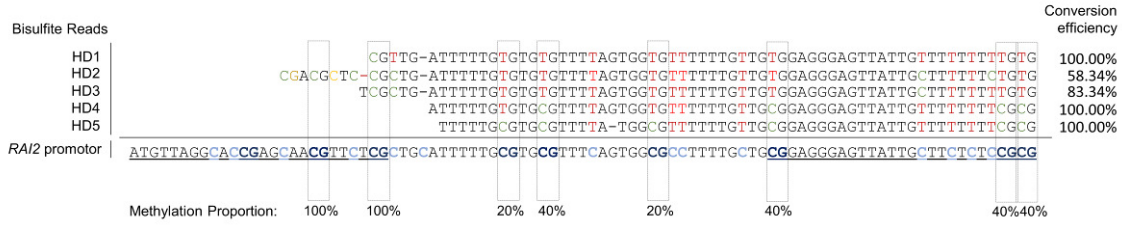


**Fig. 3-23** Methylation profile of RAI2 promotor detected by bisulfide sequencing (BSSQ) in PBMCs of five healthy donors. **A**, Representation of the individual processing steps of the EDTA blood up to bisulfite specific PCR for sequencing. **B**, Bisulfite converted sequence of RAI2 from the PBMCs of five healthy donors (HD1-HD5) was aligned with unconverted sequence. Underlined regions represent the primer region used by Yan et al. for methylation status determination by methylation specific PCR. Conversion efficiency was calculated based on the conversion of light blue cytosines © to red thymdines due to bisulfite conversion and subsequent PCR. Dark blue colour represents the CpG islands prone for methylation. Methylated Cs in are shown in green after bisulfite conversion.

### 3.13.2 Gene expression analysis of CTCs from metastatic prostate cancer patients

In order to find out whether it is possible to detect *RAI2* mRNA expression in circulating tumours cells and to find out if expression correlates with prostate cancer progression, a pilot study including 36 patients with metastatic prostate carcinoma was conducted. In total 40 EDTA blood samples were enriched for CTCs based on the immunomagnetic cell selection system of the AdnaTest ProstateCancerSelect Kit from Qiagen. The mRNA was isolated from enriched cells and transcribed into cDNA by Dr. Laura Keller. Subsequent, cDNA was preamplified before expression of selected transcripts was analysed by qRT-PCR. Next to *RAI2* gene expression analysis, each sample was profiled for expression of *AR, AR-V7, PSA (KLK3), PSMA (FOLH1), HOXB13, MRP1, PI3KCA, EPCAM, EGFR, KRT19, CD45* and the reference genes *GAPDH*, *ACTB* and *HPRT1*. Obtained Cq-values were first compensated for variations between instrument runs and corrected for the presence of genomic DNA before the "GenEx" software was applied to process and analyse the data. Missing data from the reference gene measurements (*GAPDH* value for PCa-24 and *ACTB* value for PCa-17) was replaced using the "impute" option of "GenEx", leading to an interpolation of missing values using information from all samples. Remaining missing data was replaced with a Cq-value of 36. GAPDH was identified by NormFinder (algorithm included in GenEx) as the most stably expressed gene and was further used for ΔCq calculation. For multivariate analysis ΔCq-values were converted for each gene separately into relative quantities, relative to the sample with the maximum Cq (lowest expression) and transformed into logarithmic scale using base 2. Data was mean-centred and analysed by dendogram, heat map and principle component analysis (PCA).

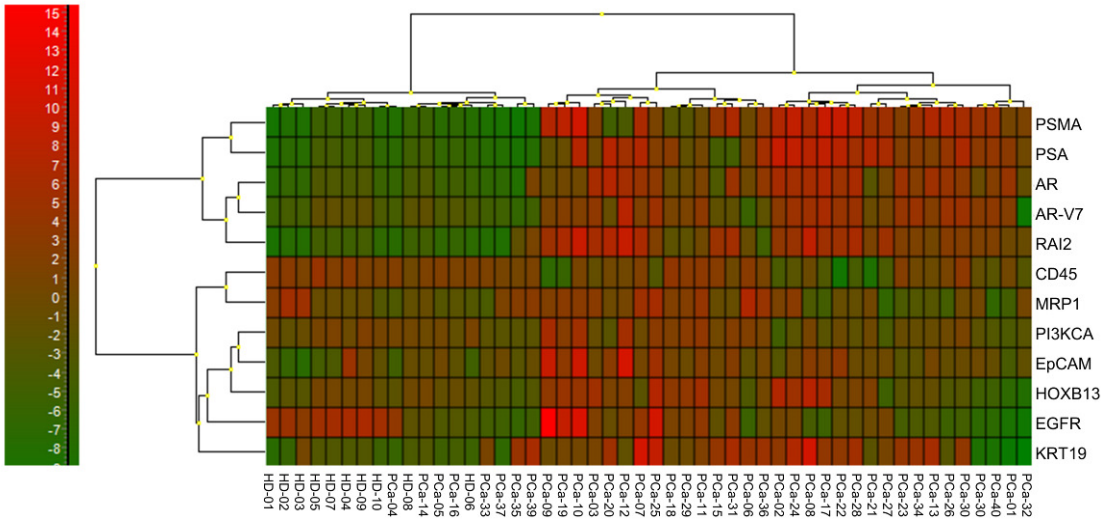


**Fig. 3-24** Classification of analysed genes and CTC samples from healthy donors (HD) and metastatic prostate cancer patients (PCa) visualised with dendograms and a heat map showing expression levels. Red, high gene expression; green, low gene expression

The expression based hierarchical clustering of patient and healthy donor samples grouped eight patients together with all healthy donor samples, indicating a CTC negative status in those samples (Fig. 3-24). CTC positivity for the patients cohort (80%) was mainly characterised by positive expression of *PSMA, PSA, RAI2, AR*, and *AR-V7* and low *CD45* expression, as visualised in fig 3-24.

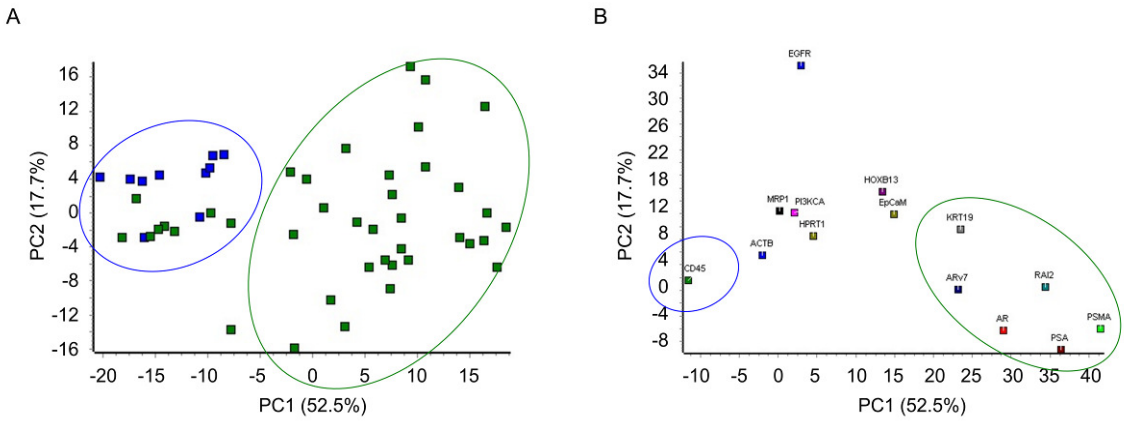


**Fig. 3-25** Classification of samples and genes by principle component analysis (PCA). **A**, AdnaTest enriched samples from healthy donors (blue squares) and prostate cancer patients(green squares) were grouped based on their gene expression profile into two different clusters, separating the CTC negative (blue circled samples) and the CTC positive (green circled samples) samples. **B**, PCA of genes shows the most differentially expressed genes between the groups. Blue circle, genes predominantly expressed in CTC negative cluster; green circle, genes mostly expressed in CTC positive cluster

Furthermore, principle component analysis (PCA) shows a clear separation of the healthy donors and the CTC-negative samples from the CTC-positive samples (Fig. 3-25, A). Moreover, the genes *CD45* and *PSA*, *PSMA*, *RAI2*, *AR* as well as *AR-V7* and *KRT19* show highest influence on PC1 variation and thereby a higher influence on the separation of the analysed samples based on the transcription profile (Fig. 3-25, B). In comparison the gene cluster of *ACTB*, *HRPT*, *MRP1* and *PI3CA* have an lower influence on the separation of the two tested groups, showing a similar distribution between the samples (Fig. 3-25, B).Conspicuously, *RAI2* was clustered in both multivariate analyses with the AR receptors and their target genes *PSA* and *PSMA* expression, supporting the hypotheses of a functional link between RAI2 expression and the hormone response.

The Pearson correlation method was used to measure the linear relationship between RAI2 and the other tested genes. A significantly positive correlation was verified for RAI2 and the hormone response related genes such as *AR*, *AR-V7*, *PSA*, *PSMA*, with coefficients ranging from 0.71 for *AR* to 0.62 for *AR-V7* and corresponding p values below 0.05. A correlation value of –0.38 detected a negative correlation of *CD45* and the *RAI2* mRNA in metastatic prostate cancer patients (Fig. 3-26).

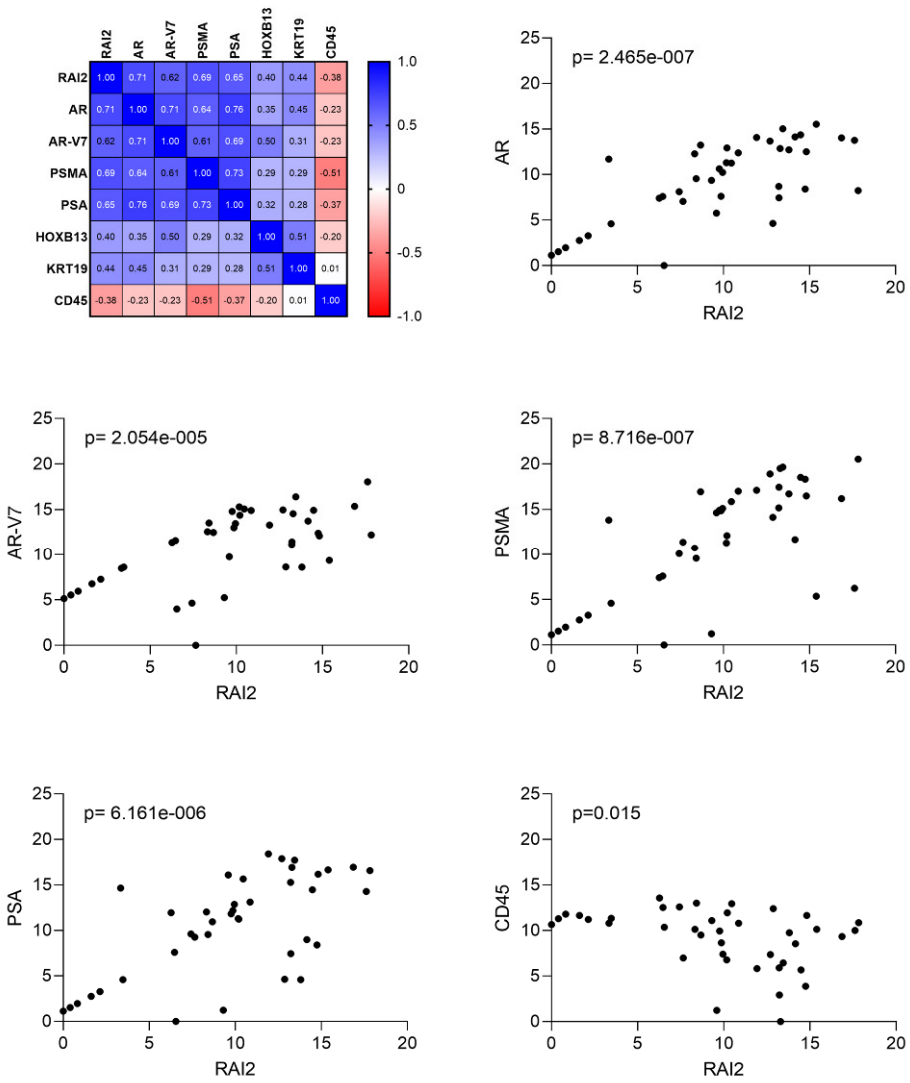


**Fig. 3-26** Pearson correlation. Correlation coefficients visualised in a correlation matrix and scatterplots showing relation between *RAI2* and either *AR*, *AR-V7*, *PSMA*, *PSA* or *CD45* expression in CTCs of metastatic prostate cancer patients.

Furthermore, it was analysed, whether *RAI2* mRNA expression in CTCs is different in patient groups of responder and non-responders to the therapy administered at the time of blood draw. Without dividing the patients to the different therapy applications they received, including chemo-, radio- or hormone therapy, high *RAI2* mRNA in CTCs was significantly associated with no response to treatment and thus with disease progression. A similar trend was obtained correlating *RAI2* mRNA expression with response to hormone therapy (Fig. 3-27, A). Additionally, correlation of *RAI2* mRNA expression with clinical parameters like PSA, lactate dehydrogenase (LDH), alkaline phosphatase (ALP) or haemoglobin (Hb) level in the patients' blood showed a positive week correlation with the serum PSA levels (Pearson's correlation coefficient r= 0.385,

p= 0.017) and a week negative one with the haemoglobin amount (Pearson's correlation coefficient r= -0.395, p=0.016) (Fig. 3-27, B).

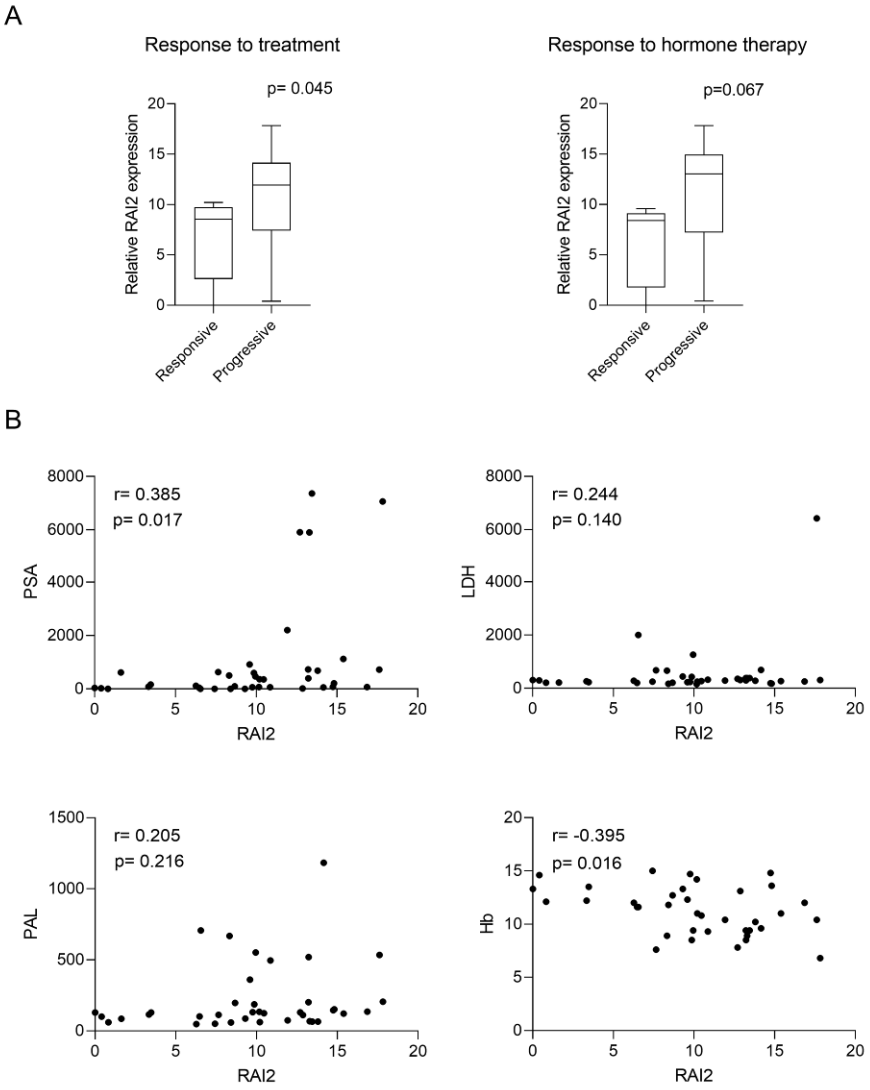


**Fig. 3-27** Correlation of *RAI2* mRNA expression in CTCs with clinical parameters of metastatic prostate cancer patients. **A**, *RAI2* mRNA expression (log2FC) grouped according to response to either any treatment type or hormone therapy at the of blood draw. **B**, Scatterplots showing *RAI2* mRNA expression (log2FC) plotted against serum levels of clinical parameters including PSA(ng/mL), LDH (U/L), ALP (U/L) and Hb (g/dL), which were assessed at time of blood draw. Pearson's correlation coefficient ® and corresponding p-value describing the relationship between the plotted values is visualized within the graphs. PSA, prostate-specific antigen; LDH, lactate dehydrogenase; ALP, alkaline phosphatase; Hb, haemoglobin

In order to analyse a potential prognostic implication of *RAI2* mRNA expression in CTCs on patients overall survival, the patients were divided based on detectable Cq values after qRT-PCR into a RAI2 negative or positive group and analysed by Kaplan Meyer estimations. The corre-

sponding curves in figure 3-28 show a negative correlation of overall survival with *RAI2* expression which did not reaching significance, mirroring moreover the efficiency of treatment in RAI2 negative patients, since *RAI2* expression correlated with progression upon given treatment and with-it with CTCs in the blood of patients.

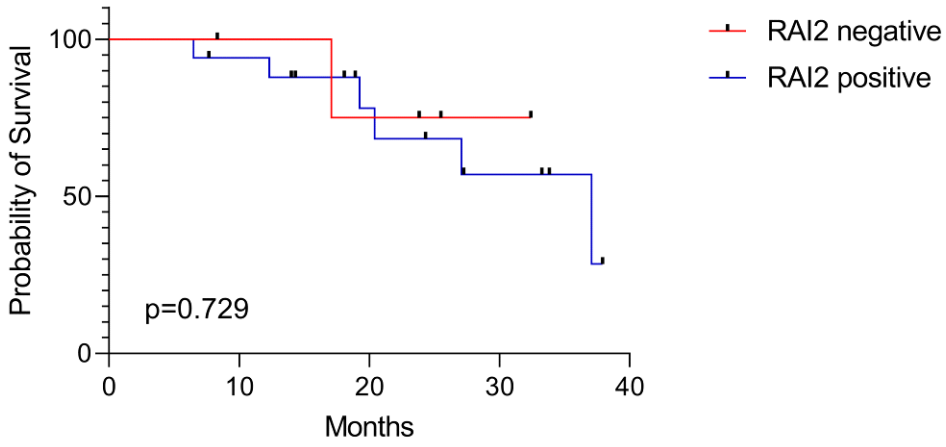


**Fig. 3-28** Kaplan Meyer estimation showing overall survival in months of metastatic prostate cancer patients based on RAI2 expression in CTCs and available follow up data. Patients were divided according to raw expression data (detectable Cq-value) into RAI2-negative (n=5) and RAI2-positive group (n=17). P-value was calculated with the Log-rank (Mantel-Cox) test.

# 4 Discussion

Breast and prostate cancer are the two most frequent cancer types worldwide and are considered to share several biological similarities. These are mainly due to dependency on the steroid hormones, oestrogen and androgen, that are not only responsible for the development and function of the two anatomically different organs, but are also known to drive primary and recurrent breast and prostate cancer, respectively[44]. These hormones exert their effect by binding to their specific hormone receptor, ER for the oestrogens and AR for the androgens, which are transcription factors that regulate in close interaction with a multitude of coregulators the expression of a wide range of target genes[43]. The activation or repression of these target genes in turn is essential for cancer cell viability, proliferation and invasion[141]. Thus the inhibition of ER and AR signalling is the main target of hormonal therapies used in ER-positive breast cancer subtypes and as a standard treatment for prostate cancer. Despite initial response to hormone therapy, most patients with advanced disease develop resistances, while the tumours still continue to rely on the action of the respective hormone receptor[44]. In both cancer entities similar mechanisms have been considered to maintain HR-signalling even under low hormone concentrations[43,44,56]. Increased understanding has led to development of several targeted agents, however develop new resistances and eventually die from their metastatic disease[44,142]. To better control cancer growth in future, further research is needed to elucidate the ER and AR action and the function of the coregulatory proteins involved in the hormone-dependent signalling.

The present study investigated the role of RAI2 in the progression of breast and prostate cancer, focusing on a possible functional link of RAI2 to hormone response and its contribution to hormone therapy resistant disease. The *RAI2* gene was first identified as a novel tumour suppressor gene in breast cancer patients with hormone-dependent disease[118]. Moreover, low RAI2 expression was significantly associated with early occurring bone metastasis and poor patient's outcome[118]. Molecular characterization of the RAI2 protein in the ER-positive, luminal breast cancer cell lines suggests that the RAI2 protein acts as a transcriptional co-regulator involved in differentiation of hormone-dependent breast cancer cells and might play an active part in the transcriptional network of hormonal response[118]. In addition GATTELLI et al. have shown that the introduction of the MMTV-virus into the murine RAI2 gene locus is associated with recurrent and hormone-independent breast cancer in this organism, emphasizing a role for RAI2 in the progression from hormone-dependent to independent tumors.

In concordance with the results in breast cancer cell lines, previous work from our institute have shown that RAI2 is predominately expressed in more differentiated, AR positive and hormone-dependent growing LNCaP and VCaP cells compared to the hormone-independent and more

aggressive PC-3 and DU145 cells. Furthermore, an altered transcription of AR-target genes was detected in VCaP cells after RAI2 depletion. Together, these results point to an overlapping function or even similar functions of the RAI2 protein in both hormone-dependent cancer entities and laid the foundation for this work.

Within the scoop of this study, databank analyses were performed to analyze the prognostic relevance of RAI2 expression in prostate cancer. Modifications of RAI2 expression, pharmacologic inhibitions of the hormone receptors and the identification of potential interaction partners should furthermore contribute to the understanding of the role of the RAI2 protein within the hormone response in breast and prostate cancer cell lines. On the other hand it was investigated whether loss of RAI2 protein is able to increase the tumorigenicity of cancer cells by analyzing their proliferation, susceptibility to pharmacologic inhibition, the migratory capability *in vitro* and the outgrowth and dissemination *in vivo*. Finally, a liquid biopsy test was established to detect the gene expression of RAI2, AR, AR-V7, androgen receptor target genes and other selected genes relevant for PCa-progression in CTCs. The feasibility of this test and its clinical relevance was tested on a pilot study of 36 prostate cancer patients with metastatic disease.

## 4.1 Prognostic relevance of RAI2 based on published datasets

In order to get first impressions of the prognostic relevance of *RAI2* gene expression in prostate cancer, the *RAI2* mRNA expression was analysed in two publicly available GEO datasets at the beginning of this study. In both evaluated datasets, *RAI2* mRNA expression was significantly lower expressed in metastatic prostate tumour tissue compared to localized prostate tumours (Fig. 3-1). Together with the previously cell line analyses previously performed at our institute, that have shown highest *RAI2* expression in more differentiated and less tumorigenic prostate cancer cells, these result are supporting the hypothesis that the expression of RAI2 might play not only play a role in the progression of breast cancer but might also be crucial in the progression of prostate cancer.

## 4.2 Relevance of RAI2 expression on the hormone response

WERNER et al. and GATTELLI et al. were the first to identify a possible causative link of RAI2 and the hormone response. Besides the particular significant impact of low RAI2 expression as a prognostic factor for poor overall survival in ER-positive breast tumours, the RAI2 gene was furthermore suggested to play a role in the progression from hormone-dependent to hormone-independent breast tumours[118,122]. On the molecular level RAI2 protein expression has been shown to

correlated with the ERα status in breast cancer tissue and to be highest expressed in breast cancer cell lines corresponding to the ER-positive, luminal subtype including the KPL-1 and MCF-7 cell lines[118]. In addition, depletion of the RAI2 protein expression in KPL-1 and MCF-7 breast cancer cell lines led to downregulation of ERα protein in both cell lines and to the assumption of a possible functional link between both proteins[118]. In concordance with the breast cancer cell lines, RAI2 expression was predominantly found in AR-positive hormone-dependent VCaP and LNCaP prostate cancer cell lines, whereas the hormone-independent and more tumorigenic PC-3 and DU145 cell lines were negative for both proteins[123]. To test whether depletion of RAI2 has the same effect on the AR protein expression and whether modification of either the ERα or the AR has an impact on the RAI2 expression, the RNAi technology was used to deplete RAI2 or the ERα in KPL-1 and MCF-7 breast cancer cell lines or RAI2 and AR in VCaP and LNCaP prostate cancer cell lines, respectively. The combined results of both breast and prostate cancer cell line experiments revealed a downregulation of the respective hormone receptor protein expression after shRNA-mediated knockdown of RAI2, in accordance with the previously published results. On the other hand, depletion of the ERα or AR induced the expression of the RAI2 protein in all tested cell lines (Fig. 3-2 and 3-3). Even though, the induction was clearly present, it was not significant in MCF-7 and LNCaP cells after Western blot quantification and statistical evaluation of all replicates. However, these results further strengthen the hypothesis of a functional link between RAI2 and the growth promoting hormone receptors by showing an interdependent regulation of the proteins in both cancer entities. Thus, the ERα or AR seem to downregulate the RAI2 protein, while the RAI2 protein stabilises protein expression of the hormone receptor under normal condition in an unknown manner. So far, no ERα or AR binding sites have been found in the RAI2 promoter region, which implies that RAI2 is not directly regulated by either transcription factor. However, two putative AP-2 (activator protein-2) binding domains were identified within the RAI2 promoter, suggesting that the RAI2 expression could be controlled by this transcription factor[120]. Target genes with AP-2 binding sites in their promoter sequence are described as being involved in biological processes like cell growth and differentiation and include, for instance, genes coding for insulin-like growth factor binding protein 5 (IGFBP5) but importantly also the oestrogen receptor[143]. The activity of the AP-2 proteins is controlled at multiple levels, their transcriptional potential, their DNA binding, their degradation and subcellular localisation can be modified by interaction with various proteins[143].

In line with the knockdown experiment, increase of the RAI2 protein could be observed after treatment of both breast cancer cell lines with the anti-oestrogen fulvestrant (ICI), which is known to accelerates the degradation of the ER protein leading to a decreased protein ER level as verified by Western blot in fig.3-4[84]. Similarly, complete hormone removal from the growth medium resulted in a clear, but - due to the strong intensity differences between the replicates - partly not

significant upregulation of the RAI2 protein in the tested breast and prostate cancer cell lines. In terms of the hormone receptor expression, the cells reacted differently to the stress situation caused by the hormone deprivation. While the KPL-1 and VCaP cells significantly induced the ER or AR expression, a reduction of ER in MCF-7 and an unchanged AR level in LNCaP cells could be observed, showing that the cell lines might activate different mechanisms to maintain the growth (Fig 3-4 and 3.-5). In the prostate cancer cells, treatment with the second generation antiandrogen enzalutamide again did not significantly increased the RAI2 protein expression or the AR protein expression which reached significance in the VCaP cell lines (Fig 3-5). Increase of the ER or AR after hormone deprivation has been shown by several studies[144,145]. Based on the knockdown experiments, it might be assumed that the induced RAI2 level may stimulate or stabilize the respective hormone receptor expression, but since the Western blots are only snapshots representing the protein level after ten days of treatment, no conclusions can be drawn about the dynamics of the protein expression. Thus, it would be interesting to analyse the expression of both proteins over a period of time, e.g. hourly or daily. Interestingly, treatment of the prostate cancer cell lines with the first generation antiandrogen bicalutamide significantly decreased the RAI2 protein expression in VCaP cells, but maintained or even slightly induced the expression in the LNCaP cells. Concomitantly, the levels of the AR remained unchanged in both cell lines. To summarise, the Western blot analyses have shown that pharmacologic inhibition of the hormone receptors affects and in most cases induces the expression of RAI2. Whether the induction of RAI2 consequently has an influence on hormone receptor expression needs to be shown in further experiments. Thus, analysing the effect of hormone deprivation or pharmacologic inhibition after RAI2 depletion could furthermore give more insight into a possible feedback regulation.

Due to the functional association between RAI2 and the hormone receptors, it was reasonable to test whether RAI2 depletion has an effect on expression of AR target genes in course of the hormone response. Therefore, Alexandra Weglarz from our working group first analysed the expression of AR-target genes, using an RT$^2$ Array from Qiagen, in RAI2 depleted VCaP cells after stimulating the AR with a synthetic androgen. She identified an increased induction of several genes such as the serine/threonine kinase 1 (*SGK-1*) and the membrane metallo-endonuclease (*MME*)[123]. In order to find out whether the increased induction of these genes can be validated in LNCaP prostate cancer cells, the genome of parental LNCaP cells were first edited by CRISPR/Cas9 to generate a RAI2-KO cell line (Fig. 3-7). Subsequently, LNCaP cells with RAI2-knockout were cultured in hormone-deprived medium before the AR was stimulated with DHT and *PSA*, *MME*, *SGK-1* gene expression was detected by qRT-PCR and compared to the parental cell line (Fig. 3-8). An increased *PSA* mRNA level was detected in parental and RAI2-KO LNCaP cells after the addition of DHT, showing that the ligand-dependent activation of the AR was successful. However, no significant changes could be observed in the induction of MME and *SGK-1*

between parental and RAI2-KO cells in course of AR-activation. Interestingly, increased expression of the *PSA* and *SGK-1* mRNA were detected after RAI2 knockout under standard growth conditions, showing that loss of RAI2 has a regulatory influence on the expression of AR-target genes, moreover suggesting an inhibitory effect of RAI2 on the transcription of AR-responsive genes.

The possibility that RAI2 regulates transcription of AR-targeted genes as a coregulator via direct interactions with the AR could not be supported through colocalisation studies by immunofluorescence staining. Even though both proteins were mainly distributed within the nucleus, their fluorescence signals showed no overlap, concluding that there is no direct interaction between RAI2 and the AR under normal growth conditions (Fig. 3-6). Furthermore, RAI2 protein contains neither a FXXLF nor a LXXLL motif, which has been shown to interact with the AF-2 domain of the AR, the major protein-protein interaction surface of nuclear receptors[55]. However, it would furthermore be of interest to perform Co-immunoprecipitation (CO-IP) analysis under different conditions including normal growth, AR-inhibiting or AR-stimulating conditions and test for a direct interaction between RAI2 and AR but also the CtBP1 and CtBP2 protein. Colocalization of RAI2 and both CtBP proteins in nuclear speckles has been demonstrated in breast cancer cell lines overexpressing the RAI2 protein[118]. A direct interaction between those proteins via the bipartite ALDLS motif of RAI2 could further be validated in RAI2-overexpressing BrCa and HEK-293T cells by Co-IP and mass spectrometry based analysis[118,146]. In this study a colocalization of CtBP1 and endogenous RAI2 protein could be observed in VCaP prostate cancer cells under RAI2 inducing conditions (Fig. 3-6). Interestingly, CtBP1 has been shown to interact with the ligand-bound AR at AR-binding sites, where it represses at early time points of AR-action the transcription of adjacent androgen-responsive genes by inhibiting histone demethylation[147]. Subsequently, CtBP1 is reduced by its antisense, non-coding RNA leading to activation of the AR transcription activity[148]. On the other hand, the closely related transcriptional regulator CtBP2 has been shown to interact with the AR at a later time point following androgen treatment, due to androgen-dependent induction of CtBP2 gene expression. In addition, CtBP2 activated the AR-mediated transcription by repressing the expression of AR corepressors like *NCOR* and *RIP140*. In contrast to CtBP1, overexpression of CtBP2 was correlated with poor prognosis in patients[149]. Thus, a better understanding of the interaction-dynamics of RAI2 and both CtBP proteins could further help to elucidate the role of RAI2 within the hormone response. Several coregulators that directly bind to the AR or ER have been shown to interact through PXDLS motifs with the CTBP proteins such as the corepressors LCoR, ZNF366 or the CtBP2 regulated RIP140 protein, suggesting that competition exists between those RAI2 and proteins, which have been observed to accumulate in nuclear speckles either alone or together with CtBP protein[150–153]. Furthermore it has been shown that the nuclear localisation of CtBP proteins is not only influenced by its NLS motif but also by

binding to PXDLS motif partner proteins[115], implying a role for RAI2 in the transcriptional regulation of hormone responsive genes either by facilitating the nuclear localisation or even storage of CtBP proteins or by being part of a corepressor complex that directly regulates the ER or AR-mediated transcription of genes.

## 4.3 Effect of RAI2 depletion on BrCa and PCa progression

Since the RAI2 expression was decreased in metastasising breast cancer tumours and metastatic prostate cancer tissue (Fig. 3-1)[118], it was of interest to determine whether loss of RAI2 expression alone might increase the tumorigenic potential of hormone-dependent breast and prostate cancer cells[118]. Therefore, RAI2-knockout (RAI2-KO) cells were established by CRISPR-Cas9 genome editing before functional assays were performed to evaluate multiple hallmarks of cancer, and especially those related to hormone response. In addition to the MCF-7- and VCaP RAI2-KO systems that were previously generated by our members of our working group, a RAI2-knockout was successfully generated in the LNCaP cells and verified by sequencing and Western blot analysis in course of this project (Fig. 3-9).The ability of parental and RAI2-KO cells to proliferate and evade growth suppression was assessed using the MTT and colony formation assay, which allowed measurement of the viability and outgrowth of single cells into colonies under different proliferation inhibitory conditions. Thus, breast and prostate cancer cells were grown in hormone-depleted medium or medium supplemented with the antioestrogens tamoxifen and fulvestrant or with the antiandrogens bicalutamide and enzalutamide to inhibit the activity of the respective hormone receptor with approved drugs used in the clinic. Given that shRNA-mediated depletion of the RAI2 protein in KPL-1 and MCF-7 breast cancer cell lines led to the activation of the proliferation activating AKT kinase, cells were furthermore treated with the AKT inhibitor MK2206 or the mTOR inhibitor RAD001[118]. The mTOR kinase is a downstream effector of AKT, whose substrates regulate the transcription and translation of critical growth genes[154].

MCF-7 breast cancer cells showed a significantly increased cell viability as measured by MTT-assay in hormone deprived medium after RAI2 loss, which could, however, not be observed under treatment with both antioestrogens (Fig. 3-10). This show on the one hand that the cells proliferation still depends on ERα signalling after RAI2 loss, but on the other hand these are not as dependent on the ligand as the parental cells. The increased growth of RAI2-KO cells compared to parental cells in complete hormone deprived medium could be possible due to ligand-independent ER activation or by activating an alternative proliferation pathway that is bypassing the survival inhibiting conditions by providing a substitute survival signal. The increased sensitivity of RAI2-KO cells to the AKT and mTOR inhibitors observed in the same experimental setting, indicates an increased activation of the PI3K/AKT/mTOR pathway and a higher influence of this

pathway on the proliferation of these cells compared to the parental MCF-7 cells. Besides the general growth and oncogenesis promoting effect of the PI3K pathway in many cancer types, a cross-talk between ER/ AR and this pathway has been observed in which both pathways can co-ordinately support survival[155] Members of the pathway have not only shown the capability to activate the ER ligand independent by phosphorylation of the receptors but also to influence the ER binding and recruitment of the transcriptional network, leading to hormone-independent growth[80,97,155]. However, little is known about the interplay between the ER and the PI3K/AKT/mTOR pathway in which RAI2 also seems to play a role. The additional stimulation of proliferation by this pathway could also explain the noted increased growth of the RAI2-KO MCF-7 cells in standard growth medium, which however only showed significance in the DMSO control while a tendency could be observed for the cells in standard medium (Fig. 3-10). Additional replicates, could show whether this tendency can reach a significance level or if the observed increase in proliferation is DMSO-specific and thus related to stress mechanisms, that might be activated by this solvent and regulated by RAI2.

Of note, parallel analyses carried out by other members of the working group have shown an increased growth of KPL-1 breast cancer cell line after RAI2 loss in hormone deprived medium and medium supplemented with the antioestrogen fulvestrant, showing the potential of RAI2 to promote hormone-independent growth. Unfortunately, growth of KPL-1 cells was not assessed under PI3K/AKT/mTOR inhibitory conditions, which makes a precise comparison with the MCF-7 cells difficult, even though an activation of this pathway was assumed, according published AKT activation after RAI2 knockdown[118]. In order to further analyse whether the reduced sensitivity of KPL-1 RAI2-KO cells towards fulvestrant treatment might be explained by the activation of serine/threonine kinases a screening of activated kinases was performed. Surprisingly, an increased activation of various MAP-kinases (MAPK1/ERK2, MAPK3/ERK1, MAPK13 and MAPK14) and cycline-dependent kinases (CDK2, CDK3 and CDK6) was found instead of the kinases involved into the PI3K/AKT/mTOR pathway (Fig. 3-18). Like the PI3K/AKT/mTOR pathway, an activation of the MAPK/ERK signalling pathway and the cell cycle regulators is known to be associated with resistance to hormone therapies[80]. However, after the discovery of the activated kinases, which were assessed based on phosphorylation of immobilised peptides on an array, a verification of the data also using MCF-7 as model system needs to be performed for further conclusions. Furthermore, it is of interest to additionally analyse the expression and activation of receptor-tyrosine kinases (RTK) which act upstream of the serine/threonine kinases The RTK that is predominantly activated in breast cancer is HER2, which acts through activation of the MAPK/ERK and PI3K/AKT/mTOR signalling pathways. Moreover, several studies observed a switch from ER to HER2 as the preferred singling pathway and *vice-versa*, as a result of targeted therapies against the respective growth driving molecules[80]. Whether RAI2 is able to facilitate the

switch from ER to HER2 or another RTK pathway needs to be further elucidated in subsequent studies. Preliminary ongoing results have not yet given clear results.

The influence of RAI2 expression on the viability and growth of the prostate cancer cell lines was also analysed by MTT and colony formation assays. In addition to the inhibition of the AR and PI3K/AKT/mTOR pathway as mentioned before, the response of the cells to taxane-based chemotherapeutics paclitaxel and docetaxel was analysed. Striking was a significant ~2-fold increase of the proliferation and colony formation of LNCaP cells as a result of the RAI2 loss and in absence of any component. Furthermore this growth advantage of RAI2 depleted LNCaP cells could be maintained under treatment with the AKT and mTOR inhibitors as well as both chemotherapeutic drugs as shown by the MTT (Fig. 3-11) and colony formation assays (Fig. 3-13). The LNCaP cells responded most strongly to inhibition of the AR signalling, although the RAI2-knockout cell still displayed a significantly increased growth after treatment with bicalutamide and enzalutamide in at least one of the performed assays. However, this growth advantage of the RAI2-KO cells was completely abolished under complete hormone depletion and decreased to the level of parental cells, implying that the growth of both LNCaP cell lines is mainly determined by the AR action.

In order to find out whether the increased proliferation of RAI2 depleted cells under bicalutamide treatment is due to additional activation of serine/threonine kinases, a functional kinomic profiling was performed with whole cell lysates similar to the KPL-1 breast cancer cells. The comparison of the STK activity in parental and RAI2-KO cells, however, small differences only and the upregulation of the barely characterised kinases DCAMKL3, MLCK4/SGK085 and CDKL2 in RAI2 depleted cells (Fig. 3-19). None of these kinases is known so far to be associated with resistances to hormone therapy in breast or prostate cancer and not much has been published about the functional characteristics of DCAMKL3 and MLCK4/SGK085. Nevertheless, the MLCK4/SGK085 kinase is a member of the myosin light chain kinase (MLCK) family, which catalyses the phosphorylation of the regulatory light chain of myosin and is associated with the regulation of the invasiveness of metastatic cancer cells[156]. Additionally, treatment of dunning rat prostatic adenocarcinoma cells with MLCK inhibitors resulted in marked reduction of invasiveness, which was principally due to impaired cellular motility, whereas the ability to survive and proliferate were minimally affected[156]. Hence, the influence of this kinase on the proliferation of the LNCaP RAI2-KO cells under bicalutamide treatment seems to be negligible. Similarly, the cycline dependent kinase like 2 (CDKL2) have been shown to promote EMT and enhance migration ability in breast and prostate cancer cells[157]. At this point it should be emphasized that no commonality in the activation of STK between the KPL-1 breast cancer cells and the LNCaP prostate cancer cells, indicating that the observed resistance to hormone treatments as a result of RAI2-depletion might not be due to the activation of same mechanism. Unpublished results from our working group show an increased AR expression in the RAI2-KO cells compared to the parental LNCaP cells. The increase

of the AR is a known mechanism to maintain proliferation under low levels which is associated with higher dosage of therapeutic drugs needed for the downregulation of AR action[158–160]. These facts are a reasonable explanation for the observed differences in cell growth between parental and RAI2-KO cells and thereby confirming that AR remains the main growth promoting pathway after RAI2 depletion. Moreover, the RAI2 loss increases the expression of AR leading to decreased susceptibility to hormone therapy in LNCaP cells.

Other unpublished results from our working group show a significantly increased AR protein expression in the VCaP cells after the knockout of the RAI2 protein. Compared to the LNCaP cells, the loss of the RAI2 protein did not change the proliferation of VCaP cells under normal growth condition, nor did it lead to increased viability under pharmacologic inhibition (Fig. 3-11). On the contrary, the RAI2-depleted VCaP cells are more sensitive to treatment with the anti-androgens bicalutamide and the mTOR inhibitor, showing a RAI2 associated dependence of both molecules. Despite the similarity of the VCaP and LNCaP cell lines in terms of hormone-dependent cell growth, many differences exist between the two cell lines in the AR signalling pathway and the maintenance of AR-signalling. For instance, the VCaP cells show a 10-fold higher expression of the wildtype AR than the LNCaP cells, which is attributed to an amplification of the AR gene[161]. Besides that, VCaP cells express several alterative spliced AR isoforms, including the AR-V7 variant, which acts as a constitutively active TF[162,163]. On the other hand, LNCaP cells express a mutant AR (T877A), which results in an altered AR-signalling[162]. Futhermore, AR signaling and the response to androgens of LNCaP cells has been described to be sensitive to serial passaging and culture conditions[162]. Moreover, it has been shown that there is a difference in the activation of target genes after AR-stimulation[161]. Together these differences may have contributed to the observed differences in proliferation of those cells after RAI2 depletion. However, since these cell lines are representative of the AR heterogeneity observed in clinical prostate cancer specimens[164], it should be of further interest to clarify the functional significance of RAI2 in both cell lines. Optimally the results should be verified in further AR-dependent cell lines, such as the LAPC or DUCaP cell lines.

Besides the loss-of-function analysis, gene overexpression was used as a *modus operandi* to analyse the effect of RAI2 on the growth and behaviour of RAI2 low expression or depleted cells. The generation of a stable RAI2 overexpressing (RAI2-OE) cell line and its control (vector) counterpart was achieved through transduction of cells with retroviral particles, harbouring either the RAI2 expression plasmid or an empty control vector. The introduction of the RAI2 protein into the androgen-independent and metastatic PC-3 cell line did not affect the cell viability or the colony formation under normal growth conditions, nor under treatment with the before mentioned cytostatic drugs or kinase inhibitors (Fig.3-12 and 3.14). The cellular response to hormone deprivation and AR-inhibition (results not included) was tested only in one experiment and was not

repeated due to failing inhibition of cell viability under saturated concentrations, verifying hormone-independent growth of this cell line. Thus, the overexpression of RAI2 was not sufficient to increase sensitivity to the applied drugs or to reverse the resistance to hormone therapy.

Furthermore, constitutive overexpression of RAI2 was used to analyse whether the reintroduction of RAI2 protein expression into LNCaP RAI2-KO cells is capable of reducing the increased clonogenic capability of these cells back towards the parental level. However, overexpression of RAI2 was not able to reduce the effect of the RAI2-knockout and to restore the original state of cell proliferation (Fig. 3-15). One conclusion from this recovery experiment could be that the depletion of RAI2 is linked to irreversible changes within the cells. This assumption is supported by results from Dr. Lena Böttcher's thesis who was able to show that depletion of RAI2 in luminal breast cancer cells leads to the accumulation of double strand breaks and loss of chromosomal fragments, which are incorporated into micronuclei after mitosis[125]. The formation of micronuclei, which appear next to the nucleus in the cytoplasm of cells, is an imprint of irreversible DNA damage and serves as an indicator of chromosomal instability[165,166]. Genome instability, especially on this chromosome level, can create high levels of intratumoural heterogeneity, which is the main reason for ineffective therapeutic response and drug resistance in cancer treatment and is a hallmark of cancer[125]. The micronuclei can encompass different genes[165,166], providing one possible explanation of the heterogeneous effects observed after RAI2 loss in the different cell lines. Another explanation of the failed RAI2 recovery experiment in the LNCaP is of a technical nature and concerns the method that was used for the generation of knockout cells. Off-target effects that might have been introduced by the CRISPR/Cas9 genome editing and lead to physiological effects that are unspecific to RAI2[167]. Furthermore, the clonal expansion of single cells and testing of the first ten clones might have contributed to selection of the fittest and fastest growing LNCaP cells independent from RAI2-knockout. On the basis that cells within a cell line are observed to be heterogeneous[168,169], it is possible that LNCaP cells with increased AR were enriched after transfection with the CRISPR/Cas9 construct due to higher proliferation, resulting in higher proliferation of RAI2-KO cells compared to parental cells which cannot be reversed by RAI2 overexpression. However, the fact that VCaP RAI2-KO cells show a higher AR expression, but grow at the same rate as the parental cell line, or even slower as observed during cell culture at lower seeding number, argues against the selection of the fittest cells and favours the theory of irreversible DNA damage. To exclude the possibility that off-target effects of CRISPR/Cas9 genome editing are causing the observed difference between parental and RAI2-KO cells, unintended genomic modifications could be identified by e.g. sequencing.

Metastasis is the hallmark of cancer that is responsible for the greatest number of cancer-related deaths and requires many different properties from the cells[7]. One essential property that epithelial cancer cells have to acquire is the ability to detach from extracellular matrix and resist anoikis,

a programmed cell death, which normally prevents detached epithelial cells from colonisation[137]. One feature of anoikis resistance and metastatic spread is therefore the anchorage-independent growth[137], which was assessed in low metastatic LNCaP cells after RAI2-knockout and in the highly metastatic PC-3 cell line RAI2-overexpression. In comparison to the respective control cell line, anchorage independent growth was significantly increased in LNCaP cells after RAI2 depletion but did not change as a consequence of RAI2 overexpression in the RAI2 protein in the PC-3 cell line (Fig. 3.16). Interestingly, the analysis of a second essential property of metastatic cells, the motility of cell, which was increased in LNCaP cells after RAI2 knockout and RAI2 introduction into the PC-3 cells was able to reduce the aggressiveness of PC-3 cell *in vitro* by decreasing the migratory capacity of these cells (Fig. 3-17). One major process that is considered to drive anoikis resistance, the migratory capacity and the colonization of cancer cells is the epithelial-mesenchymal transition (EMT)[7,137]. As detected by the kinome profiling, the loss of RAI2 protein expression in the LNCaP was followed by the activation of the MLCK4/SGK085 and CDKL2 kinases (Fig. 3-19). The action of the MLCK/SGK085 and the CDKL2 kinase has been linked to increased cell motility and invasiveness and the induction of EMT that likewise resulted in an enhanced migration ability of breast and prostate cancer cells[156,157] Thus RAI2 loss might activate the EMT through those kinases leading to the acquisitions of cancer hallmark traits that are necessary for colonisation of cells. On the other hand, RAI2 overexpression decreased the migratory ability of the metastatic and AR-negative PC-3 cells. Consequently, it would be of utmost interest to analyse the expression of EMT-markers in those cells, in order to assign for certain a role of RAI2 in this process and explain the observed behaviour of the tested cells. Furthermore, due to the AR negativity of PC-3 cells and so far unpublished research that describe a connection between the AR and the activated kinases, one could conclude that the process of EMT or the control of migration is regulated independently of a possible interaction of RAI2 and the AR transcription complex i.e. the AR action. Since the CtBP protein for example has been shown to be a modulator of several cellular processes including EMT, cell migration and invasion and be recruited by various DNA-binding transcription factors to carry out their function, it should be considered that RAI2 might regulate several processes independent from AR activation through the interaction with CtBP proteins in AR positive and especially AR negative cells[170,171]. Experiments with hormone receptor negative cells could thereby give more insight into this hormone receptor independent regulation.

The functional assays have shown that loss of the RAI2 protein enhances many hallmarks of cancer traits in the LNCaP cells including proliferation, the outgrowth of individual cells into colonies, as well as resistance to anoikis and the motility of the cells. In order to test whether this more aggressive cell phenotype observed *in vitro* can be translated into more aggressive tumours with increased proliferation and cell dissemination *in vivo*, a small cohort of immunodeficient mice

were injected subcutaneously with either parental or RAI2-KO LNCaP cells. Animals were killed when their primary tumour reached size of 1000 $mm^3$. After a total follow up time of 232 days, 3 of 11 (27.3%) mice harbouring the parental LNCaP cells and only one of 16 (6.3%) mice injected with RAI2-KO cells were still alive. Despite the large difference in percentage of surviving mice in each group, the Kaplan Meyer estimations did not show a significant difference in overall survival between both groups (Fig. 3-20). Furthermore, no differences were found between both groups concerning the presence of either CTCs or DTCs in the blood or the bone marrow of sacrificed mice respectively using immunofluorescence staining as the detection method (Fig. 3-21). Additionally, members from Prof. Dr. Lange's group from the department of Anatomy (UKE) performed *Alu*-PCR as a second method for the detection of DTCs in bone marrow and lung tissue of mice. With this approach it was possible to detect a slightly increased but not significant presence of DTCs in the bone marrow of mice injected with RAI2-KO cells (Fig. 3-22). In total, these results showed that the loss of RAI2 is not sufficient to increase the tumour growth or spread of this low metastatic prostate cancer cell line in a xenograft model. However, tendencies towards faster tumour growth and increased dissemination to the bone marrow were observed. Accordingly, a repetition with larger group of animals could be considered. In the event of a second mouse experiment, several aspects could be improved, including the CTC and DTC detection. Due to high degree of cell damage after the CTC enrichment procedure, the blood of only three mice per group could be analysed. Since the CTC enrichment method via the Parsotix system and the subsequent staining of cells is well established at our institute, the observed damage must be linked to the steps prior to blood processing. The complete blood was drawn by cardiocentesis, which involves puncturing the heart through the overlying tissues and drawing the blood through a cannula into a syringe under traction. Even though the blood cells looked intact under the microscope after the blood draw, the combination of the traction forces and the pressure which is applied during the Parsotix™ enrichment, in order to squeeze the blood cells through small gaps and separate them from bigger CTCs, may have led to the destruction of the cells. Therefore, blood draw via the orbital sinus of the terminally anesthetized mice could be used. In first internal experiments, this procedure has proven to be more cell-sparing, as the blood is collected by capillary action, without pressure, into the collection tube. Furthermore, the EpCAM and pan-keratin immunofluorescence staining that was used for detection of human LNCaP cells, led to nonspecific background staining of the murine bone marrow cells. Recent experiments performed by our group members were able to assign this background to the autofluorescence of murine cells in the green Alexa-488 channel. Thus, use of antibodies coupled to an orange-fluorescing dye would be recommended in case of a second *in vivo* approach. To sum up, with the current knowledge it would be possible to extract more information concerning the dissemination of LNCaP cells after RAI2 knockout.

## 4.4 Potential of RAI2 as a novel biomarker of liquid biopsy

In addition to the characterization of the molecular function and the influence of RAI2 expression on the progression of different cancer model systems, the development of a liquid biopsy approach was another major objective of this study. By analysing tumour material released into the blood system, liquid biopsy can contribute inter alia to cancer detection, treatment decisions and monitoring of cancer progression[104]. Besides tumour-derived exosomes, miRNA and cfRNA that can be found in the patients peripheral blood, the main tumour-derived analytes analysed so far are CTCs and ctDNA[104,116]. As ctDNA reflects DNA from multiple tumour regions, it can provide broad information on the tumour genome, including the prevalence of mutations, amplifications and epigenetic changes[107,116]. Based on the publication of YAN et al., where it was shown that methylation of the RAI2 promoter is associated with low RAI2 expression and poor overall survival of CRC patients, one aim was to establish a liquid biopsy method to analyse the methylation status of RAI2 on ctDNA level[126]. Since ctDNA in blood plasma accounts for only a small portion of circulating cell free DNA (cfDNA) and the larger fraction is likely to be derived from apoptotic leukocytes, the methylation of the RAI2 promoter in the peripheral blood cells (PBMCs) had to be excluded first[107]. Therefore, the genomic DNA from PBMCs of five healthy donors was tested for methylation of the RAI2 promoter using the primer published by YAN et al. Unfortunately, it turned out that the RAI2 promoter region in the tested healthy donor samples was methylated, so that a specific analysis of the methylation status of the RAI2 promoter in on ctDNA does not seem feasible at all. Interestingly, the region which is complementary to the used reverse primer was mainly methylated in the gDNA of female donors (HD4 and HD5, Fig. 3-23), while the gDNA from the male ones remained unmethylated. Due to this observation, as well as partially missing sequencing results of the forward primer region, a repetition of the experiment with a larger group might be of benefit to validate the results and exclude gender-specific differences in the methylation of RAI2.

The other aim of this study was to establish a liquid biopsy approach that allows expression analysis of RAI2 and other genes relevant for prostate cancer progression at the CTC level. In a pilot study of 36 patients with metastatic prostate cancer, CTCs were isolated from 40 blood samples using the AdnaTest. The AdnaTest is based on an immunomagnetic cell selection system, which enables the enrichment of CTCs by targeting the epithelial and tumour-associated cell surface epitopes EpCAM, ERBB2/HER2 and EGFR[106,172]. The mRNA, that was isolated from the enriched cells, was reverse transcribed into cDNA according to the AdnaTest protocol and preamplified before gene expression analysis was performed by qRT-PCR using reagents from TATAA Biocenter. Each sample was profiled for the expression of *RAI2*, *AR*, *AR-V7*, *PSMA* and *PSA* to analyse the hormone response with the main target genes of the AR. Additionally the AR-regulated

gene *HOXB13* was included into the panel, based on the publication of MIYAMOTO et al., who published that the expression of *HOXB13* is associated with aberrant AR signalling and more aggressive hormone refractory prostate cancer and was significantly correlated with worse overall survival[173]. Since the patients in this study received various therapies, including chemo-, radio- and hormone therapy, several other genes that are associated with resistance to these therapies were also added to the panel. Thus, each sample was analysed additionally for the expression of *MRP1*, an efflux pump that is associated with lack of chemotherapy response[174]; and *PI3KCA*, as a member of the PI3K/AKT/mTOR pathway, whose activation is frequently observed when PCa progresses to resistant, metastatic disease[175,176]. In addition, the expression of *EPCAM* and *EGFR* was analysed due to their role in the enrichment procedure. On the other hand, EGFR represents another gene, whose expression is correlated with high risk of recurrence after prostatectomy and progression to hormone resistance[175]. In addition to *EPCAM* expression, *KRT19* was assessed as a marker for epithelial cells, while *CD45* served as a marker for leukocytes[177]. Finally *GAPDH*, *ACTB* and *HPRT1* were analysed as reference genes. However, *GAPDH* was identified by NormFinder from GenEx as the most stably expressed gene and was further used for final ΔCq calculations. For multivariate analysis ΔCq-values were converted for each gene separately into relative quantities, relative to the sample with the maximum Cq (lowest expression) and transformed into logarithmic scale using base 2[132]. For classification and visualisation of the genes and samples a dendogram including a heat map was generated with GenEx using the mean centred data. Unsupervised hierarchical clustering of the samples based on gene expression grouped eight PCa-samples together with ten tested healthy donor samples into one cluster, indicating a negative CTC status in these samples (Fig. 3-24). On this basis, the remaining patients' 32 (80%) samples were concluded to be positive for CTC. With regard to the classification of genes, it is striking that *RAI2* was grouped together with receptors *AR* and *AR-V7* and formed a common cluster with the receptors and the AR-target genes *PSA* and *PSMA*, supporting furthermore a connection of RAI2 protein with the hormone response and AR-activity. Concomitantly, principal component analysis (PCA), that groups samples or genes based on correlated expression in reduced space, separated the healthy donors and eight PCa-samples clearly from the other PCa-samples (Fig. 3-25, A). Intriguingly, the division of both groups was mainly influenced by the expression of *PSMA*, *PSA*, *RAI2*, the androgen receptors, *KRT19* and *CD45* as demonstrated by the high influence of these genes on the PC1 variation (Fig. 3-25, B). With regard to the CTC enrichment method, it was surprising that *EPCAM* and *EGFR* were neither highly expressed in the PCa samples, nor was their expression limited to PCa patients (Fig. 3-24). However, expression of EGFR has also been found on the surface of peripheral blood monocytes and in T-cells, which could have been enriched by the used technique and explain the detection of EGFR in healthy donor samples [178,179]. The fact that the AdnaTest does not enrich a pure CTC fraction is particularly evident in the expression of the leukocyte marker CD45 that is found in most of the tested samples and has been

described previously by other researchers[106,180]. Nevertheless, a possible utility of the AdnaTest in CTC analysis has been postulated by many studies, including the study of ANTONARAKIS et al. and the PROPHECY study, where detection of *AR-V7* in CTCs enriched by AdnaTest has been strongly associated with resistance to enzalutamide and abiraterone acetat[114,115,181]. In this study *RAI2* expression was strongest correlated with *AR*, *AR-V7*, *PSMA* and *PS*A expression, according to order, as detected by Pearson correlations (Fig. 3-26). Thus, in addition to the prior observed correlation of RAI2 and the AR protein after RAI2 knockdown and pharmacologic inhibition of the AR, a correlation of RAI2 and AR could be found in the CTCs of metastatic prostate cancer patients on transcript level.

In order to test the predictive value of *RAI2* mRNA expression, patients were divided into 'responsive' or 'progressive' groups according to their response to the therapy administered at the time of blood draw. High RAI2 mRNA in CTCs was significantly associated with no response to treatment and thus with disease progression. A similar trend was obtained correlating *RAI2* mRNA expression with response to hormone therapy (Fig. 3-27, A). Additionally, correlation of *RAI2* mRNA expression with clinical parameters like serum PSA, lactate dehydrogenase (LDH), alkaline phosphatase (ALP) or haemoglobin (Hb) level in the patients' blood were tested. Pearson's correlation showed a positive week correlation with the serum PSA levels and a negative week correlation with the haemoglobin amount (Fig. 3-27, B), implying that high *RAI2* expression is correlated with progressive disease in the mean of biochemical recurrence measured by PSA and increased anaemia[25,110,182,183]. To analyse the potential prognostic implication of *RAI2* mRNA in CTCs on patients' overall survival, the patients were divided according to detectable Cq-values after qRT-PCR analysis into RAI2 negative or RAI2 positive group and analysed by Kaplan Meyer estimations. Even though the differences were not significant *RAI2* expression was correlated with worse overall survival, which was in line with the previous correlations (Fig. 3-28). However since *RAI2* expression correlated with the presence of CTCs in the blood of patients, missing *RAI2* expression was mirroring the efficiency of the given therapy due either to responding tumours that shed less CTCs into the blood or dying CTCs in circulation and thus a better survival prognosis. In general low *RAI2* expression has been expected throughout the CTCs, since RAI2 has been published as a metastasis suppressor[118]. However, since there was no access to tissue like the primary tumour to which to compare the expression to, the data do not allow a statement as to whether the detected expression in the CTCs is low or high. Taken together, a method for the analysis of *RAI2* and other genes has been successfully established and tested in a small group of metastatic patients. Limitation of this study was the lack follow up-data for each patients at the time of analysis.

# 5 Conclusion and outlook

Decades ago it was recognized that the growth of most breast and prostate tumours is dependent on the sex steroid hormones, oestrogen and androgen, respectively[62,64]. With the discovery of the corresponding hormone receptors ER and AR, which act as ligand modulated TF driving the progression of breast and prostate cancer disease, a multitude of therapeutic options have been developed to either prevent the production of hormones or block the receptor function[43]. Although these therapies are initial effective, most patients with advanced disease develop resistance against the drugs targeting the hormonal signalling and progress to a lethal stage of cancer[44]. Increased knowledge about the involved resistance mechanisms has led to development of several targeted agents, however patients progress with new resistances and eventually die from their metastatic disease[44,142]. To better control hormone-dependent cancer growth in future, further research is needed to elucidate the exact ER and AR action and the function of the coregulatory proteins involved in the hormone-dependent signalling.

The present study investigated the role of RAI2 in the progression of breast and prostate cancer, focusing on a possible functional link of RAI2 to hormone response and its contribution to hormone therapy resistant disease. In addition to the already published prognostic value of RAI2 for the progression of ER positive cancer[118], the present study has shown for the first time a possible prognostic relevance of RAI2 protein for prostate cancer as well. More precisely, clinical database analyses showed in line with the breast cancer data an association of low RAI2 expression with metastatic prostate cancer. Based on the fact that both cancer entities grow hormone-dependent and RAI2 expression is predominantly found in ER- and AR-positive breast cancer or prostate cancer cell lines, a possible functional association of these two proteins was analysed. Knockdown experiments of either ER/AR or RAI2 proteins revealed an interdependent regulation of the proteins, in which RAI2 protein seems to stabilise the hormone receptor expression, while the receptors inhibit the expression of RAI2 under normal growth condition in hormone-dependent breast and prostate cancer cells. Furthermore, inhibition of ER and AR with in the clinic used pharmacologic drugs showed significant changes in RAI2 expression, which mostly correlated with the expression of the respective growth driving hormone receptor. Taken together, these results indicate the existence of a possible regulatory feedback loop between RAI2 and the respective hormone receptor and thus a potential influence of RAI2 on the effectiveness of hormone receptor regulating drugs used for the treatment of both tested hormone-dependent cancer entities. However, little is known about the regulation of the RAI2 expression. Besides the influence of RAI2 promoter methylation on RAI2 expression which has been shown by YAN et al.[126], it is assumed that RAI2 is regulated by AP-2 transcription factor through its specific binding domains which

has been identified within the RAI2 promoter[120]. Thus it would be of interest to analyse whether the depletion of this protein would have direct influence on RAI2 protein expression. For example, the induction of the RAI2 protein could be tested under conditions that normally stimulate RAI2 expression, such as the addition of retinoic-acid or hormone deprivation after a knockdown of the AP-2 protein. Furthermore, an analysis of the AP-2 expression at different time points of ER and AR activation would show whether the availability of the protein is dependent on the hormone response and give a first impression whether RAI2 is indirectly regulated by ER or AR through regulation of the AP-2 expression, degradation etc. Finally, chromatin immunoprecipitation (ChIP) technique could be used to analyse more specifically the interaction between AP-2 and its postulated DNA binding site within *RAI2* promoter region e.g. under normal and hormone stimulated conditions.

Based on the relation found between RAI2 and the hormone receptors, another goal was to analyse whether RAI2 has an influence on the hormone response. Unpublished analyses from our laboratory analysing the expression of several AR target genes showed an increased induction of AR-regulated genes in VCaP cells after RAI2 knockdown. However, examination of the *SGK-1* and *MME* gene expression, which was particularly strongly induced in the experiment with the VCaP cells, showed no increased induction of transcripts in LNCaP cells after RAI2-knockout and ligand-induced activation of the AR. Nevertheless, an induction of the *PSA* and *SGK-1* genes in the LNCaP RAI2-knockout cells under normal growth conditions was observed, which could be explained either by an increased AR expression in the cells after RAI2 loss or by a prolonged AR activity. Colocalisation of RAI2 with the CtBP1 protein in VCaP cells and the previous published direct interaction of both proteins in BrCa cell lines furthermore supports a possible role of the RAI2 protein as a transcriptional coregulator[118]. The assumption is thereby mainly based on the knowledge that the CtBP proteins act as coregulators of the ER/ AR- mediated transcription of gene in an interplay with other coregulators, containing ALDLS motifs[147,149,153]. However, it has to be elucidated whether RAI2 controls the localisation and availability of the CtBP protein within the nucleus or whether it interacts with CtBP protein within a transcriptional complex at the AR binding sites where it might be involved in organising chromosome architecture. Despite the IF-staining that didn't show any colocalisation of RAI2 and the AR, e.g. a coimmunoprecipitation analysis with a pulldown of the CtBP proteins after the induction of a hormone response and the detection of precipitated RAI2 and AR, could help to exclude the interaction of all proteins in one complex in course of AR activation.

Although the knockdown experiments led to comparable results in regard to regulation of RAI2 and ER/AR protein expression in all cell lines of both cancer entities, the knockout of the RAI2 protein did not result in uniform cellular behaviour. With regard to cancer cell viability and growth, discrepancies were not only detected between breast and prostate cancer cell lines after

RAI2 loss, but also between the tested cell lines of the same entity, which makes a general conclusions about the effect of RAI2 on cancer cell progression difficult. However it was possible to show that knockout of the RAI2 protein leads to a more aggressive LNCaP phenotype which is characterised by increased cell viability/growth, decreased sensitivity to antiandrogens and taxane based chemotherapeutic drugs, resistance to anoikis and increased cell motility *in vitro*. Conversely, RAI2-overexpression in the highly aggressive PC-3 cells decreased the migratory capability of this cells, although the cell viability and growth of this cells remained unchanged. Kinome profiling has furthermore revealed an activation of the MLCK4/SGK085 and CDKL2 kinases in LNCaP cells after RAI2-knockout, which are known to promote invasiveness and EMT of cancer cells and could explain the increased observed motility. However, these results have to be validated in independent experiments. Additionally, in order to verify the possible role of RAI2 in regulation of cell plasticity, EMT-markers should be analysed in the RAI2 modified LNCaP and PC-3 cells. Nevertheless, despite the increased aggressiveness of the LNCaP cells after RAI2 depletion *in vitro*, neither increased tumour growth nor enhanced dissemination of RAI2- depleted LNCaP cells could be detected *in vivo*, showing that the inactivation of RAI2 alone is not able to increase the tumorigenicity of this cell line in the more complex xenograft model.

Within the framework of this study, it was furthermore possible to establish a liquid biopsy approach, which not only enables the detection of *RAI2* expression but also allows the analysis of other genes that are relevant for the progression of prostate cancer in the CTCs enriched from patients' blood. In a small pilot study including prostate cancer patients with metastatic disease, a correlation of RAI2 and AR expression could be detected in CTCs on the transcript level, which was in line with the prior observed correlation of RAI2 and the AR in the prostate cancer cell lines. RAI2 expression was furthermore correlated with a positive CTC status, increasing PSA levels, anemia and resistance to therapy. Concordantly, survival analysis showed a trend towards worse overall survival of patients with detectable RAI2 expression.

Taken together, these results show that RAI2 expression correlates with different markers of progressive disease in advanced prostate cancer patients. Thus, these findings contradict the putative role of RAI2 as a tumour- or metastasis suppressor in breast cancer[118]. However, also in this study the initial database analysis of RAI2 expression in primary prostate tumours clearly showed a reduced *RAI2* gene expression in more advanced tumours, which is in line with the RAI2 expression in breast and other cancer entities[118,126]. Nevertheless, all these analyses are based on relative *RAI2* gene expression levels, whereas deletions of the RAI2 genomic locus have not been reported for any cancer entity so far. Thus, it seems reasonable that RAI2 gene expression might change by e.g. epigenetic regulation at different stages of prostate cancer progression. In the primary tumour the RAI2 protein might in fact act as a tumour suppressor as indicated by various survival analyses

and functional assays. Whereas in later stages of prostate cancer progression high RAI2 gene expression could indicate constitutive AR activation and progression towards hormone independence as suggested by results of the newly established Liquid biopsy assay. Another explanation for the high RAI2 expression level in CTCs is that it simply acts as a marker of epithelial differentiation and thus can only be detected in CTC positive blood samples. Also, in breast cancer high RAI2 protein expression shows strong correlation to several markers of epithelial differentiation[118].

Nevertheless, since there was no access to other tissue such as matching primary tumour tissue or metastases to compare the detected expression levels to, it is not possible to draw direct comparisons or to state whether the observed levels of RAI2 in the CTC are higher or lower compared to the corresponding primary tumour or metastatic tissue. Furthermore, it should be noted that the RAI2 expression of the entire CTC-fraction of a blood sample was measured within this study. Consequently, it might still be possible that single RAI2 negative cells are among the analysed CTCs-fraction, that invade and cause metastases. Hence. a mRNA expression profile at single CTC level would allow to examine the intra-patient heterogeneity of CTCs and to analyse their specific effect on PCa-progression. In case of a larger patient cohort, it would have furthermore been of interest to correlate the expression levels of RAI2, e.g. low and high, within the CTC positive patient group to clinical data as well as patients' outcome. An advantage of the used method is, that expression analysis of additional genes is possible. One possibility to improve the method in future would be to analyse the a leukocytes fraction of each patient in parallel, in order to use the obtained values for background normalisation later on.

Taken together the results of this study have clearly show a strong association between the RAI2 protein and the steroid hormone receptors ER and AR in cell line models and patients material. Although a role of RAI2 as transcriptional coregulator within the hormone response seems to be possible and supported mainly due to RAI2s interaction with CtBP proteins, the exact function of RAI2 in this process remains unclear. Since the hormone response is a dynamic process in which up to 300 coregulators are involved in a time-dependent and target-gene specific manner[184], it is reasonable to run further analysis at different time points after e.g. receptor activation or inhibition to capture the dynamics. Moreover, it is of utmost interest to analyse whether the impaired DNA repair mechanism observed by Dr. Lena Böttcher in RAI2 depleted luminal breast cancer are caused by an altered hormone receptor action. Several studies have already documented a crosslink between the DNA damage response (DDR)and repair machinery and hormone signalling pathways[185,186], implying that RAI2 might be a functional component in the crosstalk between both these processes, possibly by regulating chromosome architecture and structure. Furthermore the identification of additional interaction partners should be of great interest and might help to clarify the function of RAI2. Thus, besides the ALDLs motifs, one proline-rich domain, and five

other predicted protein motifs has been identified in the protein sequence of RAI2, whose functions have not yet been defined. In order to further define the potential role of RAI2 as a biomarker for prostate cancer progression it would be of interest to analyse the expression of RAI2 throughout all stages, thereby including the analysis of primary tumour tissue, matched CTCs and metastases samples. In addition following the RAI2 expression from the start of hormone therapy administration to development of hormone resistant disease, preferably through several lines of hormone treatment, could furthermore show whether the detection of RAI2 on CTCs can be used as a biomarker to monitor patient's response to hormone therapy treatment.

# 6 Appendix

## A Heat maps of phosphorylated peptides /PAMstation

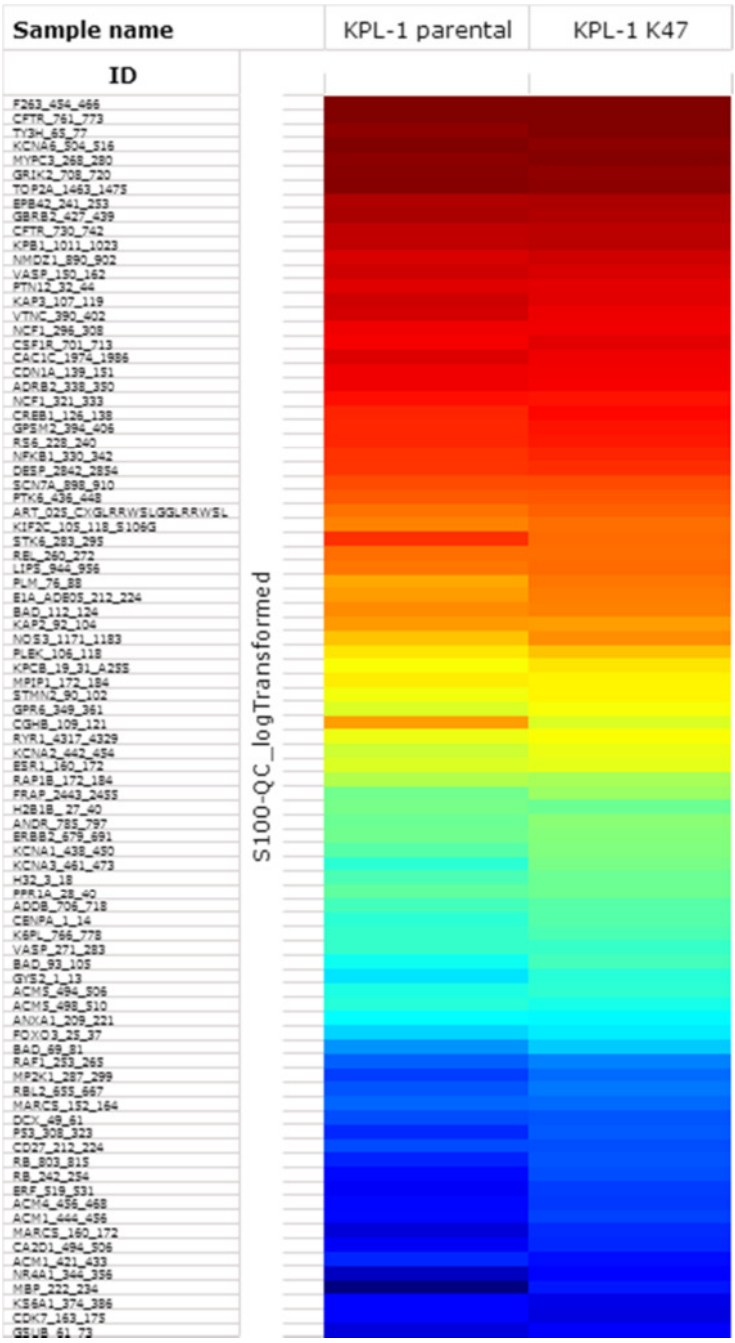


**Fig. 6-1** Heat map visualising log2 transformed signal intensities of phosphorylated peptides after incubation with whole cell extracts from parental and RAI2-KO (K47 clone) KPL-1 breast cancer cells. The phosphorylation signals are sorted from high (red) to low (blue) intensities.

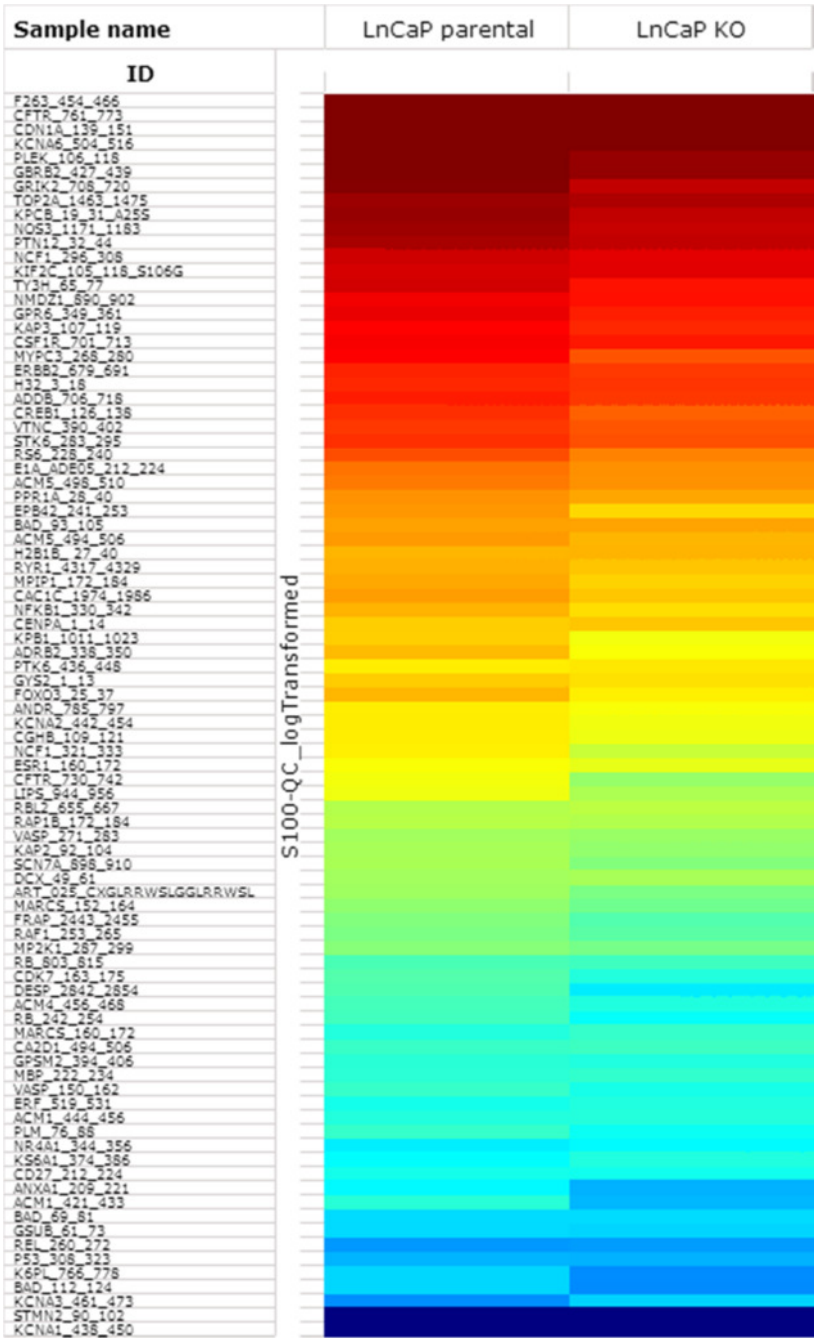


**Fig. 6-2** Heat map visualising log2 transformed signal intensities of phosphorylated peptides after incubation with whole cell extracts from parental and RAI2-KO LNCaP prostate cancer cells. The phosphorylation signals are sorted from high (red) to low (blue) intensities.

# 7 Bibliography


1. Global Burden of Disease Cancer Collaboration. Europe PMC Funders Group The Global Burden of Cancer 2013. *JAMA Oncol.* **1**, 505–527 (2015).

2. International Agency for Reasearch on Cancer 2018. Cancer Tomorrow. *GLOBOCAN 2018* https://gco.iarc.fr/tomorrow/home (2020).

3. White, M. C. *et al.* Age and cancer risk: A potentially modifiable relationship. *Am. J. Prev. Med.* **46**, S7–S15 (2014).

4. Lambert, A. W., Pattabiraman, D. R. & Weinberg, R. A. Emerging Biological Principles of Metastasis. *Cell* **168**, 670–691 (2017).

5. Hanahan, D. & Weinberg, R. A. The Hallmarks of Cancer. *Cell* **100**, 57–70 (2000).

6. Hanahan, D. & Weinberg, R. A. Hallmarks of Cancer: The Next Generation. *Cell* **144**, 646–674 (2011).

7. Fares, J., Fares, M. Y., Khachfe, H. H., Salhab, H. A. & Fares, Y. Molecular principles of metastasis: a hallmark of cancer revisited. *Signal Transduct. Target. Ther.* **5**, (2020).

8. Joosse, S. A., Gorges, T. M. & Pantel, K. Biology, detection, and clinical implications of circulating tumor cells. *EMBO Mol. Med.* **7**, 1–11 (2015).

9. Massagué, J. & Obenauf, A. C. Metastatic colonization by circulating tumour cells. *Nature* **529**, 298–306 (2016).

10. Thiery, J. P., Acloque, H., Huang, R. Y. J. & Nieto, M. A. Epithelial-Mesenchymal Transitions in Development and Disease. *Cell* **139**, 871–890 (2009).

11. Nieto, M. A., Huang, R. Y. Y. J., Jackson, R. A. A. & Thiery, J. P. P. Emt: 2016. *Cell* **166**, 21–45 (2016).

12. Pastushenko, I. *et al.* Identification of the tumour transition states occurring during EMT. *Nature* **556**, (2018).

13. Kalluri, R. & Weinberg, R. A. The basics of epithelial-mesenchymal transition. *J. Clin. Invest.* **119**, 1420–1428 (2009).

14. Culp, M. B. B., Soerjomataram, I., Efstathiou, J. A., Bray, F. & Jemal, A. Recent Global Patterns in Prostate Cancer Incidence and Mortality Rates. *Eur. Urol.* **77**, 38–52 (2020).

15. Baade, P. D., Youlden, D. R. & Krnjacki, L. J. International epidemiology of prostate cancer: Geographical distribution and secular trends. *Mol. Nutr. Food Res.* **53**, 171–184 (2009).

16. Zeigler-Johnson, C. M. *et al.* Genetic susceptibility to prostate cancer in men of African

descent: implications for global disparities in incidence and outcomes. *Can. J. Urol.* **15**, 3872–3882 (2008).

17. International Agency for Research on Cancer 2018. Cancer Today, Top cancer per country, estimated number of new cases in 2018, males, all ages. *GLOBOCAN 2018* https://gco.iarc.fr/today/online-analysis-map?v=2018&mode=cancer&mode_population=continents&population=900&populations=900&key=total&sex=1&cancer=39&type=0&statistic=5&prevalence=0&population_group=0&ages_group%5B%5D=0&ages_group%5B%5D=17&nb_items=10&grou (2020).

18. Robert Koch-Institut (Hrsg.) & Gesellschaft der epidemiologischen Krebsregister in Deutschland e.V.(Hrsg.). Krebs in Deutschland für 2015 / 2016 Krebs in Deutschland. *Berlin* **12. Ausgab**, (2019).

19. McNeal, J. E. The zonal anatomy of the prostate. *Prostate* **2**, 35–49 (1981).

20. Wright, J. L. & Ellis, W. J. Improved prostate cancer detection with anterior apical prostate biopsies. *Urol. Oncol. Semin. Orig. Investig.* **24**, 492–495 (2006).

21. Zhang, D., Zhao, S., Li, X., Kirk, J. S. & Tang, D. G. Prostate Luminal Progenitor Cells in Development and Cancer. *Trends in Cancer* **4**, 769–783 (2018).

22. Xu, J. *et al.* HOXB13 is a susceptibility gene for prostate cancer: Results from the International Consortium for Prostate Cancer Genetics (ICPCG). *Hum. Genet.* **132**, 5–14 (2013).

23. Nicolosi, P. *et al.* Prevalence of Germline Variants in Prostate Cancer and Implications for Current Genetic Testing Guidelines. *JAMA Oncol.* **5**, 523–528 (2019).

24. Barlow, L. J. & Shen, M. M. SnapShot: Prostate Cancer. *Cancer Cell* **24**, 400-400.e1 (2013).

25. Sathianathen, N. J., Konety, B. R., Crook, J., Saad, F. & Lawrentschuk, N. Landmarks in prostate cancer. *Nat. Rev. Urol.* **15**, 627–642 (2018).

26. Epstein, J. I. *et al.* The 2014 International Society of Urological Pathology (ISUP) Consensus Conference on Gleason Grading of Prostatic Carcinoma. *Am. J. Surg. Pathol.* **40**, 1 (2015).

27. Pospihalj, B. Staging of prostate cancer: a review with reference for further refinement. *Anal. Quant. Cytopathol. Histopathol.* **37**, 69–74 (2015).

28. Chen, Y., Clegg, N. J. & Scher, H. I. Anti-androgens and androgen-depleting therapies in prostate cancer: new agents for an established target. *Lancet Oncol.* **10**, 981–991 (2009).

29. Oncology, guidlines. Interdisziplinäre Leitlinie der Qualität S3 zur Früherkennung , Diagnose und Therapie der verschiedenen Stadien des Prostatakarzinoms. 1–99 (2014).

30. Harris, W. P., Mostaghel, E. A., Nelson, P. S. & Montgomery, B. Androgen deprivation therapy: Progress in understanding mechanisms of resistance and optimizing androgen

depletion. *Nat. Clin. Pract. Urol.* **6**, 76–85 (2009).

31. Urology Care Foundation. What is Advanced Prostate Cancer? *Urology Health* https://www.urologyhealth.org/patient-magazine/magazine-archives/2016/spring-2016/what-is-advanced-prostate-cancer (2016).

32. Deutsche Krebsgesellschaft DK, A. Interdisziplinäre Leitlinie derQualität S3 zur Früherkennung, Diagnose und Therapie der verschiedenen Stadien des Prostatakarzinoms. Kurzversion 5.1. *Leitlinienprogramm Onkologie* https://www.leitlinienprogramm-onkologie.de/fileadmin/user_upload/Downloads/Leitlinien/Prostata_5_0/LL_Prostatakarzinom_Kurzversion_5.1.pdf (2019).

33. Bray, F. *et al.* Global cancer statistics 2018: GLOBOCAN estimates of incidence and mortality worldwide for 36 cancers in 185 countries. *CA. Cancer J. Clin.* **68**, 394–424 (2018).

34. Hossain, M. S., Ferdous, S. & Karim-Kos, H. E. Breast cancer in South Asia: A Bangladeshi perspective. *Cancer Epidemiol.* **38**, 465–470 (2014).

35. Winters, S., Martin, C., Murphy, D. & Shokar, N. K. Breast Cancer Epidemiology, Prevention, and Screening. in *Progress in Molecular Biology and Translational Science* vol. 151 1–32 (Elsevier Inc., 2017).

36. Allemani, C. *et al.* Global surveillance of cancer survival 1995-2009: Analysis of individual data for 25 676 887 patients from 279 population-based registries in 67 countries (CONCORD-2). *Lancet* **385**, 977–1010 (2015).

37. Harbeck, N. *et al. Breast cancer*. *Nature Reviews Disease Primers* vol. 5 (2019).

38. Gallardo-Alvarado, L. N. *et al.* Prevalence of germline mutations in the TP53 gene in patients with early-onset breast cancer in the Mexican population. *BMC Cancer* **19**, 1–10 (2019).

39. Shiovitz, S. & Korde, L. A. Genetics of breast cancer: A topic in evolution. *Ann. Oncol.* **26**, 1291–1299 (2015).

40. Onkologie, L. Interdisziplinäre S3-Leitlinie für die Früherkennung , Nachsorge des Mammakarzinoms Wesentliche Neuerungen durch die. 32–45 (2018).

41. Secretan, B. L. *et al.* Spe ci a l R e p or t Breast-Cancer Screening — Viewpoint of the IARC Working Group. 2353–2358 (2015).

42. Njor, S. *et al.* Breast cancer mortality in mammographic screening in Europe: A review of incidence-based mortality studies. *J. Med. Screen.* **19**, 33–41 (2012).

43. Risbridger, G. P., Davis, I. D., Birrell, S. N. & Tilley, W. D. Breast and prostate cancer: More similar than different. *Nat. Rev. Cancer* **10**, 205–212 (2010).

44. Groner, A. C. & Brown, M. Role of steroid receptor and coregulator mutations in

hormone-dependent cancers. *J. Clin. Invest.* **127**, 1126–1135 (2017).

45. Bain, D. L., Heneghan, A. F., Connaghan-Jones, K. D. & Miura, M. T. Nuclear Receptor Structure: Implications for Function. *Annu. Rev. Physiol.* **69**, 201–220 (2007).

46. Claessens, F. *et al.* Diverse roles of androgen receptor (AR) domains in AR-mediated signaling. *Nucl. Recept. Signal.* **6**, (2008).

47. Nakamura, Y. *et al.* Type 5 17β-hydroxysteroid dehydrogenase (AKR1C3) contributes to testosterone production in the adrenal reticularis. *J. Clin. Endocrinol. Metab.* **94**, 2192–2198 (2009).

48. Rosner, W., Hryb, D. J., Saeed Khan, M., Nakhla, A. M. & Romas, N. A. Sex hormone-binding globulin: Anatomy and physiology of a new regulatory system. *J. Steroid Biochem. Mol. Biol.* **40**, 813–820 (1991).

49. Dunn, J. F., Nisula, B. C. & Rodbard, D. Transport of Steroid Hormones: Binding of 21 Endogenous Steroids to Both Testosterone-Binding Globulin and Corticosteroid-Binding Globulin in Human Plasma. *J. Clin. Endocrinol. Metab.* **53**, 58–68 (1981).

50. Russell, D. W. & Wilson, J. D. Steroid 5alpha-Reductase: Two Genes/Two Enzymes. *Annu. Rev. Biochem.* **63**, 25–61 (1994).

51. Bruchovsky, N. & Wilson, J. D. The intranuclear binding of testosterone and 5-alpha-androstan-17-beta-ol-3-one by rat prostate. *J. Biol. Chem.* **243**, 5953–60 (1968).

52. Smith, D. F. & Toft, D. O. The intersection of steroid receptors with molecular chaperones: Observations and questions. *Mol. Endocrinol.* **22**, 2229–2240 (2008).

53. Berrevoets, C. A., Doesburg, P., Steketee, K., Trapman, J. & Brinkmann, A. O. Functional interactions of the AF-2 activation domain core region of the human androgen receptor with the amino-terminal domain and with the transcriptional coactivator TIF2 (transcriptional intermediary factor 2). *Mol. Endocrinol.* **12**, 1172–1183 (1998).

54. Brinkmann, A. O. *et al.* Mechanisms of androgen receptor activation and function. **69**, 307–313 (1999).

55. Heemers, H. V. & Tindall, D. J. Androgen receptor (AR) coregulators: A diversity of functions converging on and regulating the AR transcriptional complex. *Endocr. Rev.* **28**, 778–808 (2007).

56. Feldman, B. J. & Feldman, D. The development of androgen-independent prostate cancer. *Nat. Rev. Cancer* **1**, 34–45 (2001).

57. Savkur, R. S. & Burris, T. P. The coactivator LXXLL nuclear receptor recognition motif. *J. Pept. Res.* **63**, 207–212 (2004).

58. Plevin, M. J., Mills, M. M. & Ikura, M. The LxxLL motif: a multifunctional binding sequence in transcriptional regulation. *Trends Biochem. Sci.* **30**, 66–69 (2005).

59. He, B., Minges, J. T., Lee, L. W. & Wilson, E. M. The FXXLF motif mediates androgen receptor-specific interactions with coregulators. *J. Biol. Chem.* **277**, 10226–10235 (2002).

60. Chi, D. *et al.* Estrogen receptor signaling is reprogrammed during breast tumorigenesis. *Proc. Natl. Acad. Sci. U. S. A.* **166**, 11437–11443 (2019).

61. Copeland, B. T., Du, J., Pal, S. K. & Jones, J. O. Factors that influence the androgen receptor cistrome in benign and malignant prostate cells. *Mol. Oncol.* **13**, 2616–2632 (2019).

62. Beatson, G. T. Treatment of Cancer by Oöphorectomy. *Br. Med. J.* **2**, 1195 (1926).

63. Huggins, C. Endocrine-Induced Regression of Cancers1 Phosphorus Metabolism in Genital Tract. *Cancer Res.* **27**, 1925–1930 (1967).

64. Huggins, C. & Hodges, C. V. Studies on prostatic cancer i. the effect of castration, of estrogen and of androgen injection on serum phosphatases in metastatic carcinoma of the prostate. *Cancer Res.* **1**, 293–297 (1941).

65. Nishiyama, T., Hashimoto, Y. & Takahashi, K. The influence of androgen deprivation therapy on dihydrotestosterone levels in the prostatic tissue of patients with prostate cancer. *Clin. Cancer Res.* **10**, 7121–7126 (2004).

66. Wong, Y. N. S., Ferraldeschi, R., Attard, G. & De Bono, J. Evolution of androgen receptor targeted therapy for advanced prostate cancer. *Nat. Rev. Clin. Oncol.* **11**, 365–376 (2014).

67. Akaza, H. *et al.* Combined androgen blockade with bicalutamide for advanced prostate cancer: Long-term follow-up of a phase 3, double-blind, randomized study for survival. *Cancer* **115**, 3437–3445 (2009).

68. Schmitt, B., Bennett, C., Seidenfeld, J., Samson, D. & Wilt, T. J. Maximal androgen blockade for advanced prostate cancer. *Cochrane Database Syst. Rev.* **115**, 3437–3445 (1999).

69. Watson, P. A., Arora, V. K. & Sawyers, C. L. Emerging mechanisms of resistance to androgen receptor inhibitors in prostate cancer. *Nat. Rev. Cancer* **15**, 701–711 (2015).

70. Quinn, D. I., Sandler, H. M., Horvath, L. G., Goldkorn, A. & Eastham, J. A. The evolution of chemotherapy for the treatment of prostate cancer. *Ann. Oncol.* **28**, 2658–2669 (2017).

71. Dagher, R. N. *et al.* Approval summary: Docetaxel in combination with prednisone for the treatment of androgen-independent hormone-refractory prostate cancer. *Clin. Cancer Res.* **10**, 8147–8151 (2004).

72. Tran, C. *et al.* Development of a Second-Generation Antiandrogen for Treatment of Advanced Prostate Cancer. *Science (80-. ).* **324**, 787–790 (2009).

73. Potter, G. A., Barrie, S. E., Jarman, M. & Rowlands, M. G. Novel Steroidal Inhibitors of Human Cytochrome P45017.alpha.-Hydroxylase-C17,20-lyase): Potential Agents for the Treatment of Prostatic Cancer. *J. Med. Chem.* **38**, 2463–2471 (1995).

74. U.S. Food and Drug Administration. Prescribing Information for ZYTIGA. 1–34 https://www.accessdata.fda.gov/drugsatfda_docs/label/2018/202379s024lbl.pdf (2018).

75. U.S. Food and Drug Administration. Prescribing Information for XTANDI. 1–31 https://www.accessdata.fda.gov/drugsatfda_docs/label/2019/203415s015lbl.pdf (2019).

76. Armstrong, C. M. & Gao, A. C. Drug resistance in castration resistant prostate cancer: resistance mechanisms and emerging treatment strategies. *Am. J. Clin. Exp. Urol.* **3**, 64–76 (2015).

77. Johnston, S. J. & Cheung, K.-L. Endocrine Therapy for Breast Cancer: A Model of Hormonal Manipulation. *Oncol. Ther.* **6**, 141–156 (2018).

78. Simpson, E. R. Sources of estrogen and their importance. *J. Steroid Biochem. Mol. Biol.* **86**, 225–230 (2003).

79. Williams, N. & Harris, L. N. The renaissance of endocrine therapy in breast cancer. *Curr. Opin. Obstet. Gynecol.* **26**, 41–47 (2014).

80. Rani, A., Stebbing, J., Giamas, G. & Murphy, J. Endocrine resistance in hormone receptor positive breast cancer–from mechanism to therapy. *Front. Endocrinol. (Lausanne).* **10**, (2019).

81. Razavi, P. *et al.* The Genomic Landscape of Endocrine-Resistant Advanced Breast Cancers. *Cancer Cell* **34**, 427-438.e6 (2018).

82. Shang, Y., Hu, X., DiRenzo, J., Lazar, M. A. & Brown, M. Cofactor Dynamics and Sufficiency in Estrogen Receptor–Regulated Transcription. *Cell* **103**, 843–852 (2000).

83. Shang, Y. & Brown, M. Molecular determinants for the tissue specificity of SERMs. *Science (80-. ).* **295**, 2465–2468 (2002).

84. Osborne, C. K., Wakeling, A. & Nicholson, R. I. Fulvestrant: an oestrogen receptor antagonist with a novel mechanism of action. *Br. J. Cancer* **90**, S2–S6 (2004).

85. Visakorpi, T. *et al.* In vivo amplification of the androgen receptor gene and progression of human prostate cancer. *Nat. Genet.* **9**, 401–406 (1995).

86. Jeselsohn, R. *et al.* Emergence of constitutively active estrogen receptor-α mutations in pretreated advanced estrogen receptor-positive breast cancer. *Clin. Cancer Res.* **20**, 1757–1767 (2014).

87. Robinson, D. *et al.* Integrative clinical genomics of advanced prostate cancer. *Cell* **161**, 1215–1228 (2015).

88. Carlson, K. E., Choi, I., Gee, A., Katzenellenbogen, B. S. & Katzenellenbogen, J. A. Altered ligand binding properties and enhanced stability of a constitutively active estrogen receptor: Evidence that an open pocket conformation is required for ligand interaction. *Biochemistry* **36**, 14897–14905 (1997).

89. Gregory, C. W., Johnson, R. T., Mohler, J. L., French, F. S. & Wilson, E. M. Androgen receptor stabilization in recurrent prostate cancer is associated with hypersensitivity to low androgen. *Cancer Res.* **61**, 2892–2898 (2001).

90. Cai, C. *et al.* Intratumoral De Novo steroid synthesis activates androgen receptor in castration-resistant prostate cancer and is upregulated by treatment with CYP17A1 inhibitors. *Cancer Res.* **71**, 6503–6513 (2011).

91. Simpson, E. R. *et al.* Estrogen - The good, the bad, and the unexpected. *Endocr. Rev.* **26**, 322–330 (2005).

92. De Jong, P. C. *et al.* Inhibition of breast cancer tissue aromatase activity and estrogen concentrations by the third-generation aromatase inhibitor vorozole. *Cancer Res.* **57**, 2109–2111 (1997).

93. Toy, W. *et al.* ESR1 ligand-binding domain mutations in hormone-resistant breast cancer. *Nat. Genet.* **45**, 1439–1445 (2013).

94. Hu, D. G. *et al.* Identification of Androgen Receptor Splice Variant Transcripts in Breast Cancer Cell Lines and Human Tissues. *Horm. Cancer* **5**, 61–71 (2014).

95. Kallio, H. M. L. *et al.* Constitutively active androgen receptor splice variants AR-V3, AR-V7 and AR-V9 are co-expressed in castration-resistant prostate cancer metastases. *Br. J. Cancer* **119**, 347–356 (2018).

96. Hart, C. D. *et al.* Challenges in the management of advanced, ER-positive, HER2-negative breast cancer. *Nat. Rev. Clin. Oncol.* **12**, 541–552 (2015).

97. DeGraffenried, L. A. *et al.* Inhibition of mTOR activity restores tamoxifen response in breast cancer cells with aberrant Akt activity. *Clin. Cancer Res.* **10**, 8059–8067 (2004).

98. Wen, Y. *et al.* HER-2/neu promotes androgen-independent survival and growth of prostate cancer cells through the Akt pathway. *Cancer Res.* **60**, 6841–6845 (2000).

99. McDonnell, T. J., Hsieh, J. T. & Campbell, M. L. Expression of the Protooncogene bcl-2 in the Prostate and Its Association with Emergence of Androgen-independent Prostate Cancer. *Cancer Res.* **52**, 6940–6944 (1992).

100. Colombel, M. *et al.* Detection of the apoptosis-suppressing oncoprotein bcl-2 in hormone-refractory human prostate cancers. *Am. J. Pathol.* **143**, 390–400 (1993).

101. Gundem, G. *et al.* The evolutionary history of lethal metastatic prostate cancer. *Nature* **520**, 353–357 (2015).

102. Bardelli, A. & Pantel, K. Liquid Biopsies, What We Do Not Know (Yet). *Cancer Cell* **31**, 172–179 (2017).

103. Werner, S., Stenzl, A., Pantel, K. & Todenhöfer, T. Expression of Epithelial Mesenchymal Transition and Cancer Stem Cell Markers in Circulating Tumor Cells. in vol. 994 205–228 (2017).

104. Lianidou, E. & Pantel, K. Liquid biopsies. *Genes Chromosom. Cancer* **58**, 219–232 (2019).

105. Ashworth, T. R. A case of cancer in which cells similar to those in the tumours were seen in the blood after death. *Aust Med J.* **14**, 146 (1869).

106. Bredemeier, M. *et al.* Gene expression signatures in circulating tumor cells correlate with response to therapy in metastatic breast cancer. *Clin. Chem.* **63**, 1585–1593 (2017).

107. Pantel, K. & Alix-Panabières, C. Liquid biopsy and minimal residual disease — latest advances and implications for cure. *Nat. Rev. Clin. Oncol.* **16**, 409–424 (2019).

108. Larsson, A. M. *et al.* Longitudinal enumeration and cluster evaluation of circulating tumor cells improve prognostication for patients with newly diagnosed metastatic breast cancer in a prospective observational trial. *Breast Cancer Res.* **20**, 1–14 (2018).

109. Bidard, F. C. *et al.* Circulating tumor cells in breast cancer patients treated by neoadjuvant chemotherapy: A Meta-analysis. *J. Natl. Cancer Inst.* **110**, 560–567 (2018).

110. Pantel, K., Hille, C. & Scher, H. I. Circulating tumor cells in prostate cancer: From discovery to clinical utility. *Clin. Chem.* **65**, 87–99 (2019).

111. Paoletti, C. *et al.* Heterogeneous estrogen receptor expression in circulating tumor cells suggests diverse mechanisms of fulvestrant resistance. *Mol. Oncol.* **10**, 1078–1085 (2016).

112. Paolillo, C. *et al.* Detection of activating estrogen receptor gene (ESR1) mutations in single circulating tumor cells. *Clin. Cancer Res.* **23**, 6086–6093 (2017).

113. Babayan, A. *et al.* Heterogeneity of Estrogen Receptor Expression in Circulating Tumor Cells from Metastatic Breast Cancer Patients. *PLoS One* **8**, 1–11 (2013).

114. Antonarakis, E. S. *et al.* AR-V7 and resistance to enzalutamide and abiraterone in prostate cancer. *N. Engl. J. Med.* **371**, 1028–1038 (2014).

115. Antonarakis, E. S. *et al.* Androgen receptor splice variant 7 and efficacy of taxane chemotherapy in patients with metastatic castration-resistant prostate cancer. *JAMA Oncol.* **1**, 582–591 (2015).

116. Heitzer, E., Haque, I. S., Roberts, C. E. S. & Speicher, M. R. Current and future perspectives of liquid biopsies in genomics-driven oncology. *Nat. Rev. Genet.* **20**, 71–88 (2019).

117. U.S. Food and Drug Administration. Prescribing Information for PIQRAY. 1–21 https://www.accessdata.fda.gov/drugsatfda_docs/label/2019/212526s000lbl.pdf (2019).

118. Werner, S. *et al.* Suppression of Early Hematogenous Dissemination of Human Breast Cancer Cells to Bone Marrow by Retinoic Acid-Induced 2. *Cancer Discov.* **5**, 506–519 (2015).

119. Jonk, L. J., de Jonge, M. E., Vervaart, J. M., Wissink, S. & Kruijer, W. Isolation and developmental expression of retinoic-acid-induced genes. *Dev. Biol.* **161**, 604–14 (1994).

120. Walpole, S. M. *et al.* Identification and characterization of the human homologue (RAI2) of a mouse retinoic acid-induced gene in Xp22. *Genomics* **55**, 275–283 (1999).

121. Gattelli, A. *et al.* Progression of Pregnancy-Dependent Mouse Mammary Tumors after Long Dormancy Periods . Involvement of Wnt Pathway Activation Progression of Pregnancy-Dependent Mouse Mammary Tumors after Long Dormancy Periods . Involvement of Wnt Pathway Activation. 5193–5199 (2004).

122. Gattelli, A., Zimberlin, M. N., Meiss, R. P., Castilla, L. H. & Kordon, E. C. Selection of Early-Occurring Mutations Dictates Hormone-Independent Progression in Mouse Mammary Tumor Lines. *J. Virol.* **80**, 11409–11415 (2006).

123. Besler, K. *et al.* Abstract 3736: Role of RAI2 protein in progression of breast and prostate cancer to hormone independent disease. *Cancer Res.* **78**, 3736 LP – 3736 (2018).

124. Dcona, M. M., Morris, B. L., Ellis, K. C. & Grossman, S. R. CtBP- an emerging oncogene and novel small molecule drug target: Advances in the understanding of its oncogenic action and identification of therapeutic inhibitors. *Cancer Biol. Ther.* **18**, 379–391 (2017).

125. Böttcher, L. The role of RAI2 protein in the maintenance of genomic stability. *Universiy of Hamburg* (University of Hamburg, 2019).

126. Yan, W. *et al.* Retinoic acid-induced 2 (RAI2) is a novel tumor suppressor, and promoter region methylation of RAI2 is a poor prognostic marker in colorectal cancer. *Clin. Epigenetics* **10**, 69 (2018).

127. Ran, F. A. *et al.* Genome engineering using the CRISPR-Cas9 system. *Nat. Protoc.* **8**, 2281–2308 (2013).

128. Guzmán, C., Bagga, M., Kaur, A., Westermarck, J. & Abankwa, D. ColonyArea: An ImageJ plugin to automatically quantify colony formation in clonogenic assays. *PLoS One* **9**, 14–17 (2014).

129. Borowicz, S. *et al.* The Soft Agar Colony Formation Assay. *J. Vis. Exp.* 1–6 (2014) doi:10.3791/51998.

130. Choudhry, P. High-Throughput method for automated colony and cell counting by digital image analysis based on edge detection. *PLoS One* **11**, 1–23 (2016).

131. Lange, T. *et al.* Aberrant presentation of HPA-reactive carbohydrates implies selectin-independent metastasis formation in human prostate cancer. *Clin. Cancer Res.* **20**, 1791–1802 (2014).

132. Dzamba, D., Valihrach, L., Kubista, M. & Anderova, M. The correlation between expression profiles measured in single cells and in traditional bulk samples. *Sci. Rep.* **6**, 1–9 (2016).

133. Menyhárt, O. *et al.* Guidelines for the selection of functional assays to evaluate the hallmarks of cancer. *Biochim. Biophys. Acta - Rev. Cancer* **1866**, 300–319 (2016).

134. Jensen, J. Role of the RAI2 protein in endocrine resistance of luminal breast cancer cells. *Master Thesis* (2017).

135. Puck, T. T., Marcus, P. I. & Cieciura, S. J. CLONAL GROWTH OF MAMMALIAN CELLS IN VITRO. *J. Exp. Med.* **103**, 273–284 (1956).

136. Woolston, C. & Stewart, M. Analysis of Tumor and Endothelial Cell Viability and Survival Using Sulforhodamine B and Clonogenic Assays. *Methods Mol. Biol.* **740**, p.7-12 (2011).

137. Taddei, M. L., Giannoni, E., Fiaschi, T. & Chiarugi, P. Anoikis: An emerging hallmark in health and diseases. *J. Pathol.* **226**, 380–393 (2012).

138. Müller, I. & Ullrich, S. The PFP/RAG2 Double-Knockout Mouse in Metastasis Research: Small-Cell Lung Cancer and Prostate Cancer. *Methods Mol. Biol.* **1070**, 191–201 (2014).

139. Xu, L. *et al.* Optimization and evaluation of a novel size based circulating tumor cell isolation system. *PLoS One* **10**, 1–23 (2015).

140. Parrish, R. R., Day, J. J. & Lubin, F. D. Direct Bisulfite Sequencing for Examination of DNA Methylation with Gene and Nucleotide Resolution from Brain Tissues. *Curr. Protoc. Neurosci.* **60**, 1–14 (2012).

141. Munkley, J. *et al.* Glycosylation is an Androgen-Regulated Process Essential for Prostate Cancer Cell Viability. *EBioMedicine* **8**, 103–116 (2016).

142. Rugo, H. S., Vidula, N. & Ma, C. Improving Response to Hormone Therapy in Breast Cancer: New Targets, New Therapeutic Options. *Am. Soc. Clin. Oncol. Educ. B.* **36**, e40–e54 (2016).

143. Eckert, D., Buhl, S., Weber, S., Jäger, R. & Schorle, H. The AP-2 family of transcription factors. *Genome Biol.* **6**, (2005).

144. Jeng, M. H. *et al.* Estrogen receptor expression and function in long-term estrogen-deprived human breast cancer cells. *Endocrinology* **139**, 4164–4174 (1998).

145. Olson, B. M. *et al.* Prostate cancer cells express more androgen receptor (AR) following androgen deprivation, improving recognition by AR-specific T cells. *Cancer Immunol. Res.* **5**, 1074–1085 (2017).

146. Werner, S. *et al.* Abstract 2696: Deciphering the interactome of the metastasis-suppressor protein RAI2. *Cancer Res.* **78**, 2696 LP – 2696 (2018).

147. Takayama, K.-I. *et al.* Androgen-responsive long noncoding RNA CTBP1-AS promotes prostate cancer. *EMBO J.* **32**, 1665–80 (2013).

148. Takayama, K. I. *et al.* Androgen-responsive long noncoding RNA CTBP1-AS promotes prostate cancer. *EMBO J.* **32**, 1665–1680 (2013).

149. Takayama, K. I. *et al.* CtBP2 modulates the androgen receptor to promote prostate cancer progression. *Cancer Res.* **74**, 6542–6553 (2014).

150. Verger, A. *et al.* Mechanisms Directing the Nuclear Localization of the CtBP Family Proteins. *Mol. Cell. Biol.* **26**, 4882–4894 (2006).

151. Palijan, A. *et al.* Ligand-dependent corepressor LCoR is an attenuator of progesterone-regulated gene expression. *J. Biol. Chem.* **284**, 30275–30287 (2009).

152. Jalaguier, S. *et al.* Complex regulation of LCoR signaling in breast cancer cells. *Oncogene* 4790–4801 (2017) doi:10.1038/onc.2017.97.

153. Lopez-Garcia, J. *et al.* ZNF366 is an estrogen receptor corepressor that acts through CtBP and histone deacetylases. *Nucleic Acids Res.* **34**, 6126–6136 (2006).

154. Zitzmann, K. *et al.* The novel mTOR inhibitor RAD001 (everolimus) induces antiproliferative effects in human pancreatic neuroendocrine tumor cells. *Neuroendocrinology* **85**, 54–60 (2007).

155. Vasan, N., Toska, E. & Scaltriti, M. Overview of the relevance of PI3K pathway in HR-positive breast cancer. *Ann. Oncol. Off. J. Eur. Soc. Med. Oncol.* **30**, x3–x11 (2019).

156. Tohtong, R., Phattarasakul, K., Jiraviriyakul, A. & Sutthiphongchai, T. Dependence of metastatic cancer cell invasion on MLCK-catalyzed phosphorylation of myosin regulatory light chain. *Prostate Cancer Prostatic Dis.* **6**, 212–216 (2003).

157. Li, L. *et al.* CDKL2 promotes epithelial-mesenchymal transition and breast cancer progression. *Oncotarget* **5**, 10840–10853 (2014).

158. Dart, D. A., Ashelford, K. & Jiang, W. G. AR mRNA stability is increased with AR-antagonist resistance via 3′UTR variants. *Endocr. Connect.* **9**, 9–19 (2020).

159. Nelson, W. G. & Yegnasubramanian, S. Resistance Emerges to Second-Generation Antiandrogens in Prostate Cancer. *Cancer Discov.* **3**, 971–974 (2013).

160. Feng, Q. & He, B. Androgen Receptor Signaling in the Development of Castration-Resistant Prostate Cancer. *Front. Oncol.* **9**, 1–10 (2019).

161. Makkonen, H., Kauhanen, M., Jaaskelainen, T. & Palvimo, J. J. Androgen receptor amplification is reflected in the transcriptional responses of Vertebral-Cancer of the Prostate cells. *Mol. Cell. Endocrinol.* **331**, 57–65 (2011).

162. Sampson, N., Neuwirt, H., Puhr, M., Klocker, H. & Eder, I. E. In vitro model systems to study androgen receptor signaling in prostate cancer. *Endocr. Relat. Cancer* **20**, (2013).

163. Ho, Y. & Dehm, S. M. Androgen receptor rearrangement and splicing variants in resistance to endocrine therapies in prostate cancer. *Endocrinology* **158**, 1533–1542 (2017).

164. Li, Q. *et al.* Linking prostate cancer cell AR heterogeneity to distinct castration and enzalutamide responses. *Nat. Commun.* **9**, (2018).

165. Bhatia, A. & Kumar, Y. Cancer Cell Micronucleus: An Update On Clinical And Diagnostic Applications. *Apmis* **121**, 569–581 (2013).

166. Ye, C. J. *et al.* Micronuclei and genome chaos: Changing the system inheritance. *Genes (Basel).* **10**, 1–21 (2019).

167. Zhang, X.-H., Tee, L. Y., Wang, X.-G., Huang, Q.-S. & Yang, S.-H. Off-target Effects in CRISPR/Cas9-mediated Genome Engineering. *Mol. Ther. - Nucleic Acids* **4**, e264 (2015).

168. Ben-David, U. *et al.* Genetic and transcriptional evolution alters cancer cell line drug response. *Nature* **560**, 325–330 (2018).

169. Hynds, R. E., Vladimirou, E. & Janes, S. M. The secret lives of cancer cell lines. *DMM Dis. Model. Mech.* **11**, 1–5 (2018).

170. Chinnadurai, G. The transcriptional corepressor CtBP: A foe of multiple tumor suppressors. *Cancer Res.* **69**, 731–734 (2009).

171. Blevins, M. A., Huang, M. & Zhao, R. The role of CtBP1 in oncogenic processes & its potential as a therapeutic target. *Mol. Cancer Ther.* **16**, 981–990 (2017).

172. Danila, D. C. *et al.* Clinical validity of detecting circulating tumor cells by AdnaTest assay compared with direct detection of tumor mRNA in stabilized whole blood, as a biomarker predicting overall survival for metastatic castration-resistant prostate cancer patients. *Cancer J. (United States)* **22**, 315–320 (2016).

173. Miyamoto, D. T. *et al.* An RNA-based digital circulating tumor cell signature is predictive of drug response and early dissemination in prostate cancer. *Cancer Discov.* **8**, 288–303 (2018).

174. Sánchez, C. *et al.* Chemotherapy sensitivity recovery of prostate cancer cells by functional inhibition and knock down of multidrug resistance proteins. *Prostate* **71**, 1810–1817 (2011).

175. Bitting, R. L. & Armstrong, A. J. Targeting the PI3K/Akt/mTOR pathway in castration-resistant prostate cancer. *Endocr. Relat. Cancer* **20**, 83–99 (2013).

176. Toren, P. & Zoubeidi, A. Targeting the PI3K/Akt pathway in prostate cancer: Challenges and opportunities (Review). *Int. J. Oncol.* **45**, 1793–1801 (2014).

177. Gorges, T. M. *et al.* Accession of tumor heterogeneity by multiplex transcriptome profiling of single circulating tumor cells. *Clin. Chem.* **62**, 1504–1515 (2016).

178. Minutti, C. M. *et al.* Epidermal Growth Factor Receptor Expression Licenses Type-2 Helper T Cells to Function in a T Cell Receptor-Independent Fashion. *Immunity* **47**, 710-722.e6 (2017).

179. Chan, G., Nogalski, M. T. & Yurochko, A. D. Activation of EGFR on monocytes is required for human cytomegalovirus entry and mediates cellular motility. *Proc. Natl. Acad. Sci. U. S. A.* **106**, 22369–22374 (2009).

180. Škereňová, M. *et al.* Gene Expression Analysis of Immunomagnetically Enriched Circulating Tumor Cell Fraction in Castration-Resistant Prostate Cancer. *Mol. Diagnosis*

*Ther.* **22**, 381–390 (2018).

181. Armstrong, A. J. *et al.* Prospective multicenter validation of androgen receptor splice variant 7 and hormone therapy resistance in high-risk castration-resistant prostate cancer: The PROPHECY study. *J. Clin. Oncol.* **37**, 1120–1129 (2019).

182. Van Belle, S. J. P. What is the value of hemoglobin as a prognostic and predictive factor in cancer? *Eur. J. Cancer, Suppl.* **2**, 11–19 (2004).

183. Ibrahim, U. A., Yusuf, A. A. & Ahmed, S. G. The Pathophysiologic Basis of Anaemia in Patients with Malignant Diseases. *Gulf J. Oncolog.* **1**, 80–89 (2016).

184. Dai, C., Heemers, H. & Sharifi, N. Androgen signaling in prostate cancer. *Cold Spring Harb. Perspect. Med.* **7**, (2017).

185. Matta, J. *et al.* Estrogen receptor expression is associated with DNA repair capacity in breast cancer. *PLoS One* **11**, 1–14 (2016).

186. Schiewer, M. J. & Knudsen, K. E. Linking DNA Damage and Hormone Signaling Pathways in Cancer. *Trends Endocrinol. Metab.* **27**, 216–225 (2016).

# Danksagung

Nach jahrelanger Forschung und intensiver Schreibarbeit findet auch dieser Lebensabschnitt sein Ende. Und so möchte ich die nächsten Zeilen nutzen, um mich bei allen Beteiligten zu bedanken, die mich in diesen Jahren gefördert, gefordert oder mir den Weg mit Rat und Tat geebnet haben.

Zunächst möchte ich mich bei Prof. Dr. Klaus Pantel bedanken, für die Möglichkeit meine Doktorarbeit unter exzellenten Bedingungen am Institut für Tumorbiologie anfertigen zu dürfen. Besonders danke ich Ihnen jedoch für die Unterstützung und die Wertschätzung, welche Sie mir entgegengebracht haben. Danke auch für die vielen kleinen Gespräche auf dem Flur oder im Fahrstuhl, über Wissenschaft und die Welt, welche mir nicht selten den Anlass für eine neue Idee gegeben haben.

Mein besonderer Dank gilt meinen Mentoren Dr. Stefan Werner und Prof. Dr. Haiju Wikman. Wie bei jeder anspruchsvollen Arbeit gibt es stressige Phasen sowie Hindernisse, doch über allem habt ihr mich in diesen Zeiten nicht nur geleitet, sondern auch stets motiviert und was am wichtigsten ist, inspiriert. Selbst die Herausforderungen, welchen man sich nur alleine stellen kann, gehen leichter von der Hand, wenn man um den Lehrmeister weiß, welcher einem immer den Rücken stärkt und, sollte es den mal wirklich nötig werden, unter die Arme greift. Ich bin euch dankbar, für das Vertrauen welches ihr mir und meiner Arbeit entgegen gebrach habt, sowie für die Möglichkeiten mich zu entfalten und an meinen Aufgaben zu wachsen. Danke auch dafür, dass ihr mir alle Facetten der Forschung gezeigt habt, von der einfachen Arbeit im Labor, über das Anwerben von Forschungsgeldern bis hin zum wissenschaftliche Austausch im Rahmen internationaler Kongresse. Doch auch unsere kleinen Sommer- und Winterausflüge, welche die Zeit wesentlich verschönert haben, sollten nicht vergessen bleiben.

Ich bedanke mich herzlich bei Herrn Prof. Dr. Christian Lohr, nicht nur für die Begleitung währende der Promotionszeit und die Begutachtung meiner Dissertation, sondern auch für die spannenden Vorlesungen im Rahmen meines Biologie Bachelorstudiums. Ebenso großen Dank schulde ich Herrn Prof. Dr. Tim Gilberger, Herrn PD Dr. Hartwig Lüthen und Frau PD Dr. Sabine Riethdorf für ihre bereitwillige Zusage als Mitglieder meiner Prüfungskommission zu fungieren.

Außerdem gilt mein besonderer Dank an Frau Prof. Dr. Gunhild von Amsberg für die tolle Zusammenarbeit und Rekrutierung der Patienten. An dieser Stelle möchte ich mich auch außerordentlich bei Dr. Laura Keller bedanken, die ihr Patientenmaterial mit mir teilte und so einen erheblichen Beitrag zu dieser Arbeit leistete.

Ein großer Dank gilt auch Herrn Prof. Dr. Tobias Lange und Herrn Tobias Gosau für die enorme Unterstützung bei dem Mausexperiment und die Zeit, die sie sich genommen haben, um mich in

der Präparation der Mäuse zu schulen. Ohne eure Expertise wäre der Versuch so nicht möglich gewesen.

Ebenfalls bedanken möchte ich mich bei Dr. Volker Aßmann, PD Dr. Sabine Riethdorf, Dr. Kai Bartkowiak und Dr. Simon Joosse für die wertvollen Gespräche und Anregungen sowie die Bereitschaft nicht nur ihr Fachwissen, sondern auch ihre Gerätschaften und vieles mehr zu teilen.

Bei Carol Kloevenkorn und Dr. Linda Scarrott bedanke ich mich für die Durchsicht der Arbeit auf die Korrektheit der englische Sprache.

Sehr hervorheben möchte ich meinen Dank an die Mitglieder der AG Wikman, allen voran an Alexandra und Christina, die Vorarbeiten zu dieser Arbeit geleistet haben. Ganz besonderer Dank gilt meiner lieben Jolante, ich konnte mich immer auf dich verlassen. Du bist der Ruhepol der Arbeitsgruppe und das Ass im Ärmel, mit dem man jedes Spiel gewinnt. Ich danke meinen engsten Begleitern, Svenja und Lena, mit euch an meiner Seite erschien alles leicht. Es war eine der besten Fügungen, dass wir die Promotion zeitgleich angefangen haben. Über jede Hürde konnten wir gemeinsam springen und haben uns perfekt ergänzt. Ich danke euch für das Aushelfen, das Brainstoming und vor allem den Spaß den wir bei der Arbeit und privat hatten! Vielen Dank auch an Yassine für das Aufrechterhalten meines Blutzuckerspiegels, das Entertainment und die vielen Lacher im Labor. Großen Dank auch an Desirée, welche mir oft mit Rat und Tat zur Seite stand, und neben ihrer eigenen Arbeit auch immer Zeit für mich hatte.

Danke auch an Pari, Ines, Johanna, Sonja, Leonie, Yang, Sandra, Maha und Sebastian für den wiss. Austausch und die Freundschaft! Besonderer Dank gilt auch Antje, Conny, Sonja, Bettina, Malgorzata und Sandra für die Unterstützung im Laboraltag und die netten Gespräche.

Ich danke meinen Eltern, Alexander und Lina Besler, und meinen Großeltern für die absolute Liebe und den ewigen Halt. Danke, dass ihr immer an mich glaubt, immer für mich da seid und mir alles ermöglicht habt. Ohne euch wäre ich nicht da, wo ich jetzt stehe.

Ich danke auch meinen „Schwiegereltern“, Diana Fütterer und Herbert Merdes, die immer ein offenes Ohr für meine Scherereien hatten und mich während der Bachelor-, Master- und der Promotionszeit angefeuert haben.

Zuletzt möchte ich Silvester danken, der immer an meiner Seite war. Du hast mir in Zeiten wo ich dir selbst nicht viel geben konnte, alles gegeben und mich stets umsorgt. Ich danke dir für den bedingungslosen Rückhalt und die tausend Wege die du findest mich in jeder Situation zum Lachen zu bringen.

# Eidesstattliche Erklärung

Ich erkläre hiermit, dass ich diese Dissertation selbstständig ohne Hilfe Dritter und ohne Benutzung anderer als der angegebenen Quellen und Hilfsmittel verfasst habe. Alle den benutzten Quellen wörtlich oder sinngemäß entnommenen Stellen sind als solche einzeln kenntlich gemacht.

Diese Arbeit ist bislang keiner anderen Prüfungsbehörde vorgelegt worden und auch nicht veröffentlicht worden.

---

Ort, Datum, Unterschrift

# English certificate

Dr. Linda Scarrott
[redacted]

Universitätsklinikum Hamburg-Eppendorf
Institut für Tumorbiologie
Martinistraße 52, 20246 Hamburg

Hamburg, 27.04.2020

**Subject: English Language Thesis Certification for Katharina Besler**

To whom it may concern,

Katharina Besler, who was born on 14.12.1988 in Kostanay, Kazakhstan, is submitting her doctoral dissertation in English. The title of the thesis is "Role of RAI2 protein in the progression of prostate and breast cancer".

I hereby certify as a native English speaker and molecular biologist that the English language used in this thesis is sufficiently correct for submission.

Yours Sincerely,

Linda Scarrott

Dr. Linda Scarrott